Authors' Response to referee comments for 'Modeling studies for SOA formation from α-pinene ozonolysis'

The authors would like to thank both referees for the careful consideration of the manuscript and for the constructive comments and suggestions made to improve the manuscript. According to the reviewers' comments, the authors have further improved the manuscript. All comments and changes in the manuscript are addressed below. In the case, we do not concur with the reviewers' comments, adequate reasons are given.

Comments from referees are presented in blue, these are followed by authors' response in black, and changes to the manuscript are in green.

Referee #1

Major/General comments

However, the theory and assumptions behind the derived Eq. 2 and 3 is not easy to follow by only reading Sect. 2.2.2. E.g. for me it is not possible to understand what the Q_{i} steady state term stand for and what the overall gasside mass transfer coefficient is ($K_{\mathrm{g},i}$). If the theory is taken directly from Zaveri et al. (2014) then I suggest that you remove Eq. 2–4 from Sect. 2.2.2 and only put the equations in Appendix A where you describe Q_{i} and $K_{\mathrm{g},i}$. In Sect. 2.2.2 you instead just mention that you have implemented and used the model/theory from Zaveri et al. (2014).

In this Section, Sect. 2.2.2, the authors aimed at clarifying which equations of the approach proposed by Zaveri et al. (2014) have been implemented in the box model SPACCIM. Therefore, we have presented Eqs. (2 – 4) to clarify that the equations for a general system and polydisperse particles are utilized. In the paper of Zaveri et al. (2014), at first the general solution for a closed system is derived, then single particle equations with the approximation for a general system including fast and slow reactions are deduced and at the end the polydisperse equations for the two approximations are given. SPACCIM is a spectral parcel model (Wolke et al., 2005) and for this reason, the polydisperse equations are appropriate for implementation. The equations suitable for a general system were utilized because this approach should be subsequently applied in our 3-D model COSMO-MUSCAT (Wolke et al., 2012) and, therefore, extensive sensitivity studies are needed. Further, the mass balance equations of SPACCIM (Eqs. (6) and (8) of the presented paper) are based on Eqs. (2 – 4) and, consequently, it is necessary to introduce the model equations accounting for gas-to-particle phase mass transfer. Whereas, Eqs. (2 – 4) are deduced shortly in the Appendix of the presented paper to introduce the theory behind the kinetic approach for the sake of completeness. According to the reviewer's comment the description of Q_{i} and $K_{\mathrm{g},i}$ is expanded in Sect. 2.2.2 as follows:

Q_{i} represents the ratio of the average particle-phase concentration $\overline{A}_{\mathrm{i}}$ to the surface concentration $A_{\mathrm{i}}^{\mathrm{S}}$ at steady-state and is named quasi-steady-state term (see Appendix A). N_m denotes the number concentration, $r_{\mathrm{p},m}$ the respective particle radius, $k_{\mathrm{g},i}$ is the gas-side mass transfer coefficient, and

$K_{g,i}$ is the overall gas-side mass transfer coefficient, which is needed for the application of the two film theory (see Appendix A for details).

To me it is not clear what is new with the model approach presented in this study compared to Zaveri et al. (2014) The only new detail if I understand it correctly is the consideration of reversible particle phase reactions. The authors state that the kinetic gas-particle approach has been implemented in SPACCIM model and that it can be used for 3D-Eularian model simulations but this is never tested or evaluated. What is evaluated is the kinetic gas-particle approach from Zaveri et al. (2014) if I understand the manuscript correctly. If this is the case it should be clearly stated and the Sect. 2.2.1 could be replaced with one sentence where it is stated that evaluated kinetic gas-particle approach from Zaveri et al. (2014) has been implemented in SPACCIM. But since I don't think you don't test how the approach is working or supposed to work in SPACCIM I don't see the point in describing this model in detail. E.g. you write in Sect. 2.2.1 that SPACCIM considers size-resolved particle and cloud droplet formation, evolution and evaporation using a one-dimensional sectional approach. But this is not used in the current study where you only consider one particle size at the time and if I understand it correctly you use a fixed particle radius in the model despite that you simulate SOA growth experiments where the particles growth over time. If you state that the tested approach will be used in the particle and cloud droplet size resolved model SPACCIM you as referee/reader want to see some results where you demonstrate how the model can simulate the particle number size distribution evolution during some SOA experiments and how the different model parameters (e.g. bulk diffusion coefficient and particle phase reaction rates) influence the particle number size distribution evolution. E.g. as in the study by Zaveri et al. (2014).

The presented paper comprises different novelties concerning application as well as development of the kinetic approach. The utilization of the kinetic approach to a multiphase chemistry mechanism describing α-pinene degradation and SOA formation, extensive sensitivity studies concerning this reaction system, and simulating a chamber study are three novelties. On the model development level, the implementation of additional backward reactions in the particle phase and a composition dependent diffusion coefficient D_m are new for this model approach. Further, the influence of HOMs on SOA formation is outlined in detail and accounts for existing vapor pressure estimation uncertainties on the partitioning of this compound groups. Further, supporting results concerning the applicability of the weighted bulk diffusion coefficient will be presented later in this document and has been added to the presented paper, which is an additional novelty. Therefore, the presented paper comprises several new results, which are not part of the investigations of Zaveri et al. (2014).
Within the LEAK chamber studies, seed aerosol with a quite narrow particle distribution is injected, which can be captured in one bin in a model. Due to the SOA formation, the aerosol spectrum is shifted to a larger aerosol size, but stays almost monodisperse. Therefore, for the simulation of the chamber studies, the mean radius of the initialized aerosol spectrum is utilized for the model initialization. The authors know that the fixed particle radius can not model the reality, however, the aim of this approach was to avoid overlapping sensitivity effects within this investigation.
The functionality of the polydisperse model features, using the kinetic approach, were evaluated with test scenarios because these features are important for the subsequent application, e.g. in the 3-D model. However, for the conducted sensitivity studies the consideration of a polydisperse aerosol distribution will increase the degree of freedom as well as the complexity and for the simulation of the LEAK chamber studies, this feature was not required because of the nearly monodisperse aerosol spectrum within the experiment.
Based on the reviewer's comment, the novelty of the paper is highlighted straighter in the introduction and information on the narrow range of seed aerosol particles is given in the chamber experiment section as follows:

Sect. 1 Introduction:
Within this study, the kinetic partitioning approach by Zaveri et al. (2014) have been applied and further developed. Therefore, the kinetic partitioning approach was deployed the first time to a comprehensive gas-phase chemistry mechanism, describing α-pinene ozonolysis and box model simulations have been achieved for sensitivity and chamber studies. Since the kinetic partitioning is a more complex approach than the absorptive partitioning (Pankow, 1994), we conducted extensive sensitivity studies to explore the influence of the individual parameters on SOA formation. Particularly, particle-phase bulk diffusion coefficients, mass accommodation coefficients, and rate constants for particle phase reactions in the way of oligomerization are uncertain or less characterized for SOA particles. Therefore, sensitivity studies were conducted to reveal their influence on SOA formation. In addition to these more technical studies, two further investigations were carried out to study the influence of highly oxidized multifunctional organic compounds (HOMs) and a composition dependent particle-phase bulk diffusion coefficient. HOMs have been successfully identified in laboratory and field studies recently (Ehn et al., 2012, 2014; Zhao et al., 2013; Jokinen et al., 2014; Mentel et al., 2015; Mutzel et al., 2015; Berndt et al., 2016). Their possible existence was already proposed in 1998 (Kulmala et al., 1998), but their influence on the early growth of fresh SOA particles is the subject of ongoing investigations (Riipinen et al., 2012; Donahue et al., 2012, 2013). The consideration of HOMs in gas-phase chemistry mechanisms seems to be indispensable because the total molar HOM yield from the reactions of α-pinene with OH as well as O_3 is about 6 % (Berndt et al., 2016), also the predicted vapor pressures of HOMs are rather low (Kurtén et al., 2016). Thus, in the second part of this modeling study, the gas-phase chemistry mechanism has been extended to include the measured HOM yields for α-pinene ozonolysis in order to examine their influence on the initial formation of SOA and the overall SOA yield. The second investigation focuses on the importance of the particle-phase bulk diffusion coefficient of SOA particles for the overall SOA mass yield. The particle-phase bulk diffusion coefficient might be rather composition dependent than constant and, therefore, should change with the increasing organic matter in the particle phase. This investigation is also important for modeling of chamber experiments where wet seed aerosols are often used because water is known to have a plasticizer effect on SOA (O'Meara et al., 2016). The implementation of a composition dependent particle-phase bulk diffusion coefficient within the kinetic approach of Zaveri et al. (2014) constitutes a further development of the basic approach and the applicability of this new feature is tested in this study. Moreover, this study provides how a composition dependent particle-phase bulk diffusion coefficient can be applied and how it influences the SOA formation. The second further development of the kinetic approach concerns the particle-phase reactivity. Additional backward reactions in the particle phase have been considered to enable a treatment of reversible particle-phase reactions under formation of a reaction equilibrium. The effect of this process is also subject of the extensive sensitivity studies.

Sect. 2.1 Chamber experiments:
The experiments were performed in the presence of ammonium sulfate seed particles, which aerosol size distribution span a narrow range around a mean particle radius of 35 nm.

Sect. 2.3 Performed sensitivity studies:
Polydisperse test cases have been performed, but for the conducted sensitivity studies, the consideration of a polydisperse aerosol distribution will increase the degree of freedom as well as the complexity. Further, for the simulation of the LEAK chamber studies, this feature was not required because of the nearly monodisperse aerosol spectrum existent within this type of experiment.

...There are a range of more advanced models for smog chamber SOA formation simulations such as KM-GAP and ADCHAM that the authors refer to and the model from Zaveri et al. (2014) which I think already have been implemented in regional and maybe even global chemistry transport models.

Thus, the authors need to clearly demonstrate what is unique and important with their approach. In the current form of the manuscript this is not clear.

As described in our original manuscript, more kinetic model approaches exist, which also consider the particle-phase diffusion coefficient as a model parameter. The applications of these very detailed models differ from the aim of the investigations shown in the presented paper. KM-GAP considers a detailed description of the particle phase and, therefore, the influence of the aerosol composition and morphology on the gas-to-particle mass transfer can precisely investigated with this model (Shiraiwa et al., 2013). Further, the model is utilized for investigations concerning water uptake as well as ice nucleation by organic aerosols (Berkemeier et al., 2014). With ADCHAM, smog chamber studies beyond SOA formation are investigated, e.g. simulations concerning organic salt formation, the influence of heterogeneous reactions, and chamber wall effects (Roldin et al., 2014). This advanced model features are beyond the fields of application of SPACCIM, which treats the particle phase as bulk and, therefore, not contains the required model infrastructure. Consequently, more advanced models require the specification of a greater number of model parameters, e.g. to describe the particle phase in more detail. Since not all of these parameters might be determined by experimental studies as a consequence thereof more assumptions for additional parameters have to be made (e.g., diffusion coefficient for every particle layer). A recent study by Berkemeier et al. (2016) presented an approach to extend the dimensions of the experimental input data to maintain the advanced model description for a complex system. Nevertheless, this method is only applicable for detailed experimental studies on distinct compounds.
However, the kinetic approach of Zaveri et al. (2014) utilizes the basic assumption of a constant particle-phase bulk diffusion coefficient and an analytical solution for the description of SOA formation. As investigated by O'Meara et al. (2016), numerical solutions for aerosol transformation processes are computationally expensive and, therefore, a numerical approach with a constant bulk diffusion coefficient requires approximately 20 times more computational effort than an analytical approach (O'Meara et al., 2017). The analytical kinetic approach of Zaveri et al. (2014) is preferred to save computational effort and, therefore, was analyzed/tested for utilization in future 3-D model simulations.
To the authors' knowledge, the results of a 3-D model utilizing the approach of Zaveri et al. (2014) for SOA formation is up to now not presented in a peer-reviewed journal. Nevertheless, the authors showed preliminary results of the 3-D model COSMO-MUSCAT with this kinetic partitioning approach at the EGU General Assembly 2017 (http://meetingorganizer.copernicus.org/EGU2017/EGU2017-4557.pdf).
However, the authors are not aware of the application of the kinetic approach from Zaveri et al. (2014) in a regional or global model published in a peer-reviewed journal.
The highlights of this manuscript are already addressed in response to the first comment raised by the reviewer #1.

I understand that the efficiency of the reactive uptake will be different for liquid and semi-solid particles but I don't understand how the phase-state can have such a tremendous influence on the SOA formation if the particle phase reactions are negligible slow (Fig 1b and 4c). To me the SOA phase state should not have a large influence on the SOA formation as long as the particle surface layer is composed of amorphous SOA material with the same composition as the SOA bulk. Then based on Raoul's law the saturation concentration of any gas-phase species above the particles would not differ between semi-solid and liquid particles. Even if the particles would be composed on solid crystalline salts (e.g. dry ammonium sulfate seed particles) organic molecules start to grow these particles if the gas-phase concentration of some organic species reaches above their pure-liquid saturation concentration. But the current model approach does not seem to capture this. I wonder if there is some fundamental assumption that is wrong/limiting the use of Eq. 2 and 3?

The total particle-phase concentration within this kinetic approach depends on the gas-phase concentration of the condensable organic compounds, the transport of this compounds to the particle surface as well as the transport into the particle. As described in Mai et al. (2015), three different limitations for SOA formation exist for a kinetic approach: gas-phase-diffusion-limited partitioning, interfacial-transport-limited partitioning, and particle-phase-diffusion-limited partitioning. Due to the relatively small particle sizes and the mass accommodation coefficient of $\alpha = 1$ within the majority of the presented studies, consequently particle-phase-diffusion-limited partitioning can be observed for decreased particle-phase bulk diffusion coefficients within several sensitivity studies. The particle-phase bulk diffusion coefficient determines the transport into the particle bulk. An important parameter to interpret the interaction of the individual model parameters characterizing the particle bulk is the dimensionless diffusion-reaction parameter q_i (Zaveri et al., 2014), which is defined as the ratio of the particle radius r_p and the reacto-diffusive length $\sqrt{D_{\mathrm{b},i}/k_{\mathrm{c},i}}$ (Pöschl et al., 2007):

$$q_i = r_\mathrm{p}\sqrt{\frac{k_{\mathrm{c},i}}{D_{\mathrm{b},i}}}\,. \tag{1}$$

Therein, $D_{\mathrm{b},i}$ is the particle-phase bulk diffusion coefficient and $k_{\mathrm{c},i}$ represents the pseudo-first-order rate constant for particle reactions of the compound i. In Fig. 4 of Zaveri et al. (2014), the normalized concentration profiles for the steady-state case are displayed for different q_i (see Fig. 1a). For the

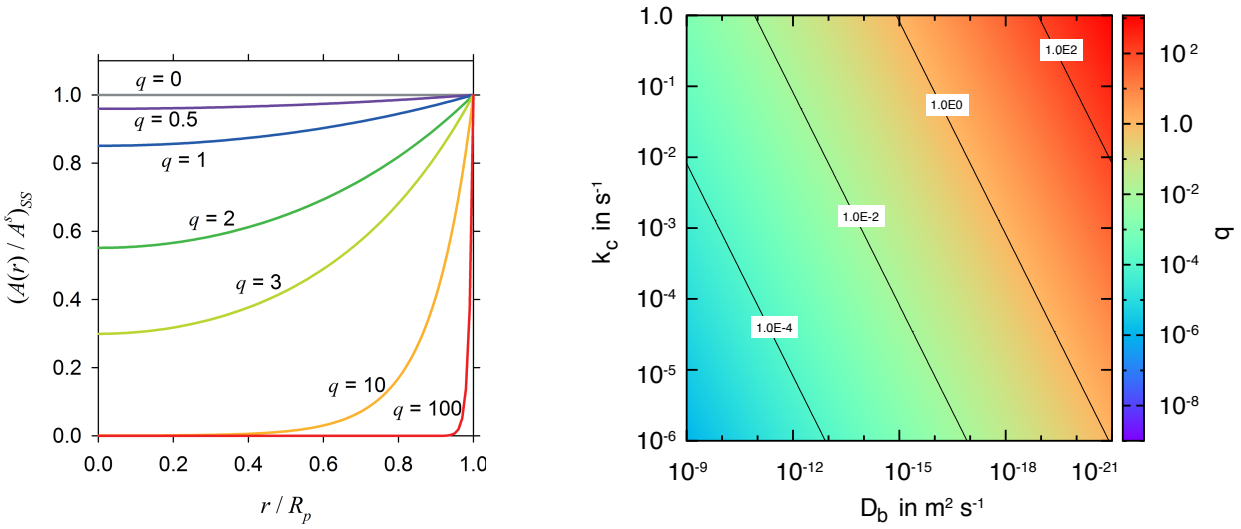

Figure 1: a) Normalized $(A(r)/A^\mathrm{s})_\mathrm{ss}$ profiles as a function of r/r_p (R_p in the variable declaration of Zaveri et al. (2014)) for different values of the dimensionless diffusion-reaction parameter q_i. Therein, $A(r)$ stands for the particle-phase concentration A in dependence of the particle radius r, which is normalized by the surface concentration of the particle A^s, and is displayed for the steady state (indicated by the index "ss"); Figure taken from Zaveri et al. (2014). b) $\log(q)$ values for the sensitivity study of case 1 from Table 1 in Gatzsche et al. (2017).

simulations performed in the sensitivity study of case 1 in Table 1 of the presented paper, q_i cover the entire spectrum displayed in Fig. 1a. From Eq. (A3) of the presented paper it is obvious, that the total organic mass in the particle bulk can be calculated by the integral of the solute concentration over the sphere volume. From the distribution of $(A(r)/A^\mathrm{s})_\mathrm{ss}$ in Fig. 1a, we can conclude that with an increasing value of q the particulate organic mass have to decrease because the organic mass only concentrates like a film on the outside of the particle. With regard to the variation of the diffusion coefficient of the sensitivity study case 1 (see Table 1 of the presented paper), the following values of q have to be considered. For these studies, a constant particle radius of $r_\mathrm{p} = 35\,\mathrm{nm}$ have been utilized. For

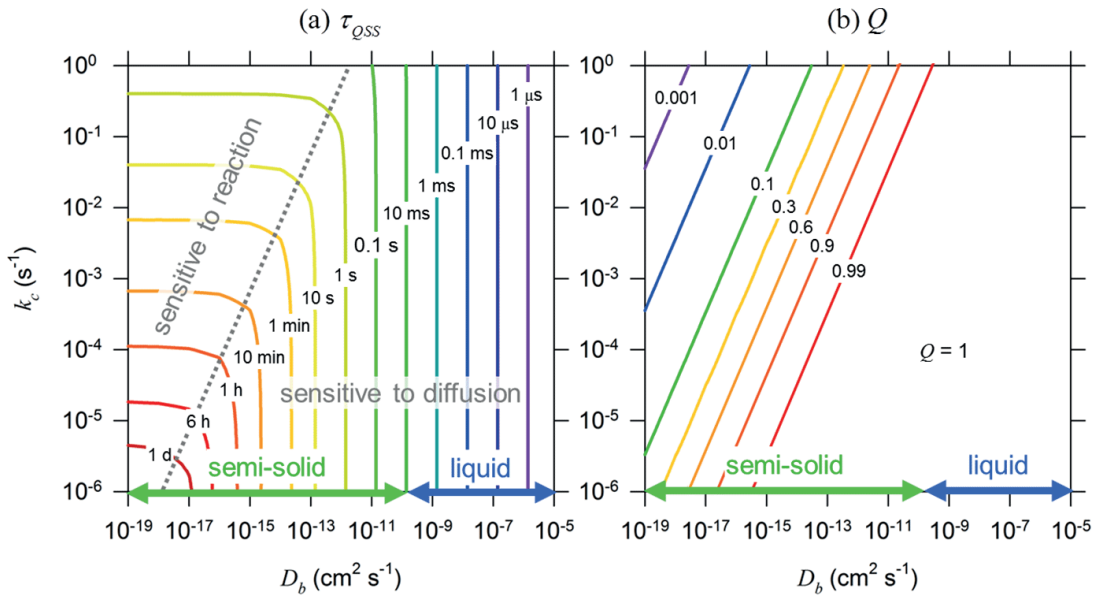

Figure 2: Contour plots of a) the quasi-steady-state timescale τ_{QSS} of the particle-phase and b) the quasi-steady-state parameter $Q = (\overline{A}/A^S)_{\mathrm{QSS}}$, both as functions of the particle-phase bulk diffusion coefficient D_{b} and the pseudo-first-order rate constant k_{c} for a fixed particle size of d_{p}=100 nm; Figure taken from Zaveri et al. (2014).

the highest rate constant of $k_{\mathrm{c}} = 1\,\mathrm{s}^{-1}$ and $D_{\mathrm{b}} = 10^{-9}\,\mathrm{m}^2\,\mathrm{s}^{-1}$, the dimensionless diffusion-reaction parameter equals $q = 1.11\times10^{-3}$ (see Fig. 1b). When decreasing the reaction rate to $k_{\mathrm{c}} = 10^{-6}\,\mathrm{s}^{-1}$, q calculates to $q = 1.11 \times 10^{-6}$ (Fig. 1b). Thus for liquid particles ($q \to 0$), the concentration ratio at steady state, displayed in Fig. 1a, is near unity in the whole particle. Therefore, the organic mass contained in the particle phase reaches their maximum. For semi-solid particles $D_{\mathrm{b}} = 10^{-21}\,\mathrm{m}^2\,\mathrm{s}^{-1}$ and $k_{\mathrm{c}} = 1\,\mathrm{s}^{-1}$, q calculates to $q = 1.11 \times 10^3$ (see Fig. 1b). For this value of q, a highly non-uniform concentration ratio profile can be observed in the particle, which means that the condensed organic compounds are mainly located at the surface of the particle (like a film, see Fig. 1a). The organic mass reaches a minimum. Therefore, no further condensation of organic compounds on the particle will occur because a particle-phase-diffusion-limited partitioning occurs (Mai et al., 2015). For slow particle-phase reactions $k_{\mathrm{c}} = 10^{-6}\,\mathrm{s}^{-1}$, the dimensionless diffusion-reaction parameter equals to $q = 1.11$ (Fig. 1b), which indicates a slightly non-uniform concentration ratio in the particle (see Fig. 1a). In this case, the concentration gradient in the particle phase is not high, however, the particle phase reactions are too slow to shift the equilibrium towards the particle phase and leading to further condensation from the gas phase.

It is not clear how the SOA material that are formed after the heterogeneous reactions are treated in the model. Is it assumed to be non-volatile but still part of the amorphous SOA phase that allows more dissolution of SVOCs into the particle phase? This needs to be explained.

To address the reviewer's comment, the description of the considered particle phase chemistry has been extended in Sect. 3.1.2. as follows:

As indicated in Eq. (1), the organic compounds, which are partitioned from the gas phase into the particle phase, can further react in the particle phase with a constant reaction rate k_{c}. The from the gas into the particle phase partitioned organic compounds are named p-products. The products, which have been caused due to the reactions in the particle phase, are termed r-products. The r-products do not stay in equilibrium with the gas-phase compounds and, therefore, can not evaporate from

the particle phase. The r-products comprise particle-phase compounds resulting from aging of the condensed organic compounds (e.g., dimers, trimers or oligomers).

The model framework does not take into account the Kelvin effect if I understand this correct. If this is the case it cannot be used to study new particle formation. Please clarify and clearly state this if this is the case. I don't understand how you can assume that the particle radius is fixed. In any SOA new particle formation experiment (without seed) the particle size will grow from initially around 1 nm to larger sizes. I am skeptical to weather this model framework can handle this size dependent particle growth? Doesn't the model framework handle the gradual growth of the particles and can it take into account coagulation?

The Kelvin effect describes the change of the vapor pressure due to a curved liquid-vapor interface and is especially important for small particles because of their higher curvature (Seinfeld and Pandis, 2006; Pruppacher and Klett, 2010). The partial vapor pressure of a compound i over a curved interface $p_i^{\ominus}$ (atm) can be related to the vapor pressure over a flat surface $p_{\mathrm{sat},i}$ (atm) with the following equation (Riipinen et al., 2010):

$$p_i^{\ominus} = x_i \gamma_i p_{\mathrm{sat},i} \exp\left(\frac{4 M_i \sigma_\mathrm{p}}{R T_\mathrm{p} \rho_\mathrm{p} d_\mathrm{p}}\right) = x_i \gamma_i p_{\mathrm{sat},i} \exp\zeta \tag{2}$$

The exponential term of Eq. (2) describes the Kelvin effect, whereas the multiplication with the mole fraction x_i and the activity coefficient γ_i owes to Raoult's law. Further, M_i is the molar weight ($\mathrm{g\,mol^{-1}}$) of the species i in the particle with the diameter d_p (m), ρ_p ($\mathrm{kg\,m^{-3}}$) the density, and σ_p ($\mathrm{N\,m^{-1}}$) the surface tension of the particle. The particle temperature T_p and the universal gas constant R ($8.314\,\mathrm{J\,mol^{-1}\,K^{-1}}$) are included. The vapor pressure over the curved interface always exceeds the vapor pressure over a flat surface considering the same species. The surface tension is defined as the amount of energy, which is required to increase the area of a surface by 1 unit (Seinfeld and Pandis, 2006). The pure water surface tension $\sigma_{\mathrm{w}0}$ can be estimated in dependence of the temperature T (in K, Pruppacher and Klett, 2010):

$$\sigma_{\mathrm{w}0} = 0.0761 - 1.55 \times 10^{-4}(T - 273)\,\mathrm{N\,m^{-1}}\,, \tag{3}$$

within a temperature range of -40 to 40°C. Dissolution of other compounds in water alter its surface tension. Salts increase the surface tension of the droplet, e.g. for ammonium sulfate the following expression is valid (Seinfeld and Pandis, 2006):

$$\sigma_\mathrm{w}(m_{(\mathrm{NH_4})_2\mathrm{SO_4}}, T) = \sigma_{\mathrm{w}0} + 2.17 \times 10^{-3} m_{(\mathrm{NH_4})_2\mathrm{SO_4}}\,, \tag{4}$$

with $m_{(\mathrm{NH_4})_2\mathrm{SO_4}}$ ($\mathrm{mol\,l^{-1}}$) the molality of ammonium sulfate. In contrast to that, organics decrease the surface tension of a droplet because their surface tension is lower than that of pure water. For pure saturated organic liquids, the surface tensions alter between 20 and $40\,\mathrm{mN\,m^{-1}}$ in the temperature range $280-320\,\mathrm{K}$ (Jasper, 1972; Seinfeld and Pandis, 2006; Butt et al., 2004). In aerosol particles, water, dissolved inorganic salts, and organics are mixed and together effect the resulting surface tension. Different investigations on the surface tension of mixed aerosols/cloud droplets exist (Facchini et al., 1999; Hitzenberger et al., 2002; Ervens et al., 2004, 2005). Facchini et al. (1999) proposed a specific relation between the surface tension σ and the dissolved organic carbon concentration $[C]$ (in $\mathrm{mol\,l^{-1}}$):

$$\sigma = 72.8 - 0.0187\,T \ln(1 + 628.14\,[C])\,\mathrm{mN\,m^{-1}}\,, \tag{5}$$

which is derived by fitting the Szyszkowski-Langmuir equation to their measurement data from Po valley fog. Whereby, Ervens et al. (2004) state that the application of Eq. (5) is only appropriate for higher molecular weight organic compounds because of the huge overestimation of the surface tension effect of small dicarboxylic acids (Shulman et al., 1996). The value of the surface tension for

a complex mixed aerosol particle/droplet is not definitely known. However, Eq. (2) indicates that the Kelvin effect is a correction to the vapor pressures over a flat surface $p_{\mathrm{sat},i}$, which are utilized in the presented paper. If only organic droplets are considered, the correction term is for particles smaller than 10 nm and surface tensions higher than 30 mN m^{-1} greater than 2 (see Fig. 3a). For water

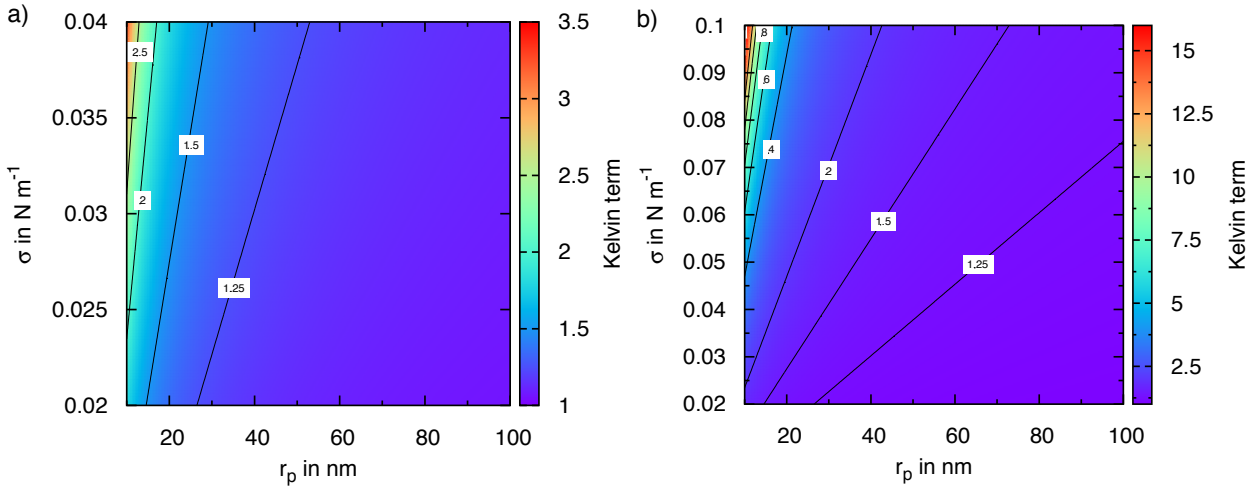

Figure 3: Kelvin term ($\exp\zeta$ in Eq. 2) depending on the surface tension σ and the particle radius r_{p} for a) a typical surface tension range for organics and b) a typical surface tension range for water with ammonium sulfate.

containing ammonium sulfate, the Kelvin term reaches greater values for particles with $r_{\mathrm{p}} \leq 10$ nm, which might imply a larger effect for the first organic compounds that condense on small particles (see Fig. 3b). Thus, only for the smallest particles in our simulations ($r_{\mathrm{p}} = 11$ nm) the Kelvin effect might affect the initial condensation of the organic compounds on the particles (see Fig. 3a, b). Nevertheless in the presented paper, a group contribution method (EVAPORATION, Compernolle et al., 2011) is applied to estimate the liquid vapor pressures of the condensing organic species because no accurate measurements for the compounds are available as well as it is impracticable to measure the vapor pressures for the variety of compounds. An investigation of O'Meara et al. (2014) reveals that the vapor pressure estimates from the different group contribution methods vary from each other and deviate from existing measurements up to six orders of magnitude. Additionally, Kurtén et al. (2016) show the differences between the vapor pressures estimated by three different group contribution methods and COSMO-RS (conductor-like screening model for real solvents, Eckert and Klamt, 2002). Therein, 8 orders of magnitude lower vapor pressures are estimated by using group contribution methods than COSMO-RS for some highly oxidized monomers. Therefore, the correction of the vapor pressure by the Kelvin effect might be in the order of the error range of the applied group contribution method. For this reason, we have not considered the Kelvin effect in our calculations, but it is planned to be included in future investigations.

In the study of Zaveri et al. (2014), the Kelvin effect was also not considered for simplicity. In KM-GAP, the Kelvin effect is only considered for water within the Köhler equation (Shiraiwa et al., 2012). However, Roldin et al. (2014) stated that ADCHAM comprises the Kelvin effect for the organic compounds, utilizing surface tensions of 50 mN m^{-1} according to the study from Riipinen et al. (2010). Further, the simulations in the presented paper do not investigate new particle formation because seed aerosol particles are taken into account.

The parcel model SPACCIM includes coagulation as proposed in Wolke et al. (2005), wherein all microphysical features of SPACCIM have been already provided and tested. However, in the presented studies this process was not a matter of interest. The focus of the presented paper is to characterize the influence of the different model parameters on the SOA formation and not on aerosol microphysics. As explained before, the LEAK chamber studies are initialized with a quite narrow particle spectrum

with the mean radius of 35 nm. Therefore, we did not additionally vary the particle radius within this sensitivity study and use $r_p = 35$ nm, which was the mean radius of the initialized seed aerosol particles for the LEAK experiment.
To address the reviewer's comment concerning the Kelvin effect, in Sect. 3.2 it is clarified that new particle formation is not investigated and an additional section concerning the limitations of the model studies have been added. Further, in Sect. 2.2.1 the authors point out more clearly that the microphysical features of the utilized model framework are already published and are not part of the presented paper.

Sect. 2.2.2:
The size-resolved cloud microphysics of deliquesced particles and droplets including cloud droplet formation, evolution, and evaporation is considered using a one-dimensional sectional approach. Further microphysical features of SPACCIM are already described in Wolke et al. (2005) and results owing to these processes are presented in Tilgner et al. (2013); Rusumdar et al. (2016); Hoffmann et al. (2016). The implemented multiphase chemical model applies a high-order implicit time integration scheme, which utilizes the specific sparse structure of the model equations (Wolke and Knoth, 2002). SPACCIM was originally developed for parcel model studies, whereby, the considered air parcel can follow real or artificial trajectories. However, the partitioning of organic gases towards the particle phase was not considered in the original SPACCIM and the model was not exclusively designed for application on aerosol chamber studies. The existing model framework has been extended by gas-to-particle mass transfer via a kinetic partitioning approach (Zaveri et al., 2014), see Sect. 2.2.2 for details. Due to the focus of these studies on modeling aerosol chamber studies of gasSOA formation for monodisperse aerosol without entrainment and coagulation, microphysical processes are not included in the results of this study.

Sect. 3.2:
Nevertheless, the conducted simulations account not for new particle formation. The simulations without initial organic mass is consistent to previous studies, initialized with inorganic seed aerosol particles.

Sect. 3.6 Limitations of the present studies:
The presented model studies do not account for the Kelvin effect. The Kelvin effect describes the change of the vapor pressure due to a curved liquid-vapor interface and is especially important for small particles because of their higher curvature (Seinfeld and Pandis, 2006; Pruppacher and Klett, 2010). The vapor pressure of a compound i over a flat surface $p_{\mathrm{sat},i}$ (atm) can be corrected to the partial vapor pressure over a curved interface $p_i^{\ominus}$ (atm, Seinfeld and Pandis, 2006). The correction factor depends strongly on the particle size and the surface tension of the considered aerosol particle/droplet. The surface tension varies with the composition of the aerosol particle (Facchini et al., 1999; Hitzenberger et al., 2002; Ervens et al., 2004, 2005), e.g. it is increased by dissolved salts (Seinfeld and Pandis, 2006) and decreased by organic compounds (Facchini et al., 1999; Ervens et al., 2005). However, for the estimation of the vapor pressures for the partitioning compounds a group contribution method (EVAPORATION, Compernolle et al., 2011) is applied in this study. An investigation of O'Meara et al. (2014) reveals that the vapor pressure estimates from the different group contribution methods vary from each other and deviate from existing measurements up to six orders of magnitude. Further, Kurtén et al. (2016) showed the differences between the vapor pressures estimated by three different group contribution methods and COSMO-RS (conductor-like screening model for real solvents, Eckert and Klamt, 2002). Therein, 8 orders of magnitude lower vapor pressures are estimated by group contribution methods than COSMO-RS for some highly oxidized monomers. Therefore, the correction of the vapor pressure by the Kelvin effect might be in the order of the error range of the applied group contribution method. For this reason, we have not considered the Kelvin effect in our calculations.

How realistic is it to represent a dimerization or oligomerization process as a first order reaction. Dimerization will involve two organic monomers. Please clearly explain what the first order particle formation reactions are supposed to represent in the model. I would also like to see some reference on what values of k_c that has been used in previous studies, I am sure that is also exists some experimental evidence of appropriate values and what reactions it may be.

As already stated in Zaveri et al. (2014), the particle-phase reactions and their associated reaction rates are not well defined by measurements and, therefore, a constant pseudo-first-order-rate constant is introduced to approximate the particle-phase reactivity. Camredon et al. (2010) also described oligomerization with a pseudo-first-order loss rate from the monomers to consider the particle-phase reactivity in a box model study. Trump and Donahue (2014) utilize thermodynamic calculations for the equilibrium constants of organic compounds to describe oligomerization in a VBS framework. A detailed description of dimerization is contained in ADCHAM (Roldin et al., 2014), which utilizes measurements of the reaction rate coefficients for the formation of peroxyhemiactetals proposed by Antonovskii and Terent'ev (1967). The reaction rate coefficients of Antonovskii and Terent'ev (1967) are the only available measured values, which are also proposed in the review of Ziemann and Atkinson (2012).
However, Seinfeld and Pandis (2006) proposed that SOA often comprises high-molecular-weight species that are a kind of oligomers (e.g., dimers, trimers, tetramers, etc.) resulting from the reaction of VOC oxidation products (Kalberer et al., 2004; Gao et al., 2004b,a; Tolocka et al., 2004; Hall IV and Johnston, 2011). Further, oligomerization is enhanced due to the presence of strong acids (e.g., sulfuric acid, Jang et al., 2002, 2003; Iinuma et al., 2004). Barsanti and Pankow (2004, 2005) and Barsanti and Pankow (2006) suppose due to thermodynamic studies that accretion reactions are most likely for acids. Nevertheless, none of these recent studies provide a reaction mechanism and related reaction rate constants for the particle phase reactions. Up to now, the existence and qualitative values of oligomerization in the particle phase are investigated. In the study of Hosny et al. (2016), additional to the micro-viscosity measurements, monomer:dimer:trimer:tetramer signal intensities are shown and the oligomerization process is compared with the simulation of the oligomerization of oleic acid as model compound. KM-SUB (Shiraiwa et al., 2010) is utilized for the simulations in this study. However, the reactions and reaction rate coefficients therein are valid for oleic acid, which is a more investigated reaction system.
It is clear to the authors that the dimerization process can not described by using a first-order rate constant limited to the production of oligomers. This process is more accurately captured by an equilibrium reaction, but the equilibrium constants are also not well defined. Therefore, the authors' consideration was to add an additional backward reaction to initially review/verify the sensitivity of SOA formation on this additional feature. In the detailed approach of Roldin et al. (2014), the formation and degradation of dimers is also treated with two separate reactions.
To address the reviewer comment on the pseudo-first-order rate constant, text is modified/added in Sect. 3.3 and a description of the limitations of the current particle-phase reactivity scheme is added to the new inserted Sect. 3.6.

Text added/modified to Sect. 3.3:
Organic aerosol-phase reactions can be irreversible reactions such as oxidation reactions or reversible reactions as for instance dimerization/oligomerization (Hallquist et al., 2009; Ziemann and Atkinson, 2012). For the observed particle-phase dimerization, different possible reaction mechanisms can be found in the literature: (i) hemiacetal formation due to reactions between alcohols and aldehydes or carbonyl compounds (Iinuma et al., 2004; Ziemann and Atkinson, 2012; Carey and Sundberg, 2007), (ii) peroxyhemiacetal formation between hydroperoxides and carbonyl compounds (Tobias and Ziemann, 2000; Ziemann and Atkinson, 2012), (iii) aldol reaction products from the acid-catalyzed

dimerization of a ketone or aldehyde (Carey and Sundberg, 2007; Casale et al., 2007), and (iv) esterification due to reactions of carboxylic acids with alcohols (Surratt et al., 2006; Ziemann and Atkinson, 2012; Carey and Sundberg, 2007). Thermodynamic calculations indicate ester formation and peroxyhemiacetal formation as most likely (Barsanti and Pankow, 2006; DePalma et al., 2013) and suggest hemiacetal formation as thermodynamically unfavorable (Barsanti and Pankow, 2004; DePalma et al., 2013). Therefore, an irreversible representation of the aerosol chemistry might lead to an overprediction of the formed SOA mass, which means that can be only considered as an upper limit approach. The formed oligomers are complex compounds, which consist of a few monomer units. The oligomer equilibrium can be influenced by ambient conditions such as the temperature, relative humidity, and the chemical composition of the aerosol. A reversible representation of oligomerization reactions can be considered by means of an implemented backward reaction. E.g. Roldin et al. (2014) treats the kinetics of the reversible dimerization also with two separate reactions. However, an advanced kinetic treatment of particle-phase reactions is utilized considering monomer concentrations combined with second-order rate constants and dimer first-order degradation rates separated for bulk and surface layers. However, measurement data concerning dimerization reaction rates are scarce for condensed organic compounds and vary over several orders of magnitude (Antonovskii and Terent'ev, 1967). For the sensitivity study concerning the influence of the backward reaction on the predicted SOA mass, a simplified approach is tested. Therefore, we considered different backward reaction rate constants for particle-phase reactions (see Table 1, case 7) in addition to the pseudo-first-order rate constants.

Text added to Sect. 3.6 Limitations of the present studies:
This study utilizes a simplified scheme to consider particle-phase reactions in order to account for SOA aging. The kinetic approach of Zaveri et al. (2014) is divided into two reaction cases according to the rate of the particle-phase reactivity based on the achievement of the steady state. In Sect. 3.3, a modification of the particle-phase reactivity is presented in order to improve the representation of SOA aging under preservation of the basic classification/separation in fast and slow particle-phase reactions. This simplified approach is appropriate for application in 3-D models, treating organic compounds in lumped groups, and saves computational effort. However, for future chamber simulations with the focus on SOA processes combined with advanced measurement data, accounting for SOA aging or oxidation state, an improved representation of particle-phase reactivity will be implemented to further develop SPACCIM. Therefore, the pseudo-first-order rate constants will be replaced, e.g. by second-order equilibrium reactions under consideration of equilibrium rates provided by Barsanti and Pankow (2004) for hydrate and hemiacetal formation or thermodynamic calculations for equilibrium constants of DePalma et al. (2013) for individual dimers.

In Sect. 3.4 you describe an approach of how to estimate a weighted particle-phase bulk diffusion coefficient that considers particle composition (Eq. 10). I don't understand this approach. Is D_{m} referring to the diffusion coefficient of the organic compounds in the particle-phase? Is it further assumed that the organic compounds are water-soluble then and that the particles are composed on one SOA+water+inorganics phase? I think that the particles often will be composed of several phases (e.g. one hygrophobic organic phase and one water+inorganics+some water soluble organics phase). I think that differences in D_{org} over time can also be due to particle phase oligomerization processes that gradually increase the average organic molecular mass. But this Eq. 10 does not take this into consideration. To me Eq. 10 contains to many assumptions and is not evaluated properly to be able to be justified.

In SPACCIM no phase separation is considered. We assume that the particle contains only one mixed phase, which is characterized by the bulk diffusion coefficient. In our study, the particle phase comprises water, ammonium sulfate, and organics. In the kinetic approach of Zaveri et al. (2014), the particle-phase bulk diffusion coefficient is constant over the whole simulation time. A plenty of studies

indicate that SOA might have under certain conditions a higher viscosity (Renbaum-Wolff et al., 2013; Abramson et al., 2013; Pajunoja et al., 2014; Zhang et al., 2015; Grayson et al., 2016) and we try to consider this effect in our model studies. The mean particle-phase bulk diffusion coefficient D_{m}, defines the diffusion coefficient of the whole particle as the mixture of the three compounds (water, ammonium sulfate, and organics). To calculate the weighted diffusion coefficient with the Vignes type rule the self-diffusion coefficient of the organic compounds D_{org}, of the dissolved inorganic ions (here from ammonium sulfate) D_{inorg}, and of water D_{water} have to be considered. The individual self-diffusion coefficients (D_{org}, D_{inorg}, D_{water}) are constant over time (only the self diffusion coefficient of water depends on the temperature, but in our study the temperature is constant). However, the mole fraction of the organic compounds x_{org} increase with increasing organic mass in the particle phase. Due to the assumed lower self-diffusion coefficient of the organic compounds ($D_{\mathrm{org}} = 10^{-12}\,\mathrm{m^2\,s^{-1}}$ or $D_{\mathrm{org}} = 10^{-14}\,\mathrm{m^2\,s^{-1}}$) than that of water with dissolved ions ($\approx 10^{-9}\,\mathrm{m^2\,s^{-1}}$) the weighted diffusion coefficient decreases. Hosny et al. (2016) showed in their study that the viscosity increases over their experiment time and that the amount of dimers, trimers, and tetramers increases (simultaneous decrease of monomers). Therefore, the oligomerization might also decrease the particle-phase bulk diffusion coefficient. Nevertheless, there are no appropriate measurements to parameterize this effect and for the implementation of this effect in a model more assumptions than for a uniform self-diffusion coefficient for the organic compounds have to be made. Therefore, the presented sensitivity study concerning the weighted diffusion coefficient aims at investigating the effect of a decreased particle-phase bulk diffusion coefficient induced to an increased amount of organics in the particle phase on SOA formation. For this issue, two self-diffusion coefficients of the organic compounds are assumed, which are related to material more viscous than water. An assumption was made for liquid ($D_{\mathrm{org}} = 10^{-12}\,\mathrm{m^2\,s^{-1}}$) and a second for the transition to semi-solid ($D_{\mathrm{org}} = 10^{-14}\,\mathrm{m^2\,s^{-1}}$) particles. The Vignes type rule (Vignes, 1966) is used in previous studies concerning water diffusion in SOA particles (Lienhard et al., 2014, 2015; Price et al., 2015) and to study the plasticizing effect of water (O'Meara et al., 2017). To evaluate the applicability of Eq. (10) combined with the kinetic approach of Zaveri et al. (2014), additional results are added to the revised manuscript (S. O'Meara, personal communication). For this purpose, the model of Zobrist et al. (2011) have been utilized as basis for evaluation of the composition dependent particle-phase bulk diffusion coefficient. According to the reviewer's comment and the additional results, the manuscript is extended as follows:

The applicability of Eq. (10) within the kinetic approach of Zaveri et al. (2014) is checked and verified under the utilization of the model by Zobrist et al. (2011) as basis for evaluation (S. O'Meara, personal communication). Fig. S7a and S7b in the Supplement display the differences for the numerical solution from the model of Zobrist et al. (2011) and the analytical solution of the kinetic approach with the weighted particle-phase bulk diffusion coefficient for $D_{\mathrm{org}} = 10^{-11}\,\mathrm{m^2\,s^{-1}}$ and $D_{\mathrm{org}} = 10^{-13}\,\mathrm{m^2\,s^{-1}}$, respectively. For both assumed self-diffusion coefficients of the organic fraction, the numerical and analytical solution are equal within 1×10^{-6} s and 1×10^{-4} s. Thus, Eq. (10) can applied to the kinetic approach instead of a constant bulk diffusion coefficient.

Minor comments:

Page 2, Line 17-18: I think this sentence needs to be reformulated.

We have reformulated the sentence as follows in the revised manuscript:
The modeling approach, which is mainly utilized for gas-to-particle phase partitioning of semi-volatile organic compounds, based on gas-particle equilibrium for these compounds, was proposed by Pankow (1994).

Page 2, Line 25-28: This sentence is a bit hard to understand/follow. Can you reformulate it?

We have reformulated the sentence as follows in the revised manuscript:
Bulk viscosity measurements demonstrate that SOA particles only exist at a high relative humidity (RH > 75 %) in a liquid state (Renbaum-Wolff et al., 2013; Kidd et al., 2014). At a lower relative humidity, the organic particles exhibit a higher viscosity indicating a semi-solid or glassy phase state (Renbaum-Wolff et al., 2013; Abramson et al., 2013; Pajunoja et al., 2014; Zhang et al., 2015; Grayson et al., 2016).

Page 2, last word, remove "the"

We followed the reviewer comment and removed the "the":
However, the data by Hosny et al. (2016) fit well with particle-phase diffusion coefficient measurements by Price et al. (2015), which were converted by the Stokes-Einstein (SE) relation to viscosity.

Page 3, Line 33. The molar yields are not 6 %.

Adding up of the measured gas-phase HOM yields results the following:
2.4 % + 3.4 % = 5.8 % ≈ 6 %.

Page 4, Line 2-3. I don't understand this sentence. I understand that the diffusion coefficient will depend on the composition but not how it depends on increasing organic matter. Indirectly it can of course be influenced by the organic mass since this in turn can influence the composition.

With increasing organic matter, the mole fraction of the organic fraction increases in the particle phase. Therefore, the weighted particle-phase bulk diffusion coefficient will decrease because the self diffusion coefficient of the organic material ($D_{org} = 10^{-12}\,m^2\,s^{-1}$ or $10^{-14}\,m^2\,s^{-1}$) is lower than that of water with dissolved ions ($\approx 10^{-9}\,m^2\,s^{-1}$). According to the reviewer's comment the description has been improved in the introduction:

The particle-phase bulk diffusion coefficient might be composition dependent and due to a lower self-diffusion coefficient of the organic material, increasing organic matter in the particle phase decreases the weighted particle-phase bulk diffusion coefficient.

Sect. 2.1. Here you describe the experiments and the instruments that were used. What I am missing is the information about the size of the smog chamber (volume) and the wall material (e.g. Teflon) and I also miss information about how the measurement results are used in the present manuscript. E.g. how were the measurements used to derive the SOA mass in Fig. 9a? Also I miss a discussion concerning VOC and particle wall losses that is known to be important in chambers.

Detailed information concerning the chamber are provided in Iinuma et al. (2009) and Mutzel et al. (2016). Briefly, LEAK is a cylindrical, 19 m^3 Teflon bag with a surface-to-volume ratio of 2 m^{-1}. This information is now also given in the revised manuscript.
The measurement results are used in Sect. 3.2 to evaluate the simulations. Fig. 8 and Fig. 9 comprises the SOA mass measured in LEAK. As described in Gatzsche et al. (2017), the volume size distribution was measured with a scanning mobility particle sizer (SMPS), which is converted with an average density of 1 g cm^{-3} into the increase of organic mass (Mutzel et al., 2016).

Wall loss effects are not considered in the presented paper, due to the difficulties associating with modeling the size resolved wall loss for mixed organic and inorganic particles.
According to the reviewer's comment, the description of the LEAK chamber has been improved (Sect. 2.1) and the neglected wall losses have been mentioned (Sect. 3.5):

Section 2.1:
A detailed description of the LEAK chamber together with the available equipment can be found in Iinuma et al. (2009) and Mutzel et al. (2016). Briefly, LEAK is a cylindrical, 19 m^3 Teflon bag with a surface-to-volume ratio of 2 m^{-1}.

Section 3.5:
Wall loss effects are not considered in this study, due to the short experiment time (2 h). However, for longer experiment duration particle and gas wall loss might be an important process for chamber studies and have to be considered in modeling (Zhang et al., 2014).

Sect. 3.5. Why did you decide to use $k_c = 10^{-2}\,s^{-1}$ and $k_c = 10^{-3}\,s^{-1}$ and $D_{org} = 10^{-12}\,m^2\,s^{-1}$ and $D_{org} = 10^{-14}\,m^2\,s^{-1}$, respectively?

The authors decide to use $D_{org} = 10^{-12}\,m^2\,s^{-1}$ and $D_{org} = 10^{-14}\,m^2\,s^{-1}$ because previous studies (Koop et al., 2011; Renbaum-Wolff et al., 2013; Zhang et al., 2015; Grayson et al., 2016; Hosny et al., 2016) indicate that SOA particles have a higher viscosity than water droplets. The particle-phase reactivity is subject of the sensitivity studies and results from $k_c = 10^{-2}\,s^{-1}$ and $k_c = 10^{-3}\,s^{-1}$ have been chosen as reference simulations within this section.

Table S4. I am missing a unit on the pure liquid saturation vapor pressures of the HOM. I also think that you should mention that these molecules only represent the HOMs but that the HOMs is a family of many organic molecules presumably formed from autoxidation with a wide range of volatility. Can you justify why you decided to use these specific HOM molecules and specify how they are assumed to be formed? It is not either clear how these three different HOM are used in the model because in the gas-phase mechanism you only seem to have one HOM molecule.

The missing unit in Table S4 is atm. The table has been revised. These HOM molecules have been utilized because their structures have been presented by Berndt et al. (2016) and these compounds have been identified from laboratory measurements. The reaction pathway for the formation of HOMs is already described in Berndt et al. (2016). The average vapor pressure of these three compounds is utilized as an approximation for the vapor pressure in the gas-phase chemistry mechanism. Therefore, no individual products are represented in the model. The manuscript description has been extended in Sect. 3.2 as follows:

The HOM compounds are lumped to one compound group and added to the gas-phase chemistry mechanism (see Table S1, reactions 1b and 3b). As an estimate for the vapor pressure of this compound group, the average vapor pressure of the compounds listed in Table S4 from COSMO-RS have been taken.

Eq. 1. Is A_i representing a concentration of a species or is A_i a solute as stated on Line 17? In Eq. 2 C is used to represent concentrations.

Considering the reviewer's comment, the description in Sect. 2.2.2 has been changed as follows:

Thereby, the utilized parameters are the particle-phase concentration A_i of the solute i as a function of the radius r and the time t, the particle-phase bulk diffusion coefficient of the solute $D_{\mathrm{b},i}$, and the chemical reaction rate constant $k_{\mathrm{c},i}$ of the solute within the particle phase.

The title is a bit imprecise. Their exist many model studies of SOA formation from α-pinene ozonolysis. Can you make it more precise?

The title is specified:

Kinetic modeling studies of SOA formation from α-pinene ozonolysis

Referee #2
General comments
My biggest concern is how the authors justify their assumption that organic molecules must diffuse into the particle phase in order to contribute to particle growth. This assumption is crucial for all conclusions in this paper and finds too little scrutiny.

In general, the utilized kinetic approach supplies only two options for the organic compounds in the particle phase to change the equilibrium between the gas and the particle phase:

1. The organic molecules diffuse into the particle, thus at the particle surface the equilibrium between the gas and the particle phase is changed.
2. The organic molecules react in the particle phase to the corresponding r-product, which is treated as non-volatile and, therefore, the equilibrium between the gas and the particle phase is altered.

In Fig. 2a, the influence of the particle-phase bulk diffusion coefficient D_{b} and pseudo-first-order rate constant k_{c} on the steady state timescale is shown. Therewith, it can be shown that two different regimes exist for the sensitivity of the kinetic approach. For particle-phase bulk diffusion coefficients $D_{\mathrm{b}} \geq 10^{-15}\,\mathrm{m^2\,s^{-1}}$, the quasi-steady-state timescale is mainly sensitive to the value of the particle-phase bulk diffusion coefficient. In contrast, for particle-phase bulk diffusion coefficients $D_{\mathrm{b}} < 10^{-15}\,\mathrm{m^2\,s^{-1}}$ the quasi-steady-state timescale predominantly depends on the pseudo-first-order rate constant. Therefore, the particle-phase bulk diffusion coefficient and the pseudo-first-order rate constant strongly effect the SOA formation within this approach. To improve the explanation of this context in the paper, we revised the text as follows:

Modified/Added explanation to Sect. 3.1.1:
For values $D_{\mathrm{b}} < 10^{-16}\,\mathrm{m^2\,s^{-1}}$ the SOA formation is inhibited because the condensed organic material does not diffuse sufficiently into the particle bulk. According to the classification of Mai et al. (2015), this case is named particle-phase-diffusion-limited partitioning. After the formation of a thin organic shell/film around the particle, no effective SOA formation takes place because of the long mixing time inside the particle. Thus, the gas-phase concentrations of the condensing organic compounds as well as the interfacial transport of these compounds are not the limiting factors of SOA formation under these conditions.

In Sect. 2.2.2., which parts of these equations are necessary? Entrainment and outflow are not considered in this study and there is an argument for omitting it from the equations here. The authors have to add what M stands for here, is it the number of size-section? I see a term for partitioning

between aqueous and organic phases, how is this utilized in this manuscript? The manuscript never mentions phase-separation, so how does this play a role? From reading the manuscript, it is also not clear how the mass-transfer term works and when it is needed.

First of all, M is the number of size-sections. We included this in Sect. 2.2.2. of the revised version of the manuscript as follows:

Therein, $\overline{C}_{\mathrm{a},i,m}$ denotes the total average concentration of a solute i in size-section m, with M the number of size-sections.

Equation (6) and Eq. (8) summarizes the general model equations in the spectral model SPACCIM and offers the possibility to compare with previous publications using SPACCIM (Wolke et al., 2005; Rusumdar et al., 2016). The entrainment and outflow terms are included in both equations for the sake of completeness. As already indicated in the response to referee #1, the parcel model is not exclusively designed for simulation of aerosol chamber studies and additional text is provided in the revised manuscript.
At the current state, we treat the particle phase as one mixed phase without consideration of phase separation. Therefore, no partitioning term between the aqueous and the particle phase is considered. The aqueous phase transfer term (term II in Eq. (6) and Eq. (8)) describes the phase transfer between the gas and the aqueous phase with the Schwartz approach (Schwartz, 1986). According to the reviewer's comment, we changed it for the sake of clarity "aqueous phase transfer" to "gas-to-aqueous-phase mass transfer" in Eq. (6) and Eq. (8) in the revised manuscript.
The mass transfer term is already shortly described in the manuscript and a more detailed description is given in Wolke et al. (2005), which is referenced in the presented paper.

Regarding the sensitivity studies (Sect. 3.1), the authors must do a better job in highlighting that some of these simulations are probably far from reality. For example, Fig. 4c interestingly shows that omitting HOMs in the mechanism leads to an increase in SOA mass. However, the SOA mass yield is so low in these simulations that I strongly doubt their usefulness for real applications. The same argument can be made for Figs. 2b and 3b. These simulations show very different reaction regimes that might not be encountered in a simulation chamber experiment. While I find it interesting to show how a system reacts under strong perturbation, the questionable practicality must be indicated more clearly in the text.

The authors thank the reviewer for the interesting assessment concerning the simulation results with very low particle-phase bulk diffusion coefficients. Figs. 2b, 3b, and 4c display results for $D_{\mathrm{b}} = 10^{-18}\,\mathrm{m^2\,s^{-1}}$, which indicates higher viscous particles in the upper range of the semi-solid phase state. We included the figures in our paper to show that the low particle-phase bulk diffusion coefficient will impede SOA formation regardless of the settings of the remaining model parameters within this approach. This is contrary to the diffusion coefficients calculated from viscosity measurements indicating a semi-solid phase state of the SOA particles for a broad humidity range (Renbaum-Wolff et al., 2013; Zhang et al., 2015; Grayson et al., 2016). As the reviewer mentioned, the formed SOA mass for this low diffusion coefficients is not useful for real application in simulating chamber studies or for regional model studies with effective SOA formation. Therefore, we determined the particle-phase bulk diffusion coefficient as key parameter in our approach. According to the reviewer's comment, the text in the manuscript has been revised at different places highlighting that several simulations reflect extreme environmental conditions not prevalent in the simulated aerosol chamber study.

Modifications and additions to Sect. 3.1.2/Fig. 2b are given in the next paragraph.

Sect. 3.1.3/Fig. 3b
Therefore, the influence of the particle radius is higher for semi-solid particles. However, the formed SOA mass is rather small due to the limited diffusion into the particle and it should be kept in mind that this diffusion coefficient is limited to dry conditions.

Sect. 3.2/Fig. 4c
As indicated before, semi-solid aerosol particles might occur for a limited range of atmospheric conditions when the relative humidity decreases below 40 %. Therefore, the HOMs might affect SOA formation as seen in Fig. 4a and 4b, regardless of their reactivity in the particle phase.

In Sect. 3.1.2, I find it imperative to describe what the reason is that there is no particle growth at low diffusivities. I would suggest expanding on the description about what happens in the model, in words or figures.

According to the reviewer's comment, the explanation for the semi-solid particles is extended in Sect. 3.1.2 as follows:

For semi-solid particles, the kinetic approach is predominantly sensitive for particle-phase reactions as indicated in Zaveri et al. (2014). The particle-phase-diffusion-limited partitioning for the viscous aerosol particles has been step-wise raised due to the increased particle-phase reaction rate constant (see Fig. 2b). The mass enhancement factor is about 2.5 for a seven orders of magnitude higher reactivity. It is noted that organic aerosol particles might exhibit such low particle-phase diffusivities $D_b \leq 10^{-18}\,m^2\,s^{-1}$ mainly under dry conditions (RH $< 40\,\%$).

Section 3.3
I am not sure if I understand the purpose of Sect. 3.3. This section essentially looks at the effect of different equilibrium constants of the particle phase reaction, but it is presented as effect of different first-order reaction rates. I tend to think that an equilibrium constant is more straightforward here as the particle will most likely be in reactive equilibrium anyway. I find Fig. 5 very instructive and what happens in Fig. 6 is just that the share of r-products (orange bands) is reduced, is that correct? This is not a very exciting result given that all reaction rates are arbitrary guesses, or are the amounts of p-products and HOMs also affected? A normalized sensitivity coefficient of the mass of r-products and p-products to a reaction rate might be much more instructive. On a different note, would it be possible to connect these cases to real scenarios, e.g. by making more realistic assumptions of k_c and k_b for examples at high RH low RH?

Sect. 3.3. aims at the description of reversible particle-phase reactions. In the approach of Zaveri et al. (2014), only reactions in the particle phase are considered, which increase the particle mass due to the non-reversible reaction from "partitioning-products" (p-products) to "reacted-products" (r-products). In Sect. 3.1.2, it has been shown that the pseudo-first-order rate constant can be interpreted as an additional reactive uptake in the particle phase. An important detail of the kinetic approach of Zaveri et al. (2014), which might get not enough emphasis in the paper, is the distinction between two different model cases on the basis of the pseudo-first-order rate constant. For fast reactions ($k_c \geq 10^{-2}\,s^{-1}$), Eq. (2) is valid and for slow reactions ($k_c < 10^{-2}\,s^{-1}$), Eq. (3) is applied. The first difference between the two equations is the missing Q_i in Eq. (3), which is the steady state term given in the Appendix A in the presented paper. As indicated in Fig.2b, the quasi-steady-state term Q attains the value of 1 ($Q \to 1$) for the limiting case ($k_{c,i} \to 0$, $q \to 0$). The second difference is that due to the usage of the two-film theory for slow reactions an overall mass transfer coefficient

$K_{g,i}$ is defined (see Eq. (A10) in the presented paper and Zaveri et al., 2014):

$$\frac{1}{K_{g,i}} = \frac{1}{k_{g,i}} + \frac{1}{k_{p,i}} \left(\frac{C^*_{g,i}}{\sum_j \overline{A}_j} \right) . \tag{6}$$

Therefore, the choice of the pseudo-first-order rate constant influences, which regime is applied and, therefore, the partitioning equilibrium of the organic compounds. Due to the implementation of additional backward reactions, the approach of the two reaction regimes is preserved and the reaction system can be written as follows:

$$\text{p-product}_i \xrightarrow{k_c} \text{r-product}_i , \tag{7}$$

$$\text{r-product}_i \xrightarrow{k_b} \text{p-product}_i , \tag{8}$$

$$\text{p-product}_i \underset{k_b}{\overset{k_c}{\rightleftharpoons}} \text{r-product}_i . \tag{9}$$

The aging of the p-products is described by Eq. (7), the backward reaction is formulated in Eq. (8), and the net particle-phase reaction results in Eq. (9). The advantage of such a separate treatment of the production and reduction reaction of an equilibrium reaction is that the equilibrium state is adjusted over the time and is not instantaneously reached. A separate treatment of the dimerization reaction and the degradation of the dimers is also presented in Roldin et al. (2014) and an equilibrium of both reactions is reached after a distinct time. Nevertheless, the temporal evolution of dimers and monomers are solved with an own kinetic model in Roldin et al. (2014), whereby surface and bulk layers are separately handled. This approach demands a quite high computational effort inadequately for the subsequent application in a 3-D model. Further, measurements of particle-phase reactivity are scarce and the values for peroxyhemiactelas depend on acidity ranging from 2.3×10^{-25} to 3.2×10^{-23} molecules^{-1} cm^3 s^{-1} (Ziemann and Atkinson, 2012). As already mentioned above, the description of the particle phase reactivity modification in Sect. 3.3 is improved and the limitations of that approach are provided in an additional paragraph of Sect. 3.6.

Sect. 3.4
In this section, it is very hard to follow what exact calculations were performed. This leads to many open questions: What are the initial conditions for these experiments, especially x_{inorg} and x_{water}? What were the diffusivties D_{inorg} and D_{water}? On which humidity is the water concentration based? What is the hygroscopicity of these particles, how is it determined? Why is it safe to assume that organic and inorganic phases are mixed? Are we seeing an effect of D_{inorg} or an effect of D_{water} here? It would be interesting to see D_m plotted against humidity, following this framework. You could compare the humidity-dependence of your D_m for self-diffusion in SOA to the values of tracer diffusion determined in Berkemeier et al. (2014); Lienhard et al. (2015); Price et al. (2015) or Berkemeier et al. (2016).
It would be helpful if it were more explicitly explained what happens in the simulations. What does the time profile of D_m look like? I suppose it increases due to the smaller contribution of inorganics. On, p. 17, l. 33, the wording seems suboptimal. You write that using a constant bulk diffusion coefficient lowers the total SOA mass. Along the lines of the argumentation, this should be formulated the other way around: implementing a weighted particle-phase diffusion scheme increases total SOA mass. I have to wonder though, what of this effect is due to water and what is due to inorganics? It seems very clear to me that you would need to compare the diffusivity of the equilibrium SOA-water mixture and only add in the inorganics. Otherwise, you mainly make the argument that humidity leads to more SOA mass and not so much investigate the effects of a time-dependent diffusivity coefficient.

The simulation is initialized with inorganic seed particles (ammonium sulfate) with a particle radius of

$r_p = 35\,\text{nm}$. A relative humidity of 55 % leads in combination with the dissolved ammonium sulfate to the following mole fractions $x_{\text{inorg}} = 0.43$ and $x_{\text{water}} = 0.57$. The hygroscopicity is treated with the Köhler equation as described in Pruppacher and Klett (2010). For the self-diffusion coefficient of water, we utilize the relation proposed by Holz et al. (2000):

$$D_{\text{water}} = D_0[(T/T_S) - 1]^\gamma\,, \tag{10}$$

with:

$$\begin{aligned} D_0 &= (1.635 \times 10^{-8} \pm 2.242 \times 10^{-11})\,\text{m}^2\,\text{s}^{-1}\,, & (11)\\ T_S &= (215.05 \pm 1.20)\,\text{K}\,, & (12)\\ \gamma &= 2.063 \pm 0.051\,. & (13) \end{aligned}$$

This relation is valid between 0 and 100 °C and comprises an error limit of ≤1 %. The self diffusion coefficients of dissolved ions are tabulated in Cussler (2009), $D_{\text{NH}_4^+} = 1.96 \times 10^{-9}\,\text{m}^2\,\text{s}^{-1}$ and $D_{\text{SO}_4^{2-}} = 1.06 \times 10^{-9}\,\text{m}^2\,\text{s}^{-1}$. For seed particles containing water with dissolved ammonium sulfate ions, an initial weighted particle-phase bulk diffusion coefficient of $D_m = 1.78 \times 10^{-9}\,\text{m}^2\,\text{s}^{-1}$ is derived.
In the current SPACCIM version, no liquid-liquid phase separation of mixed organic-inorganic particles is considered to describe the coexistence of separate aqueous and organic phases. Therefore, this bulk approach is utilized to describe the particle as one mixed phase. To consider the additional effects of water and inorganics on partitioning, the simplified method of Zuend et al. (2010) might be implemented, which is also applicable for regional modeling.
Considering Eq. (10) of the presented paper, an effect of D_{org} can be seen because of the increase of x_{org} during the simulation.
The focus of the publications mentioned by the reviewer might not the same as that of the presented study. In the presented paper, a weighting rule for the three self-diffusion coefficients was applied to calculate a weighted particle-phase bulk diffusion coefficient D_m that replicates the effect of the increasing organic fraction in particles due to SOA formation. For the chamber experiments, the relative humidity was constant (55 %), which was also considered in the model and thus, the LWC is constant. To illustrate the temporal evolution of the weighted particle-phase bulk diffusion coefficient D_m depending on the SOA mass, an additional figure is provided in the revised manuscript (see Fig. 4). The authors decided to relate this additional figure to Sect. 3.5, where the weighted particle-phase bulk diffusion coefficient is applied to the chamber studies. The weighted particle-phase bulk diffusion coefficient D_m decreases because more organic material (characterized by a smaller self diffusion coefficient) is consumed (see Fig. 4). Therefore, an increase in organic mass results in a decrease of the weighted particle-phase bulk diffusion coefficient D_m.
According to the reviewer's comment, the description of the calculation of the weighted diffusion coefficient is expanded in the Supplement as follows and Fig. 4 as well as the interpretation of the new figure are added in Sect. 3.5:

Text added to Supplement:
All simulations are initialized with inorganic seed particles containing water and dissolved ammonium sulfate, with a particle radius of $r_p = 35\,\text{nm}$. A relative humidity of 55 % leads in combination with the dissolved ammonium sulfate to the following mole fractions $x_{\text{inorg}} = 0.43$ and $x_{\text{water}} = 0.57$. For the self-diffusion coefficient of water, we utilize the relation proposed by Holz et al. (2000):

$$D_{\text{water}} = D_0[(T/T_S) - 1]^\gamma\,, \tag{14}$$

with:

$$\begin{aligned} D_0 &= (1.635 \times 10^{-8} \pm 2.242 \times 10^{-11})\,\text{m}^2\,\text{s}^{-1}\,, & (15)\\ T_S &= (215.05 \pm 1.20)\,\text{K}\,, & (16)\\ \gamma &= 2.063 \pm 0.051\,. & (17) \end{aligned}$$

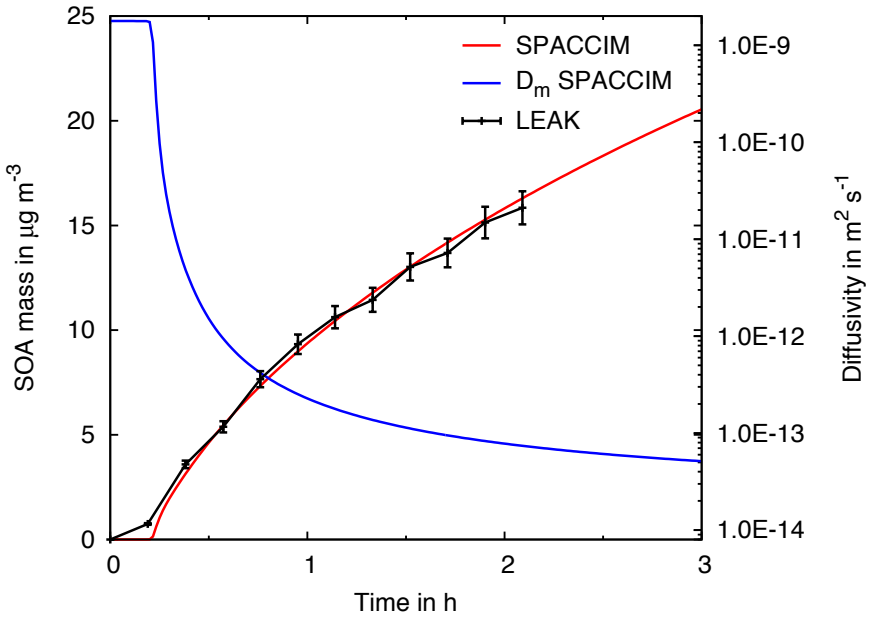

Figure 4: Simulated SOA mass as shown in Fig. 8b of Gatzsche et al. (2017) for $k_c = 10^{-2}\,s^{-1}$, $k_b = 10^{-2}\,s^{-1}$, under consideration of HOMs, and with the weighted diffusion coefficient utilizing $D_{org} = 10^{-14}\,m^2\,s^{-1}$ in comparison to the measured SOA mass from the LEAK experiment. The corresponding weighted particle-phase bulk diffusion coefficient D_m from the simulation is displayed on the secondary y-axis.

The self diffusion coefficients of dissolved ions are tabulated in Cussler (2009), $D_{NH_4^+} = 1.96 \times 10^{-9}\,m^2\,s^{-1}$ and $D_{SO_4^{2-}} = 1.06 \times 10^{-9}\,m^2\,s^{-1}$. For the aqueous ammonium sulfate seed particles an initial weighted particle-phase bulk diffusion coefficient of $D_m = 1.78 \times 10^{-9}\,m^2\,s^{-1}$ is derived. Due to the partitioning of organic compounds, the organic mole fraction x_{org} increases and D_{org} influences D_m. Since D_{org} is estimated to $D_{org} = 10^{-12}\,m^2\,s^{-1}$ or $D_{org} = 10^{-14}\,m^2\,s^{-1}$, the increase of the organic mole fraction causes a decrease of the weighted particle-phase bulk diffusion coefficient.

Sect. 3.5:
The high initial particle-phase bulk diffusion coefficient, $D_m \approx 2 \times 10^{-9}\,m^2\,s^{-1}$ (see Fig. 9), for the aqueous ammonium sulfate seed particles enables a fast diffusion in the aerosol particles. Thus, immediately partitioning HOMs can be absorbed quickly into the particle phase. Within the first 30 min of the simulation time, the SOA mass sharply increases and the weighted particle-phase bulk diffusion coefficient drops about three orders of magnitude. Consequently, the mixing time in the particle phase increases and this leads to a slower SOA mass formation. This process is depicted in Fig. 9, where for the first hour of simulation time the major changes in the weighted particle-phase bulk diffusion coefficient and the SOA mass can be seen. After the weighted particle-phase bulk diffusion coefficient has reduced to a value $D_m \approx 10^{-13}\,m^2\,s^{-1}$, the longer mixing time will cause a slower SOA formation as already shown in Fig. 1b. This effect is further pronounced due to continuous SOA formation and a concomitant decrease in particle-phase diffusion.

We agree with the reviewer's comment that the wording on, p. 17, l. 33 of the presented paper is suboptimal to describe the comparison between a constant and a weighted particle phase bulk diffusion coefficient and have thus reformulated this sentence as follows:

Fig. 7c reveals that the total SOA mass is increased by about 40 – 50 % for a weighted particle-phase bulk diffusion coefficient ($D_{org} = 10^{-14}\,m^2\,s^{-1}$) compared to simulation results with a constant

particle-phase bulk diffusion coefficient of $D_b = 10^{-14}\,m^2\,s^{-1}$. Additionally, the SOA formation is faster for the weighted particle-phase bulk diffusion coefficient.

Specific comments

p. 12, l. 27 – 28

"No initial organic mass OM_0 is utilized for the simulations with HOMs."
- This change seems arbitrary when first reading the article and gets only clear upon further reading. I wonder how the simulations would look like if no initial organic mass would be utilized for the simulations without HOMs? I find that would be much more instructive.

The partitioning approach requires initial organic mass in the aerosol phase (OM_0) according to Eq. (A7) in the presented manuscript. Therefore, a sufficient amount of organic mass is initialized to enable partitioning. For the simulations with HOMs, $\mathrm{OM}_0 \approx 2 \times 10^{-13}\,g\,m^{-3} = 2 \times 10^{-4}\,ng\,m^{-3}$ have been utilized, which is negligible. For the simulations without HOMs, $\mathrm{OM}_0 = 41.62\,ng\,m^{-3}$ have been initialized. When we initialize the simulations with considered HOMs with $\mathrm{OM}_0 = 41.62\,ng\,m^{-3}$, the rapid partitioning of HOMs quite fast exceeds the effect of the initial particulate organic mass and, therefore, we decided to initialize these simulations with the negligible amount of organic mass. According to the reviewer's comment, the information of the negligible particulate organic mass concentration is provided in Table 1 for case 6a and 6b and the indicated sentence is slightly modified in Sect. 3.2:

Almost no initial organic mass OM_0 is utilized for the simulations with HOMs.

p. 13, l. 2
"A rapid condensation of HOMs occurs due to their low vapor pressures (Fig. 4a)."
- How can this be seen in Fig. 4a? It seems not easy to see whether the solid lines take off sooner than the dashed lines. Is also does not appear as if the solid lines separate from the dashed lines within the early moments of the experiment/simulation, but rather over the first half of the experiment. Maybe referring to Fig. 5 would be helpful here if it is showing what you mean here?

We agree with the reviewer's comment that the fast condensation of the HOMs can not be seen so easily in (Fig. 4a). Therefore, we add Fig. 5 to the Supplement, which displays only the first half hour of the simulation time. Fig. 5 shows that for the first 13 minutes, the dashed red lines lay above the solid lines. However for the simulation with HOMs and $k_c = 1\,s^{-1}$ (see Fig. 5, indicated by the solid red line), the condensation of organic material begins at about 4 minutes. The SOA mass increases so fast that until 13 minutes is higher than for the simulation without HOMs. This behavior is described as a very rapid condensation.

p. 13, Fig. 3 - Since particle radius is reduced down to 11 nm, are Kelvin effects considered in this study? I don't see this mentioned in the manuscript.

Until now we have not considered the Kelvin effect because the correction of the vapor pressure due to the Kelvin term (see Eq. 2) might be smaller than the indicated error range (O'Meara et al., 2014; Kurtén et al., 2016) of the group contribution methods applied for the estimation of the vapor pressures of the partitioning compounds. A longer explanation for this assumption is already given in the response for reviewer #1 and we have added this information to a new section as indicated earlier.

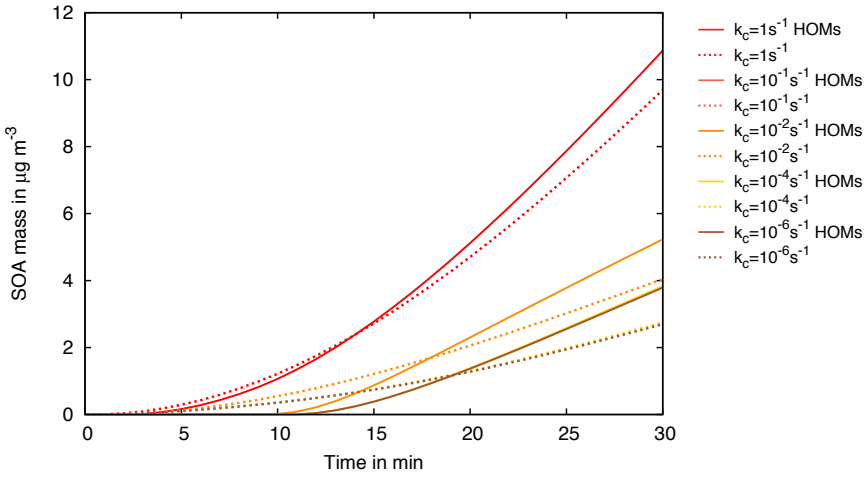

Figure 5: Simulated SOA mass including HOMs and additional variation of the pseudo-first-order rate constant of particle reactions k_c (case 6a and 6b of Table 1) for liquid ($D_b = 10^{-12}\,m^2\,s^{-1}$) aerosol particles as shown in Fig. 4a, but only for the first half hour of the simulation time.

p. 14, l. 5 – 7
"This may be the reason for the convergence of formed SOA mass for $k_c = 1\,s^{-1}$ combined with $D_b = 10^{-14}\,m^2\,s^{-1}$ and the overall more effective SOA formation without consideration of HOMs for semisolid particles ($D_b = 10^{-18}\,m^2\,s^{-1}$, Fig. 4c)."
- Would it be possible to give more explanation on this odd result of Fig. 4c? Should this be left out if not realistic?

Following the reviewer's comment, we modified the corresponding text and expanded the explanation to Fig. 4c as follows:

This may be the reason for the convergence of formed SOA mass for $k_c = 1\,s^{-1}$ combined with $D_b = 10^{-14}\,m^2\,s^{-1}$. For semi-solid particles ($D_b = 10^{-18}\,m^2\,s^{-1}$, Fig. 4c), the SOA formation without consideration of HOMs is more effective. This circumstance is caused by the missing particle-phase reactions for HOMs because the utilized kinetic approach is for $D_b < 10^{-15}\,m^2\,s^{-1}$ mainly sensitive to particle-phase reactions (Zaveri et al., 2014). Further, for semi-solid particles a particle-phase-diffusion-limited partitioning of HOMs occur with proceeding simulation time (Mai et al., 2015). Therefore, the equilibrium between the gas and the particle phase is quickly established for HOMs and their effect on the SOA mass differ from that for liquid particles.

p. 14, l. 10
"In general the HOMs provide about 27 % of the simulated final total SOA mass and introduce SOA mass formation."
- How does this compare to the molar yields in Berndt et al. (2016)? In addition, there is a comma missing after "in general".

The molar yields of Berndt et al. (2016) are determined in the gas-phase and in our study the 27 % are contained in the particle phase. The study of Berndt et al. (2016) aims not in measuring partitioning or particle-phase concentrations. Following the reviewer's comment, we added the comma after "in general" and changed "introduce" to "initiate":

"In general, the HOMs provide about 27 % of the simulated final total SOA mass and initiate SOA

mass formation."

p. 15, l. 8f
"The main benefit of the implementation of a sufficiently fast backward reaction ($k_b \leq 10^{-2}\,s^{-1}$) is the asymptotic curve shape of the SOA mass for proceeding simulation times. This behavior is also observed during chamber studies, which indicate an equilibrium state of the gas and the particle phase after a proceeding oxidation time."
- This reads interesting, but is difficult to understand without practical experience with smog chambers. Could this statement be explained in more detail and justified with examples?

This behavior is for example depicted in Fig. 1 of Ng et al. (2006) for α-pinene ozonolysis. After α-pinene is totally consumed, the maximum of organic mass is reached and remains constant thereafter. According to the reviewer's comment we have added this reference in the regarding sentence as follows:

The main benefit of the implementation of a sufficiently fast backward reaction ($k_\mathrm{b} \leq 10^{-2}\,\mathrm{s}^{-1}$) is the asymptotic curve shape of the SOA mass for proceeding simulation times. This behavior is also observed during chamber studies (Ng et al., 2006), which indicate an equilibrium state of the gas and the particle phase after a proceeding oxidation time and concomitant consumption of the hydrocarbon.

p. 18, l. 25
"Consideration of the weighted particle-phase bulk diffusion coefficient and HOMs lead to a faster SOA mass increase at the beginning of the simulation. The decreasing particle-phase bulk diffusion coefficient due to the uptake of further organic material and the backward reactions in the particle phase induce a flattening of the mass increase."
- Where can this be seen? Why should a weighted particle-phase diffusion coefficient generally speed up SOA formation?

This result can be seen in Fig. 8a in the period between $0.25-1.5\,\mathrm{h}$ of the simulation time. We did not generalize this result and for clarity we insert after "the beginning of the simulation": *"when the organic amount is low in the particle phase"*.

Consideration of the weighted particle-phase bulk diffusion coefficient and HOMs lead to a faster SOA mass increase at the beginning of the simulation when the organic amount is low in the particle phase.

p. 20, Figure 8
- In Fig. 8, it is very difficult to understand the simulation conditions of each plotted line. Am I correct that the dashed lines are showing the same results in both panels? This would be worthwhile pointing out! It would be easier to see if both panels would show the same range on the y-axis. It is also difficult to spot the line that fits the experimental data well in Fig. 8b, maybe draw these on top of the markers or highlight it in another way.

In the caption of Fig. 8 the following sentence refers to the two reference cases indicated by the dashed lines: *"For comparison, in both plots the results for a constant particle-phase bulk diffusion coefficient $D_b = 10^{-12}\,m^2\,s^{-1}$ combined with two different pseudo-first-order rate constants of particle reactions $k_c = 10^{-2}\,s^{-1}$ (ref. case I) and $k_c = 10^{-3}\,s^{-1}$ (ref. case II) are included (dashed lines)."*. As also indicated by the key, the two reference cases are the same for both figures and this is additionally

mentioned in the text of the paper: p. 18, l. 18/19.
For an improved depiction, we adjusted similar y-ranges for Fig. 8a and Fig. 8b and we increased the line width of the LEAK measurements according to the reviewer's comment (see Fig. 6).

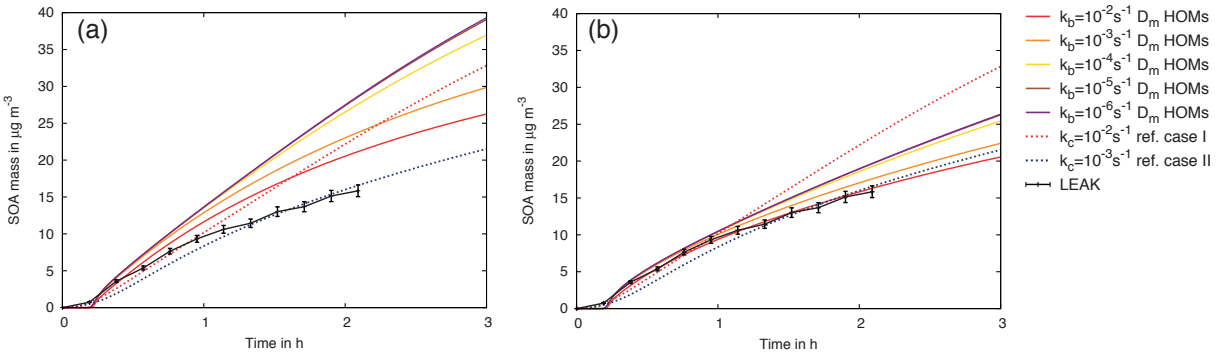

Figure 6: Simulated SOA mass considering an effective particle-phase bulk diffusion coefficient as well as HOMs, a constant pseudo-first-order rate constant of particle reactions $k_c = 10^{-2}\,s^{-1}$ and under additional variation of the chemical backward reaction rate constant of particle reactions k_b in comparison with aerosol chamber measurements from LEAK. a) Organic material is considered with a diffusion coefficient of $D_{org} = 10^{-12}\,m^2\,s^{-1}$ in the weighted diffusivity D_m (solid lines); b) Organic material is considered with a diffusion coefficient of $D_{org} = 10^{-14}\,m^2\,s^{-1}$ in the weighted diffusivity D_m (solid lines). For comparison, in both plots the results for a constant particle-phase bulk diffusion coefficient $D_b = 10^{-12}\,m^2\,s^{-1}$ combined with two different pseudo-first-order rate constants of particle reactions $k_c = 10^{-2}\,s^{-1}$ (ref. case I) and $k_c = 10^{-3}\,s^{-1}$ (ref. case II) are included (dashed lines).

p. 20, l. 4ff
"For the preferred model setup of Fig. 8b with $k_b = 10^{-2}\,s^{-1}$, the simulation is in a very good agreement with the measured concentration decrease of α-pinene (Fig. 10a)."
- Why does the α-pinene concentration depend on k_b?

The α-pinene concentration depends not on the value of k_b. We only would like to indicate with this wording that the corresponding gas-phase concentrations to this model case are displayed. According to the reviewer's comment, we improved the beginning of the paragraph describing the gas-phase concentration results as follows:

Corresponding gas-phase concentrations for the preferred model setup of Fig. 8b, with $k_b = 10^{-2}\,s^{-1}$, of the reactants α-pinene and ozone (see Fig. 10a and 10b) as well as a first reaction product named pinonaldehyde (Fig. 10c) have also been compared with smog chamber measurements. The simulation for the α-pinene depletion is in a very good agreement with the measured concentration decrease of α-pinene (Fig. 10a).

p. 21, l. 7
The depletion of ozone is slightly overestimated by the model after 1.5 hours (Fig. 10b). The measured gas-phase concentration of pinonaldehyde is underestimated by the model (Fig. 10c)."
- Do you have ideas what could be the underlying reasons here? This would add much more to the manuscript than just plotting results.

The formation of pinonaldehyde was measured by a proton-transfer-reaction mass spectrometer (PTR-

MS) at m/z 169 ($[M+H]^+$). The PTR-MS technique enables only the detection of the m/z ratio. No further information were obtained. Thus, compounds or fragments with the same m/z were detected as well resulting in an overestimation of the pinonaldehyde concentration measured by PTR-MS. This circumstance can cause the underestimation of the gas-phase concentration of pinonaldehyde (see Fig. 10c of the presented paper).
Ozone is measured with an ozone monitor (49c Ozone Analyzer, Thermo Scientific, USA) and this device is based on measuring absorption on characteristic wavelengths. For measuring ozone, the absorption at 254 nm is utilized. According to Docherty et al. (2005), the ozonolysis of α-pinene yields up to 47 % organic peroxides. As organic peroxides absorb light at 254 nm, an overestimation of the signal detected by the ozone monitor caused by the high amount of organic peroxides cannot be excluded. Therefore, with the increase of the hydroperoxide concentration over the experiment time the overestimation of the ozone concentration by the monitoring system might increase and the underestimation by the model can be caused. According to the reviewer's suggestion, we included this information in the interpretation of the results of Sect. 3.5 as follows:

The depletion of ozone is slightly overestimated by the model (see Fig. 10b). After half an hour, the measured ozone concentration decreases not so fast as initially started. Experimentally, ozone is measured with an ozone monitor (49c Ozone Analyzer, Thermo Scientific, USA) and this device is based on measuring absorption on characteristic wavelengths. For measuring ozone, the absorption at 254 nm is utilized. According to Docherty et al. (2005), the ozonolysis of α-pinene yields up to 47 % organic peroxides. As organic peroxides absorb light at 254 nm, an overestimation of the signal detected by the ozone monitor caused by the high amount of organic peroxides cannot be excluded. Therefore, with the increase of the hydroperoxide concentration over the experiment time the overestimation of the ozone concentration by the monitoring system might increase and the underestimation by the model can be caused. Further, the measured gas-phase concentration of pinonaldehyde is underestimated by the model (Fig. 10c). This cannot be caused by an excessive partitioning of pinonaldehyde into the particle phase because pinonaldehyde is characterized by a high saturation vapor pressure and there is no effective partitioning into the particle phase. However, the formation of pinonaldehyde is measured by a proton-transfer-reaction mass spectrometer (PTR-MS) at m/z 169 ($[M+H]^+$). The PTR-MS technique enables only the detection of the m/z ratio. No further information were obtained. Thus, compounds or fragments with the same m/z were detected as well resulting in an overestimation of the pinonaldehyde concentration measured by PTR-MS. This circumstance can cause the underestimation of the gas-phase concentration of pinonaldehyde (see Fig. 10c). To investigate the underestimation of pinonaldehyde concentration additionally from the site of the model, we evaluated the branching ratios of the α-pinene with ozone reaction. Based on the results of Berndt et al. (2003), the pinonaldehyde yield was artificially increased in the mechanism to investigate the sensitivity of the pinonaldehyde on this yield.

Technical comments

Figure 6 caption

"... both combined with different fast chemical backward reactions k_b."
- This sentence is difficult to understand in general and might deserve revision, but I believe what you mean here is "differently".

Caption changed to:

Simulated SOA mass including a chemical backward reaction in the particle phase for liquid (D_b =

$10^{-12}\,m^2\,s^{-1}$) aerosol particles (case 7 of Table 1) with a) a fast chemical reaction in the particle phase k_c=1 s^{-1} and b) a reduced rate constant k_c=$10^{-2}\,s^{-1}$, whereby backward reactions with different rate constants k_b are additionally included.

"The reference simulations for the regarding k_c and no k_b are shown with dashed lines."
- Do you mean "respective" instead of "regarding"? Do you mean "without backward reaction" instead of "no k_b"?

Caption changed to:

The reference simulations for the respective k_c without backward reactions (indicated by "no k_b" in the key) are shown with dashed lines.

p. 18, l. 33ff
"After 1 h simulation time, it is obvious that the simulated concentration profile agree well with the experimentally observed SOA mass with a backward reaction rate constant of k_b=$10^{-2}\,s^{-1}$."
- Do the authors mean:
"After 1 h simulation time, it is obvious that the simulated concentration profile agrees well with the experimentally observed SOA mass when using a backward reaction rate constant of k_b=$10^{-2}\,s^{-1}$."

Sentence changed to:

After 1 h simulation time, it is obvious that the simulated concentration profile agrees well with the experimentally observed SOA mass when using a backward reaction rate constant of k_b=$10^{-2}\,s^{-1}$.

Figure S5b
- This figure is not discussed in the manuscript.

Sentence added:
For semi-solid particles and moderate particle reactions, the same trend is observed but only very low SOA concentrations are formed (see Fig S5b in the Supplement). Due to the particle-phase-diffusion-limited partitioning for semi-solid particles combined with only moderate particle-phase rate constants, the formed SOA mass reaches quite small values, which are not observed under typical chamber study experiment conditions.

References

Abramson, E., Imre, D., Beranek, J., Wilson, J., and Zelenyuk, A.: Experimental determination of chemical diffusion within secondary organic aerosol particles, Phys. Chem. Chem. Phys., 15, 2983–2991, doi:10.1039/c2cp44013j, 2013.

Antonovskii, V. L. and Terent'ev, V. A.: Effect of the Structure of Hydroperoxides and Some Aldehydes on the Kinetics of the Noncatalytic Formation of α-Hydroxy Peroxides, Zhurnal Organicheskoi Khimii, 3, 1011–1015, 1967.

Barsanti, K. C. and Pankow, J. F.: Thermodynamics of the formation of atmospheric organic particulate matter by accretion reactions-Part 1: aldehydes and ketones, Atmospheric Environment, 38, 4371–4382, doi:10.1016/j.atmosenv.2004.03.035, 2004.

Barsanti, K. C. and Pankow, J. F.: Thermodynamics of the formation of atmospheric organic particulate matter by accretion reactions-2. Dialdehydes, methylglyoxal, and diketones, Atmospheric Environment, 39, 6597–6607, doi:10.1016/j.atmosenv.2005.07.056, 2005.

Barsanti, K. C. and Pankow, J. F.: Thermodynamics of the formation of atmospheric organic particulate matter by accretion reactions-Part 3: Carboxylic and dicarboxylic acids, Atmospheric Environment, 40, 6676–6686, doi:10.1016/j.atmosenv.2006.03.013, 2006.

Berkemeier, T., Shiraiwa, M., Pöschl, U., and Koop, T.: Competition between water uptake and ice nucleation by glassy organic aerosol particles, Atmospheric Chemistry and Physics, 14, 12 513–12 531, doi:10.5194/acp-14-12513-2014, 2014.

Berkemeier, T., Steimer, S., Krieger, U., Peter, T., Pöschl, U., Ammann, M., and Shiraiwa, M.: Ozone uptake on glassy, semi-solid and liquid organic matter and the role of reactive oxygen intermediates in atmospheric aerosol chemistry, Phys. Chem. Chem. Phys., 18, 12 662–12 674, doi:10.1039/C6CP00634E, 2016.

Berndt, T., Böge, O., and Stratmann, F.: Gas-phase ozonolysis of α-pinene: gaseous products and particle formation, Atmospheric Environment, 37, 3933–3945, doi:10.1016/S1352-2310(03)00501-6, 2003.

Berndt, T., Richters, S., Jokinen, T., Hyttinen, N., Kurtén, T., Otkjær, R. V., Kjaergaard, H. G., Stratmann, F., Herrmann, H., Sipilä, M., Kulmala, M., and Ehn, M.: Hydroxyl radical-induced formation of highly oxidized organic compounds, Nature Communications, 7, doi:10.1038/ncomms13677, 2016.

Butt, H.-J., Graf, K., and Kappl, M.: Physics and Chemistry of Interfaces, Wiley-VCH Verlag GmbH & Co. KGaA, doi:10.1002/3527602313, 2004.

Camredon, M., Hamilton, J. F., Alam, M. S., Wyche, K. P., Carr, T., White, I. R., Monks, P. S., Rickard, A. R., and Bloss, W. J.: Distribution of gaseous and particulate organic composition during dark α-pinene ozonolysis, Atmospheric Chemistry and Physics, 10, 2893–2917, doi:10.5194/acp-10-2893-2010, 2010.

Carey, F. and Sundberg, R.: Advanced Organic Chemistry, Part A. Structure and Mechanisms, 5th Edition, Springer US, doi:10.1007/978-0-387-44899-2, 2007.

Casale, M. T., Richman, A. R., Elrod, M. J., Garland, R. M., Beaver, M. R., and Tolbert, M. A.: Kinetics of acid-catalyzed aldol condensation reactions of aliphatic aldehydes, Atmospheric Environment, 41, 6212–6224, doi:10.1016/j.atmosenv.2007.04.002, 2007.

Compernolle, S., Ceulemans, K., and Müller, J.-F.: EVAPORATION: a new vapour pressure estimation method for organic molecules including non-additivity and intramolecular interactions, Atmospheric Chemistry and Physics, 11, 9431 – 9450, doi:10.5194/acp-11-9431-2011, 2011.

Cussler, E. L.: Diffusion: mass transfer in fluid systems, 3rd Edition, Cambridge University Press, doi:10.1017/cbo9780511805134, 2009.

DePalma, J. W., Horan, A. J., Hall IV, W. A., and Johnston, M. V.: Thermodynamics of oligomer formation: implications for secondary organic aerosol formation and reactivity, Phys. Chem. Chem. Phys., 15, 6935 – 6944, doi:10.1039/C3CP44586K, 2013.

Docherty, K. S., Wu, W., Lim, Y. B., and Ziemann, P. J.: Contributions of Organic Peroxides to Secondary Aerosol Formed from Reactions of Monoterpenes with O_3, Environmental Science & Technology, 39, 4049 – 4059, doi:10.1021/es050228s, 2005.

Donahue, N. M., Kroll, J. H., Pandis, S. N., and Robinson, A. L.: A two-dimensional volatility basis set – Part 2: Diagnostics of organic-aerosol evolution, Atmospheric Chemistry and Physics, 12, 615 – 634, doi:10.5194/acp-12-615-2012, 2012.

Donahue, N. M., Ortega, I. K., Chuang, W., Riipinen, I., Riccobono, F., Schobesberger, S., Dommen, J., Baltensperger, U., Kulmala, M., Worsnop, D. R., and Vehkamaki, H.: How do organic vapors contribute to new-particle formation?, Faraday Discussions, 165, 91 – 104, doi: 10.1039/C3FD00046J, 2013.

Eckert, F. and Klamt, A.: Fast solvent screening via quantum chemistry: COSMO-RS approach, AIChE Journal, 48, doi:10.1002/aic.690480220, 2002.

Ehn, M., Kleist, E., Junninen, H., Petäjä, T., Lönn, G., Schobesberger, S., Dal Maso, M., Trimborn, A., Kulmala, M., Worsnop, D. R., Wahner, A., Wildt, J., and Mentel, T. F.: Gas phase formation of extremely oxidized pinene reaction products in chamber and ambient air, Atmospheric Chemistry and Physics, 12, 5113 – 5127, doi:10.5194/acp-12-5113-2012, 2012.

Ehn, M., Thornton, J. a., Kleist, E., Sipilä, M., Junninen, H., Pullinen, I., Springer, M., Rubach, F., Tillmann, R., Lee, B., Lopez-Hilfiker, F., Andres, S., Acir, I.-H., Rissanen, M., Jokinen, T., Schobesberger, S., Kangasluoma, J., Kontkanen, J., Nieminen, T., Kurtén, T., Nielsen, L. B., Jørgensen, S., Kjaergaard, H. G., Canagaratna, M., Maso, M. D., Berndt, T., Petäjä, T., Wahner, A., Kerminen, V.-M., Kulmala, M., Worsnop, D. R., Wildt, J., and Mentel, T. F.: A large source of low-volatility secondary organic aerosol, Nature, 506, 476 – 9, doi:10.1038/nature13032, 2014.

Ervens, B., Feingold, G., Clegg, S. L., and Kreidenweis, S. M.: A modeling study of aqueous production of dicarboxylic acids: 2. Implications for cloud microphysics, Journal of Geophysical Research: Atmospheres, 109, doi:10.1029/2004JD004575, 2004.

Ervens, B., Feingold, G., and Kreidenweis, S. M.: Influence of water-soluble organic carbon on cloud drop number concentration, Journal of Geophysical Research: Atmospheres, 110, doi: 10.1029/2004JD005634, 2005.

Facchini, M. C., Mircea, M., Fuzzi, S., and Charlson, R. J.: Cloud albedo enhancement by surface-active organic solutes in growing droplets, Nature, 40, 257 – 259, doi:10.1038/45758, 1999.

Gao, S., Keywood, M., Ng, N. L., Surratt, J., Varutbangkul, V., Bahreini, R., Flagan, R. C., and Seinfeld, J. H.: Low-Molecular-Weight and Oligomeric Components in Secondary Organic Aerosol from the Ozonolysis of Cycloalkenes and α-Pinene, The Journal of Physical Chemistry A, 108, 10 147 – 10 164, doi:10.1021/jp047466e, 2004a.

Gao, S., Ng, N. L., Keywood, M., Varutbangkul, V., Bahreini, R., Nenes, A., He, J., Yoo, K. Y., Beauchamp, J. L., Hodyss, R. P., Flagan, R. C., and Seinfeld, J. H.: Particle Phase Acidity and Oligomer Formation in Secondary Organic Aerosol, Environmental Science & Technology, 38, 6582 – 6589, doi:10.1021/es049125k, 2004b.

Gatzsche, K., Iinuma, Y., Tilgner, A., Mutzel, A., Berndt, T., and Wolke, R.: Modeling studies of SOA formation from α-pinene ozonolysis, Atmospheric Chemistry and Physics Discussions, 2017, 1 – 33, doi:10.5194/acp-2017-275, 2017.

Grayson, J. W., Zhang, Y., Mutzel, A., Renbaum-Wolff, L., Böge, O., Kamal, S., Herrmann, H., Martin, S. T., and Bertram, A. K.: Effect of varying experimental conditions on the viscosity of α-pinene derived secondary organic material, Atmospheric Chemistry and Physics, 16, 6027 – 6040, doi:10.5194/acp-16-6027-2016, 2016.

Hall IV, W. and Johnston, M.: Oligomer Content of α-Pinene Secondary Organic Aerosol, Aerosol Science and Technology, 45, 37 – 45, doi:10.1080/02786826.2010.517580, 2011.

Hallquist, M., Wenger, J. C., Baltensperger, U., Rudich, Y., Simpson, D., Claeys, M., Dommen, J., Donahue, N. M., George, C., Goldstein, A. H., Hamilton, J. F., Herrmann, H., Hoffmann, T., Iinuma, Y., Jang, M., Jenkin, M. E., Jimenez, J. L., Kiendler-Scharr, A., Maenhaut, W., McFiggans, G., Mentel, T. F., Monod, A., Prévôt, A. S. H., Seinfeld, J. H., Surratt, J. D., Szmigielski, R., and Wildt, J.: The formation, properties and impact of secondary organic aerosol: current and emerging issues, Atmospheric Chemistry and Physics, 9, 5155 – 5236, doi:10.5194/acp-9-5155-2009, 2009.

Hitzenberger, R., Berner, A., Kasper-Giebl, A., Löflund, M., and Puxbaum, H.: Surface tension of Rax cloud water and its relation to the concentration of organic material, Journal of Geophysical Research: Atmospheres, 107, AAC 5–1 – AAC 5–6, doi:10.1029/2002JD002506, 2002.

Hoffmann, E., Tilgner, A., Schrödner, R., Bräuer, P., Wolke, R., and Herrmann, H.: An advanced modeling study on the impacts and atmospheric implications of multiphase dimethyl sulfide chemistry, Proceedings of the National Academy of Sciences, 113, 11 776 – 11 781, doi:10.1073/pnas.1606320113, 2016.

Holz, M., Heil, S. R., and Sacco, A.: Temperature-dependent self-diffusion coefficients of water and six selected molecular liquids for calibration in accurate 1H NMR PFG measurements, Physical Chemistry Chemical Physics, 2, 4740 – 4742, doi:10.1039/B005319H, 2000.

Hosny, N. A., Fitzgerald, C., Vyšniauskas, A., Athanasiadis, A., Berkemeier, T., Uygur, N., Pöschl, U., Shiraiwa, M., Kalberer, M., Pope, F. D., and Kuimova, M. K.: Direct imaging of changes in aerosol particle viscosity upon hydration and chemical aging, Chemical Science, 7, 1357 – 1367, doi:10.1039/c5sc02959g, 2016.

Iinuma, Y., Böge, O., Gnauk, T., and Herrmann, H.: Aerosol-chamber study of the α-pinene/O_3 reaction: influence of particle acidity on aerosol yields and products, Atmospheric Environment, 38, 761 – 773, doi:10.1016/j.atmosenv.2003.10.015, 2004.

Iinuma, Y., Böge, O., Kahnt, A., and Herrmann, H.: Laboratory chamber studies on the formation of organosulfates from reactive uptake of monoterpene oxides, Physical Chemistry Chemical Physics, 11, 7985 – 7997, doi:10.1039/B904025K, 2009.

Jang, M., Czoschke, N. M., Lee, S., and Kamens, R. M.: Heterogeneous Atmospheric Aerosol Production by Acid-Catalyzed Particle-Phase Reactions, Science, 298, 814 – 817, doi:10.1126/science.1075798, 2002.

Jang, M., Carroll, B., Chandramouli, B., and Kamens, R. M.: Particle Growth by Acid-Catalyzed Heterogeneous Reactions of Organic Carbonyls on Preexisting Aerosols, Environmental Science & Technology, 37, 3828 – 3837, doi:10.1021/es021005u, 2003.

Jasper, J. J.: The Surface Tension of Pure Liquid Compounds, Journal of Physical and Chemical Reference Data, 1, 841 – 1010, doi:10.1063/1.3253106, 1972.

Jokinen, T., Sipilä, M., Richters, S., Kerminen, V.-M., Paasonen, P., Stratmann, F., Worsnop, D., Kulmala, M., Ehn, M., Herrmann, H., and Berndt, T.: Rapid Autoxidation Forms Highly Oxidized RO_2 Radicals in the Atmosphere, Angewandte Chemie International Edition, 53, 14 596 – 14 600, doi:10.1002/anie.201408566, 2014.

Kalberer, M., Paulsen, D., Sax, M., Steinbacher, M., Dommen, J., Prevot, A. S. H., Fisseha, R., Weingartner, E., Frankevich, V., Zenobi, R., and Baltensperger, U.: Identification of Polymers as Major Components of Atmospheric Organic Aerosols, Science, 303, 1659 – 1662, doi:10.1126/science.1092185, 2004.

Kidd, C., Perraud, V., Wingen, L. M., and Finlayson-Pitts, B. J.: Integrating phase and composition of secondary organic aerosol from the ozonolysis of α-pinene, Proceedings of the National Academy of Sciences, 111, 7552 – 7557, doi:10.1073/pnas.1322558111, 2014.

Koop, T., Bookhold, J., Shiraiwa, M., and Pöschl, U.: Glass transition and phase state of organic compounds: dependency on molecular properties and implications for secondary organic aerosols in the atmosphere, Phys. Chem. Chem. Phys., 13, 19 238 – 19 255, doi:10.1039/c1cp22617g, 2011.

Kulmala, M., Toivonen, A., Mäkelä, J., and Laaksonen, A.: Analysis of the growth of nucleation mode particles observed in Boreal forest, Tellus B, 50, doi:10.3402/tellusb.v50i5.16229, 1998.

Kurtén, T., Tiusanen, K., Roldin, P., Rissanen, M., Luy, J., Boy, M., Ehn, M., and Donahue, N.: α-Pinene Autoxidation Products May Not Have Extremely Low Saturation Vapor Pressures Despite High O:C Ratios, The Journal of Physical Chemistry A, 120, 2569 – 2582, doi:10.1021/acs.jpca.6b02196, 2016.

Lienhard, D. M., Huisman, A. J., Bones, D. L., Te, Y.-F., Luo, B. P., Krieger, U. K., and Reid, J. P.: Retrieving the translational diffusion coefficient of water from experiments on single levitated aerosol droplets, Physical Chemistry Chemical Physics, 16, 16 677 – 16 683, doi:10.1039/C4CP01939C, 2014.

Lienhard, D. M., Huisman, A. J., Krieger, U. K., Rudich, Y., Marcolli, C., Luo, B. P., Bones, D. L., Reid, J. P., Lambe, A. T., Canagaratna, M. R., Davidovits, P., Onasch, T. B., Worsnop, D. R., Steimer, S. S., Koop, T., and Peter, T.: Viscous organic aerosol particles in the upper troposphere: diffusivity-controlled water uptake and ice nucleation?, Atmospheric Chemistry and Physics, 15, 13 599 – 13 613, doi:10.5194/acp-15-13599-2015, 2015.

Mai, H., Shiraiwa, M., Flagan, R. C., and Seinfeld, J. H.: Under What Conditions Can Equilibrium Gas-Particle Partitioning Be Expected to Hold in the Atmosphere?, Environmental Science & Technology, 49, 11 485 – 11 491, doi:10.1021/acs.est.5b02587, 2015.

Mentel, T. F., Springer, M., Ehn, M., Kleist, E., Pullinen, I., Kurtén, T., Rissanen, M., Wahner, A., and Wildt, J.: Formation of highly oxidized multifunctional compounds: autoxidation of peroxy radicals formed in the ozonolysis of alkenes - deduced from structure-product relationships, Atmospheric Chemistry and Physics, 15, 6745 – 6765, doi:10.5194/acp-15-6745-2015, 2015.

Mutzel, A., Poulain, L., Berndt, T., Iinuma, Y., Rodigast, M., Böge, O., Richters, S., Spindler, G., Sipilä, M., Jokinen, T., Kulmala, M., and Herrmann, H.: Highly Oxidized Multifunctional Organic Compounds Observed in Tropospheric Particles: A Field and Laboratory Study, Environmental Science & Technology, 49, 7754 – 7761, doi:10.1021/acs.est.5b00885, 2015.

Mutzel, A., Rodigast, M., Iinuma, Y., Böge, O., and Herrmann, H.: Monoterpene SOA – Contribution of first-generation oxidation products to formation and chemical composition, Atmospheric Environment, 130, 136 – 144, doi:10.1016/j.atmosenv.2015.10.080, 2016.

Ng, N., Kroll, J., Keywood, M., Bahreini, R., Varutbangkul, V., Flagan, R., Seinfeld, J., Lee, A., and Goldstein, A.: Contribution of First- versus Second-Generation Products to Secondary Organic Aerosols Formed in the Oxidation of Biogenic Hydrocarbons, Environmental Science & Technology, 40, 2283 – 2297, doi:10.1021/es052269u, 2006.

O'Meara, S., Booth, A. M., Barley, M. H., Topping, D., and McFiggans, G.: An assessment of vapour pressure estimation methods, Phys. Chem. Chem. Phys., 16, 19 453 – 19 469, doi:10.1039/C4CP00857J, 2014.

O'Meara, S., Topping, D. O., and McFiggans, G.: The rate of equilibration of viscous aerosol particles, Atmospheric Chemistry and Physics, 16, 5299 – 5313, doi:10.5194/acp-16-5299-2016, 2016.

O'Meara, S., Topping, D. O., Zaveri, R. A., and McFiggans, G.: An efficient approach for treating composition-dependent diffusion within organic particles, Atmospheric Chemistry and Physics Discussions, 2017, 1 – 25, doi:10.5194/acp-2016-1052, 2017.

Pajunoja, A., Malila, J., Hao, L., Joutsensaari, J., Lehtinen, K. E. J., and Virtanen, A.: Estimating the Viscosity Range of SOA Particles Based on Their Coalescence Time, Aerosol Science and Technology, 48, i – iv, doi:10.1080/02786826.2013.870325, 2014.

Pankow, J. F.: An absorption model of the gas/aerosol partitioning involved in the formation of secondary organic aerosol, Atmospheric Environment, 28, 189 – 193, doi:10.1016/1352-2310(94)90094-9, 1994.

Pöschl, U., Rudich, Y., and Ammann, M.: Kinetic model framework for aerosol and cloud surface chemistry and gas-particle interactions – Part 1: General equations, parameters, and terminology, Atmospheric Chemistry and Physics, 7, 5989 – 6023, doi:10.5194/acp-7-5989-2007, 2007.

Price, H. C., Mattsson, J., Zhang, Y., Bertram, A. K., Davies, J. F., Grayson, J. W., Martin, S. T., O'Sullivan, D., Reid, J. P., Rickards, A. M. J., and Murray, B. J.: Water diffusion in atmospherically relevant α-pinene secondary organic material, Chemical Science, 6, 4876 – 4883, doi:10.1039/C5SC00685F, 2015.

Pruppacher, H. and Klett, J.: Microphysics of Clouds and Precipitation, 2nd Edition, Springer Netherlands, doi:10.1007/978-0-306-48100-0, 2010.

Renbaum-Wolff, L., Grayson, J. W., Bateman, A. P., Kuwata, M., Sellier, M., Murray, B. J., Shilling, J. E., Martin, S. T., and Bertram, A. K.: Viscosity of α-pinene secondary organic material and implications for particle growth and reactivity, Proceedings of the National Academy of Sciences, 110, 8014 – 8019, doi:10.1073/pnas.1219548110, 2013.

Riipinen, I., Pierce, J. R., Donahue, N. M., and Pandis, S. N.: Equilibration time scales of organic aerosol inside thermodenuders: Evaporation kinetics versus thermodynamics, Atmospheric Environment, 44, 597 – 607, doi:10.1016/j.atmosenv.2009.11.022, 2010.

Riipinen, I., Yli-Juuti, T., Pierce, J. R., Petaja, T., Worsnop, D. R., Kulmala, M., and Donahue, N. M.: The contribution of organics to atmospheric nanoparticle growth, Nature Geosciences, 5, doi:10.1038/ngeo1499, 2012.

Roldin, P., Eriksson, A. C., Nordin, E. Z., Hermansson, E., Mogensen, D., Rusanen, A., Boy, M., Swietlicki, E., Svenningsson, B., Zelenyuk, A., and Pagels, J.: Modelling non-equilibrium secondary

organic aerosol formation and evaporation with the aerosol dynamics, gas- and particle-phase chemistry kinetic multilayer model ADCHAM, Atmospheric Chemistry and Physics, 14, 7953 – 7993, doi:10.5194/acp-14-7953-2014, 2014.

Rusumdar, A. J., Wolke, R., Tilgner, A., and Herrmann, H.: Treatment of non-ideality in the SPACCIM multiphase model – Part 1: Model development, Geoscientific Model Development, 9, 247 – 281, doi:10.5194/gmd-9-247-2016, 2016.

Schwartz, S. E.: Mass-Transport Considerations Pertinent to Aqueous Phase Reactions of Gases in Liquid-Water Clouds, pp. 415 – 471, Springer Berlin Heidelberg, Berlin, Heidelberg, doi:10.1007/978-3-642-70627-1_16, 1986.

Seinfeld, J. H. and Pandis, S. N.: Atmospheric Chemistry and Physics: from Air Pollution to Climate Change, 2nd Edition, John Wiley, New York, doi:10.1029/2007JD009735, 2006.

Shiraiwa, M., Pfrang, C., and Pöschl, U.: Kinetic multi-layer model of aerosol surface and bulk chemistry (KM-SUB): the influence of interfacial transport and bulk diffusion on the oxidation of oleic acid by ozone, Atmospheric Chemistry and Physics, 10, 3673 – 3691, doi:10.5194/acp-10-3673-2010, 2010.

Shiraiwa, M., Pfrang, C., Koop, T., and Pöschl, U.: Kinetic multi-layer model of gas-particle interactions in aerosols and clouds (KM-GAP): linking condensation, evaporation and chemical reactions of organics, oxidants and water, Atmospheric Chemistry and Physics, 12, 2777 – 2794, doi:10.5194/acp-12-2777-2012, 2012.

Shiraiwa, M., Zuend, A., Bertram, A. K., and Seinfeld, J. H.: Gas-particle partitioning of atmospheric aerosols: interplay of physical state, non-ideal mixing and morphology, Phys. Chem. Chem. Phys., 15, 11 441 – 11 453, doi:10.1039/C3CP51595H, 2013.

Shulman, M. L., Jacobson, M. C., Carlson, R. J., Synovec, R. E., and Young, T. E.: Dissolution behavior and surface tension effects of organic compounds in nucleating cloud droplets, Geophysical Research Letters, 23, 277 – 280, doi:10.1029/95GL03810, 1996.

Surratt, J. D., Murphy, S. M., Kroll, J. H., Ng, N. L., Hildebrandt, L., Sorooshian, A., Szmigielski, R., Vermeylen, R., Maenhaut, W., Claeys, M., Flagan, R. C., and Seinfeld, J. H.: Chemical Composition of Secondary Organic Aerosol Formed from the Photooxidation of Isoprene, The Journal of Physical Chemistry A, 110, 9665 – 9690, doi:10.1021/jp061734m, 2006.

Tilgner, A., Bräuer, P., Wolke, R., and Herrmann, H.: Modelling multiphase chemistry in deliquescent aerosols and clouds using CAPRAM3.0i, Journal of Atmospheric Chemistry, 70, 221 – 256, doi:10.1007/s10874-013-9267-4, 2013.

Tobias, H. and Ziemann, P.: Thermal Desorption Mass Spectrometric Analysis of Organic Aerosol Formed from Reactions of 1-Tetradecene and O_3 in the Presence of Alcohols and Carboxylic Acids, Environmental Science & Technology, 34, 2105 – 2115, doi:10.1021/es9907156, 2000.

Tolocka, M. P., Jang, M., Ginter, J. M., Cox, F. J., Kamens, R. M., and Johnston, M. V.: Formation of Oligomers in Secondary Organic Aerosol, Environmental Science & Technology, 38, 1428 – 1434, doi:10.1021/es035030r, 2004.

Trump, E. R. and Donahue, N. M.: Oligomer formation within secondary organic aerosols: equilibrium and dynamic considerations, Atmospheric Chemistry and Physics, 14, 3691 – 3701, doi:10.5194/acp-14-3691-2014, 2014.

Vignes, A.: Diffusion in Binary Solutions. Variation of Diffusion Coefficient with Composition, Industrial & Engineering Chemistry Fundamentals, 5, 189 – 199, doi:10.1021/i160018a007, 1966.

Wolke, R. and Knoth, O.: Numerical Solution of Differential and Differential-Algebraic Equations, 4 – 9 September 2000, Halle, Germany Time-integration of multiphase chemistry in size-resolved cloud models, Applied Numerical Mathematics, 42, 473 – 487, doi:10.1016/S0168-9274(01)00169-6, 2002.

Wolke, R., Sehili, A., Simmel, M., Knoth, O., Tilgner, A., and Herrmann, H.: SPACCIM: A parcel model with detailed microphysics and complex multiphase chemistry, Atmospheric Environment, 39, 4375 – 4388, doi:10.1016/j.atmosenv.2005.02.038, 2005.

Wolke, R., Schröder, W., Schrödner, R., and Renner, E.: Influence of grid resolution and meteorological forcing on simulated European air quality: A sensitivity study with the modeling system COSMO-MUSCAT, Atmospheric Environment, 53, 110 – 130, doi:10.1016/j.atmosenv.2012.02.085, 2012.

Zaveri, R. A., Easter, R. C., Shilling, J. E., and Seinfeld, J. H.: Modeling kinetic partitioning of secondary organic aerosol and size distribution dynamics: representing effects of volatility, phase state, and particle-phase reaction, Atmospheric Chemistry and Physics, 14, 5153 – 5181, doi:10.5194/acp-14-5153-2014, 2014.

Zhang, X., Cappa, C. D., Jathar, S. H., McVay, R. C., Ensberg, J. J., Kleeman, M. J., and Seinfeld, J. H.: Influence of vapor wall loss in laboratory chambers on yields of secondary organic aerosol, Proceedings of the National Academy of Sciences, 111, 5802 – 5807, doi:10.1073/pnas.1404727111, 2014.

Zhang, Y., Sanchez, M. S., Douet, C., Wang, Y., Bateman, A. P., Gong, Z., Kuwata, M., Renbaum-Wolff, L., Sato, B. B., Liu, P. F., Bertram, A. K., Geiger, F. M., and Martin, S. T.: Changing shapes and implied viscosities of suspended submicron particles, Atmospheric Chemistry and Physics, 15, 7819 – 7829, doi:10.5194/acp-15-7819-2015, 2015.

Zhao, J., Ortega, J., Chen, M., McMurry, P. H., and Smith, J. N.: Dependence of particle nucleation and growth on high-molecular-weight gas-phase products during ozonolysis of α-pinene, Atmospheric Chemistry and Physics, 13, 7631 – 7644, doi:10.5194/acp-13-7631-2013, 2013.

Ziemann, P. J. and Atkinson, R.: Kinetics, products, and mechanisms of secondary organic aerosol formation, Chem. Soc. Rev., 41, 6582 – 6605, doi:10.1039/C2CS35122F, 2012.

Zobrist, B., Soonsin, V., Luo, B. P., Krieger, U. K., Marcolli, C., Peter, T., and Koop, T.: Ultra-slow water diffusion in aqueous sucrose glasses, Phys. Chem. Chem. Phys., 13, 3514 – 3526, doi:10.1039/c0cp01273d, 2011.

Zuend, A., Marcolli, C., Peter, T., and Seinfeld, J. H.: Computation of liquid-liquid equilibria and phase stabilities: implications for RH-dependent gas/particle partitioning of organic-inorganic aerosols, Atmospheric Chemistry and Physics, 10, 7795 – 7820, doi:10.5194/acp-10-7795-2010, 2010.

Kinetic modeling studies of SOA formation from α-pinene ozonolysis

Kathrin Gatzsche[1], Yoshiteru Iinuma[1,*], Andreas Tilgner[1], Anke Mutzel[1], Torsten Berndt[1], and Ralf Wolke[1]

[1]Leibniz Institute for Tropospheric Research (TROPOS), Leipzig, Germany
[*]now at: Okinawa Institute of Science and Technology Graduate University (OIST), Okinawa, Japan

Correspondence to: K. Gatzsche (gatzsche@tropos.de)

Abstract. This paper describes the implementation of a kinetic gas-particle partitioning approach used for the simulation of secondary organic aerosol (SOA) formation within the SPectral Aerosol Cloud Chemistry Interaction Model (SPACCIM). The kinetic partitioning considers the diffusion of organic compounds into aerosol particles and the subsequent chemical reactions in the particle phase. The basic kinetic partitioning approach is modified by the implementation of chemical backward reaction of the solute within the particle phase as well as a composition dependent particle-phase bulk diffusion coefficient. The adapted gas-phase chemistry mechanism for α-pinene oxidation has been updated due to the recent findings related to the formation of highly oxidized multifunctional organic compounds (HOMs). Experimental results from a LEAK (Leipziger Aerosolkammer) chamber study for α-pinene ozonolysis were compared with the model results describing this reaction system.

The performed model studies reveal that the particle-phase bulk diffusion coefficient and the particle phase reactivity are key parameters for SOA formation. Using the same particle phase reactivity for both cases we find that liquid particles with higher particle-phase bulk diffusion coefficients have 310-times more organic material formed in the particle phase compared to higher viscous semi-solid particles with lower particle-phase bulk diffusion coefficients. The model results demonstrate that, even with a moderate particle phase reactivity, about 61 % of the modeled organic mass consists of reaction products that are formed in the liquid particles. This finding emphasizes the potential role of SOA processing. Moreover, the initial organic aerosol mass concentration and the particle radius are of minor importance for the process of SOA formation in liquid particles. A sensitivity study shows that a 22-fold increase in particle size merely leads to a SOA increase of less than 10 %.

Due to two additional implementations, allowing backward reactions in the particle phase and considering a composition dependent particle-phase bulk diffusion coefficient, the potential overprediction of the SOA mass with the basic kinetic approach is reduced by about 40 %. HOMs are an important compound group in the early stage of SOA formation because they contribute up to 65 % of the total SOA mass at this stage. HOMs also induce further SOA formation by providing an absorptive medium for SVOCs (semi-volatile organic compounds). This process contributes about 27 % of the total organic mass. The model results are very similar to the LEAK chamber results. Overall, the sensitivity studies demonstrate that the particle reactivity and the particle-phase bulk diffusion require a better characterization in order to improve the current model implementations and to validate the assumptions made from the chamber simulations.

The successful implementation and testing of the current kinetic gas-particle partitioning approach in a box model framework will allow further applications in a 3-D model for regional scale process investigations.

1 Introduction

The Earth's radiative budget is directly and indirectly influenced by atmospheric aerosols due to scattering and absorption of solar as well as terrestrial radiation (Haywood and Boucher, 2000; IPCC, 2013). Additionally, atmospheric aerosols affect cloud formation and provide an interface for heterogeneous chemical reactions (Andreae and Crutzen, 1997). Aerosols also markedly affect human health, in particular, respiratory and cardiovascular systems can be damaged due to exposure to aerosol particles (Harrison and Yin, 2000; Pope and Dockery, 2006). In many locations, organic matter (OM) represents the largest fraction of the aerosol mass, whereby the aerosol fine fraction consists of up to about one half of secondary organic aerosol (SOA, Jimenez et al., 2009; Hallquist et al., 2009). SOA can be divided into two main types; gasSOA (Hallquist et al., 2009) that is formed from gas to particle conversion and aqSOA (Ervens et al., 2011) that is formed from aqueous phase processes. This study investigates only gasSOA and will only be referred to as SOA henceforth.

SOA is formed via the oxidation of gas-phase organic precursor compounds by ozone, hydroxyl radical, nitrate radical, or photolysis (Hallquist et al., 2009). Thereby, the functionalization and binding ability of the product molecules result in decreased volatility (Donahue et al., 2012). If the vapor pressure of the oxidized organic compounds is low enough, they condense on a pre-existing particle surface or form new particles through nucleation. SOA formation is very complex because of the variety of organic precursor compounds in the atmosphere and numerous atmospheric degradation pathways. Due to the complexity no comprehensive mechanistic knowledge, including a complete particle product distribution, exits (Goldstein and Galbally, 2007). The modeling approach, which is mainly utilized for gas-to-particle phase partitioning of semi-volatile organic compounds, based on gas-particle equilibrium for these compounds, was proposed by Pankow (1994). The phase states of SOA particles have been investigated in more detail by a wide variety of measurement techniques recently. First indications of an amorphous (semi-)solid state for biogenic SOA particles were deduced by Virtanen et al. (2010) and were established in following studies (Virtanen et al., 2011; Cappa and Wilson, 2011; Vaden et al., 2011; Saukko et al., 2012; Zelenyuk et al., 2012). These studies have provided a first qualitative estimate of the particle phase state, however, quantitative values such as the particle-phase bulk diffusion coefficients are essential for model description. For this purpose, new measurement techniques of particle viscosity for small sample masses have been developed and verified (Zelenyuk et al., 2012; Renbaum-Wolff et al., 2013b, a; Kuimova, 2012; Hosny et al., 2013). Bulk viscosity measurements demonstrate that SOA particles only exist at a high relative humidity (RH $>$ 75 %) in a liquid state (Renbaum-Wolff et al., 2013a; Kidd et al., 2014). At a lower relative humidity, the organic particles exhibit a higher viscosity indicating a semi-solid or glassy phase state (Renbaum-Wolff et al., 2013a; Abramson et al., 2013; Pajunoja et al., 2014; Zhang et al., 2015; Grayson et al., 2016). Additionally, Grayson et al. (2016) have shown that viscosity increases when the production mass concentration of SOA decreases, however, the experimentally formed SOA mass exceeded atmospheric mass concentrations. Recently, microviscosity measurements of SOA particles have revealed a high intra-molecular heterogeneity of SOA particles concerning their phase state (Hosny et al., 2016). The measured micro-

viscosity values provided by Hosny et al. (2016) are lower than the results of bulk measurements reported by Renbaum-Wolff et al. (2013a), Zhang et al. (2015), and Grayson et al. (2016). However, the data by Hosny et al. (2016) fit well with particle-phase diffusion coefficient measurements by Price et al. (2015), which were converted by the Stokes-Einstein (SE) relation to viscosity. The break-down of the SE relation for supercooled liquids and glasses is well known from literature (Tarjus and Kivelson, 1995; Mendoza et al., 2015). This fact is also reported near the glass transition temperature for sugars (Champion et al., 1997; Rampp et al., 2000; Zhu et al., 2011; Power et al., 2013) and protein (Shiraiwa et al., 2011). All measurements indicate that the viscosity of SOA particles increases with decreasing relative humidity and that a semi-solid phase state is very likely achieved. Therefore, absorptive partitioning approaches, which are based on steady equilibrium between gas and particle phase (Pankow, 1994), may indirectly overestimate particle-phase diffusion and thus the SOA formation due to continuous partitioning.

A significant progress in the development of non-equilibrium partitioning models has been made in recent years, whereby the particle phase is resolved in different ways. Shiraiwa et al. (2010) presented KM-SUB, a novel model approach to resolve the particle phase in multiple layers, and interface the gas phase and particle phase with the introduction of a sorption layer and a surface layer. For the description of the fluxes between the many layers of the particle, diffusion coefficients for the gas and the particle phase are necessary. Thus, the phase state of the aerosol particles will influence the partitioning of gaseous compounds. The model was further developed to KM-GAP (Shiraiwa et al., 2012, 2013a, b). Later, Roldin et al. (2014) provided a second multi-layer model, ADCHAM, which has a similar layer structure to KM-SUB/KM-GAP and has been developed for the simulation of chamber studies. A third model approach with a kinetic description of VOC partitioning suitable for regional and global atmospheric models has been recently proposed by Zaveri et al. (2014) and it has been verified in MOSAIC (Model for Simulating Aerosol Interactions and Chemistry). In this approach, the particle phase is not resolved in different layers, but bulk particle-phase diffusion is considered for the solute semi-volatile species. The utilization of particle-phase bulk diffusion coefficients in partitioning approaches increases the degree of freedom for the phase transfer and, therefore, the particle-phase bulk diffusion coefficient needs to be estimated.

Within this study, the kinetic partitioning approach by Zaveri et al. (2014) have been applied and further developed. Therefore, the kinetic partitioning approach was deployed the first time to a comprehensive gas-phase chemistry mechanism, describing α-pinene ozonolysis and box model simulations have been achieved for sensitivity and chamber studies. Since the kinetic partitioning is a more complex approach than the absorptive partitioning (Pankow, 1994), we conducted extensive sensitivity studies to explore the influence of the individual parameters on SOA formation. Particularly, particle-phase bulk diffusion coefficients, mass accommodation coefficients, and rate constants for particle phase reactions in the way of oligomerization are uncertain or less characterized for SOA particles. Therefore, sensitivity studies were conducted to reveal their influence on SOA formation. In addition to these more technical studies, two further investigations were carried out to study the influence of highly oxidized multifunctional organic compounds (HOMs) and a composition dependent particle-phase bulk diffusion coefficient. HOMs have been successfully identified in laboratory and field studies recently (Ehn et al., 2012, 2014; Zhao et al., 2013; Jokinen et al., 2014; Mentel et al., 2015; Mutzel et al., 2015; Berndt et al., 2016). Their possible existence was already proposed in 1998 (Kulmala et al., 1998), but their influence on the early growth of fresh SOA particles is the subject of on-

going investigations (Riipinen et al., 2012; Donahue et al., 2012, 2013). The consideration of HOMs in gas-phase chemistry mechanisms seems to be indispensable because the total molar HOM yield from the reactions of α-pinene with OH as well as O_3 is about 6 % (Berndt et al., 2016), also the predicted vapor pressures of HOMs are rather low (Kurtén et al., 2016). Thus, in the second part of this modeling study, the gas-phase chemistry mechanism has been extended to include the measured HOM yields for α-pinene ozonolysis in order to examine their influence on the initial formation of SOA and the overall SOA yield. The second investigation focuses on the importance of the particle-phase bulk diffusion coefficient of SOA particles for the overall SOA mass yield. The particle-phase bulk diffusion coefficient might be rather composition dependent than constant and due to a lower self-diffusion coefficient of the organic material, increasing organic matter in the particle phase decreases the weighted particle-phase bulk diffusion coefficient. This investigation is also important for modeling of chamber experiments where wet seed aerosols are often used because water is known to have a plasticizer effect on SOA (O'Meara et al., 2016). The implementation of a composition dependent particle-phase bulk diffusion coefficient within the kinetic approach of Zaveri et al. (2014) constitutes a further development of the basic approach and the applicability of this new feature is tested in this study. Moreover, this study provides how a composition dependent particle-phase bulk diffusion coefficient can be applied and how it influences the SOA formation. The second further development of the kinetic approach concerns the particle-phase reactivity. Additional backward reactions in the particle phase have been considered to enable a treatment of reversible particle-phase reactions under formation of a reaction equilibrium. The effect of this process is also subject of the extensive sensitivity studies.

2 Material and methods

2.1 Chamber experiments

α-Pinene ozonolysis experiments were carried out in the aerosol chamber LEAK (Leipziger Aerosolkammer). A detailed description of the LEAK chamber together with the available equipment can be found in Iinuma et al. (2009) and Mutzel et al. (2016). Briefly, LEAK is a cylindrical, 19 m^3 Teflon bag with a surface-to-volume ratio of 2 m^{-1}. The experiments were performed in the presence of ammonium sulfate seed particles, which aerosol size distribution span a narrow range around a mean particle radius of 35 nm. O_3 was generated by UV irradiation of O_2 using an O_2 flow rate of 3 L min^{-1}. α-Pinene ($\approx$ 58 ppb) was injected into the LEAK chamber with a microliter-syringe. The oxidation of α-pinene was carried out under 55 % relative humidity (RH). Carbon monoxide (CO) was used during the experiment as an OH scavenger. The α-pinene consumption was monitored with a proton-transfer-reaction mass spectrometer (PTR-MS) over a reaction time of 2 hours. Throughout the chamber experiment, the particle-size distribution was measured every 11.5 min with a scanning mobility particle sizer (SMPS). Ozone was monitored with a 60 s time resolution. An average density of 1 g cm^{-3} was applied to calculate the produced organic particle mass (ΔOM). The particle phase was sampled on filters at the end of the experiments and analyzed afterwards by an Ultra Performance Liquid Chromatography coupled to Electrospray Ionisation Time-of-Flight Mass Spectrometer (UPLC/ESI(-)-TOFMS, Waters, MA, USA). 1.8 m^3 of the chamber volume was collected on a PTFE filter (borosilicate glass fiber filter coated with fluorocarbon, 47 mm in diameter, PALLFLEX T60A20, PALL, NY, USA), which was

connected to a denuder (URG-2000-30B5, URG Corporation, Chapel Hill, NC, USA, Kahnt et al., 2011) to avoid gas-phase artifacts. Furthermore, PTR-MS measurements were performed in order to monitor the key oxidation products of the α-pinene ozonolysis, such as pinonaldehyde.

2.2 Model framework

2.2.1 Box model SPACCIM (original code)

This study uses the SPectral Aerosol Cloud Chemistry Interaction Model (SPACCIM, Wolke et al., 2005) and has extended it by implementing a particle phase partitioning approach. The original SPACCIM version published by Wolke et al. (2005) is an adiabatic air parcel model incorporating a complex size-resolved cloud microphysical model and a multiphase chemistry model. Briefly, the interaction between both models is implemented by a coupling scheme. This coupling enables both models to run independently, as far as possible, and to apply their own time step control. The microphysics scheme of the SPACCIM model framework is based on the work of Simmel and Wurzler (2006) and Simmel et al. (2005). The cloud microphysical model describes the growth and shrinking processes of aerosol particles by water vapor diffusion as well as nucleation and growth/evaporation of cloud droplets or deliquescent particles. Other microphysical processes such as impaction of aerosol particles and collision/coalescence of droplets are also explicitly considered. The implementation of the dynamic growth rate in the condensation/evaporation processes and the droplet activation is implemented based on the Köhler theory (Köhler, 1936). The size-resolved cloud microphysics of deliquesced particles and droplets including cloud droplet formation, evolution, and evaporation is considered using a one-dimensional sectional approach. Further microphysical features of SPACCIM are already described in Wolke et al. (2005) and results owing to these processes are presented in Tilgner et al. (2013); Rusumdar et al. (2016); Hoffmann et al. (2016). The implemented multiphase chemical model applies a high-order implicit time integration scheme, which utilizes the specific sparse structure of the model equations (Wolke and Knoth, 2002). SPACCIM was originally developed for parcel model studies, whereby, the considered air parcel can follow real or artificial trajectories. However, the partitioning of organic gases towards the particle phase was not considered in the original SPACCIM and the model was not exclusively designed for application on aerosol chamber studies. The existing model framework has been extended by gas-to-particle mass transfer via a kinetic partitioning approach (Zaveri et al., 2014), see Sect. 2.2.2 for details. Due to the focus of these studies on modeling aerosol chamber studies of gasSOA formation for monodisperse aerosol without entrainment and coagulation, microphysical processes are not included in the results of this study.

2.2.2 Implementation of a kinetic partitioning approach

The existing model framework was extended by the implementation of the kinetic partitioning approach established by Zaveri et al. (2014). The general assumption of this approach is based on the description of the diffusive flux of a solute in the particle phase via Fick's second law extended by a particle phase reaction of the solute:

$$\frac{\partial A_i(r,t)}{\partial t} = D_{\mathrm{b},i}\frac{1}{r^2}\frac{\partial}{\partial r}\left(r^2\frac{\partial A_i(r,t)}{\partial r}\right) - k_{\mathrm{c},i}A_i(r,t)\,. \tag{1}$$

Thereby, the utilized parameters are the particle-phase concentration A_i of the solute i as a function of the radius r and the time t, the particle-phase bulk diffusion coefficient of the solute $D_{\mathrm{b},i}$, and the chemical reaction rate constant $k_{\mathrm{c},i}$ of the solute within the particle phase. Equation (1) is given in spherical coordinates. As a fundamental simplification the diffusion coefficient is assumed to be constant. Therefore, a particle-phase bulk diffusion coefficient $D_{\mathrm{b},i}$ is introduced. This assumption simplifies the calculation of the integral (Eq. 1). In Zaveri et al. (2014) two solutions of Eq. (1) are described. The first solution is only for usage in a Lagrangian box model in case of a "closed system". The second approach is applicable to general systems treated with 3-D Eulerian models. Therefore, the distinction of two reaction regimes concerning their reaction rates and the application of the two-film theory (Lewis and Whitman, 1924) in case of slow reactions is utilized. For a polydisperse aerosol distribution, the following equations are proposed by Zaveri et al. (2014) for fast reactions ($k_{\mathrm{c},i} \geq 0.01$ s):

$$\frac{\mathrm{d}\overline{C}_{\mathrm{a},i,m}}{\mathrm{d}t} = \xi_m k_{\mathrm{g},i,m} \left(\overline{C}_{\mathrm{g},i} - \overline{C}_{\mathrm{a},i,m} \frac{S_{i,m}}{Q_i} \right) - k_{\mathrm{c},i} \overline{C}_{\mathrm{a},i,m} \,, \tag{2}$$

and for slow reactions ($k_{\mathrm{c},i} < 0.01$ s):

$$\frac{\mathrm{d}\overline{C}_{\mathrm{a},i,m}}{\mathrm{d}t} = \xi_m K_{\mathrm{g},i,m} \left(\overline{C}_{\mathrm{g},i} - \overline{C}_{\mathrm{a},i,m} S_{i,m} \right) - k_{\mathrm{c},i} \overline{C}_{\mathrm{a},i,m} \,, \tag{3}$$

whereby, ξ_m denotes the surface area of the respective size-section m:

$$\xi_m = 4\pi r_{\mathrm{p},m}^2 N_m \,, \tag{4}$$

and $S_{i,m}$ is the saturation ratio:

$$S_{i,m} = \frac{C_{\mathrm{g},i}^*}{\sum_j \overline{C}_{\mathrm{a},j,m}} \,. \tag{5}$$

Therein, $\overline{C}_{\mathrm{a},i,m}$ denotes the total average concentration of a solute i in size-section m, with M the number of size-sections. Q_{i} represents the ratio of the average particle-phase concentration $\overline{A}_{\mathrm{i}}$ to the surface concentration $A_{\mathrm{i}}^{\mathrm{S}}$ at steady-state and is named quasi-steady-state term (see Appendix A). N_m denotes the number concentration, $r_{\mathrm{p},m}$ the respective particle radius, $k_{\mathrm{g},i}$ is the gas-side mass transfer coefficient, and $K_{\mathrm{g},i}$ is the overall gas-side mass transfer coefficient, which is needed for the application of the two film theory (see Appendix A for details). The saturation ratio $S_{i,m}$ (Eq. 5) represents the ratio of the effective saturation vapor concentration $C_{\mathrm{g},i}^*$ and the total average organic aerosol mass concentration $\sum_j \overline{C}_{\mathrm{a},j,m}$. A more detailed derivation of Eq. (2) and (3) is provided in Appendix A following Zaveri et al. (2014).

The mass balance equation in SPACCIM for the gas phase after implementation of the gas-to-particle transfer via the kinetic

approach yields to:

$$\frac{\mathrm{d}C_{\mathrm{g},i^*}}{\mathrm{d}t} = \underbrace{R_{\mathrm{g},i^*}\left(t, C_{\mathrm{g},1}, \ldots, C_{\mathrm{g},N_\mathrm{g}}\right)}_{\substack{\text{I: gas phase}\\ \text{chemistry}}} \underbrace{-\kappa_i \sum_m L_m k_{\mathrm{t},m,i}\left[C_{\mathrm{g},i^*} - \frac{C_{\mathrm{a},m,i}}{H_i}\right]}_{\substack{\text{II: gas-to-aqueous-phase}\\ \text{mass transfer}}} \underbrace{-\lambda_i \sum_m \xi_m k^{\circ}_{\mathrm{g},m,i}\left[C_{\mathrm{g},i^*} - C_{\mathrm{a},m,i} S^{\circ}_{m,i}\right]}_{\substack{\text{III: gas-to-particle-phase}\\ \text{mass transfer}}}$$

$$\underbrace{+\mu\left[c_{\mathrm{g},i^*} - c_{\mathrm{g,\,ent}}\right]}_{\substack{\text{IV: entrainment/}\\ \text{outflow}}}, \tag{6}$$

$$i^* = 1, \ldots, N_\mathrm{g};\ i = 1, \ldots, N_\mathrm{aq}, N_{\mathrm{aq}+1}, \ldots, N_\mathrm{a};\ m = 1, \ldots, M\,,$$

with

$$k^{\circ}_{\mathrm{g},m,i} = k_{\mathrm{g},m,i} \quad \text{and} \quad S^{\circ}_{m,i} = \frac{S_{i,m}}{Q_i} \quad (k_{\mathrm{c},i} \geq 0.01\,\mathrm{s}) \quad \text{or} \quad k^{\circ}_{\mathrm{g},m,i} = K_{\mathrm{g},m,i} \quad \text{and} \quad S^{\circ}_{m,i} = S_{i,m} \quad (k_{\mathrm{c},i} < 0.01\,\mathrm{s}). \tag{7}$$

The mass balance equation for the particle phase is given by:

$$\frac{\mathrm{d}C_{\mathrm{a},i}}{\mathrm{d}t} = \underbrace{L_m R_{\mathrm{a},i}\left(t, C_{\mathrm{a},1}, \ldots, C_{\mathrm{a},N_\mathrm{aq}}, C_{\mathrm{a},N_\mathrm{aq}+1}, \ldots, C_{\mathrm{a},N_\mathrm{a}}\right)}_{\text{I: aqueous and particle phase chemistry}} + \underbrace{\kappa_i L_m k_{\mathrm{t},m,i}\left[C_{\mathrm{g},i^*} - \frac{C_{\mathrm{a},m,i}}{H_i}\right]}_{\substack{\text{II: gas-to-aqueous-phase}\\ \text{mass transfer}}} + \underbrace{\lambda_i \xi_m k^{\circ}_{\mathrm{g},m,i}\left[C_{\mathrm{g},i^*} - C_{\mathrm{a},m,i} S^{\circ}_{m,i}\right]}_{\substack{\text{III: gas-to-particle-phase}\\ \text{mass transfer}}}$$

$$\underbrace{+F\left(c_{1,i} - c_{M,i}\right)}_{\substack{\text{IV: mass transfer}\\ \text{by microphysics}}} + \underbrace{\mu\left[c_{m,i} - c_{m_\mathrm{ent},i}\right]}_{\substack{\text{V: entrainment/}\\ \text{outflow}}}. \tag{8}$$

Here, R_{g,i^*} stands for all chemical reactions which take place in the gas phase (compounds $i^* = 1, \ldots, N_\mathrm{g}$) and $R_{\mathrm{a},i}$ for chemical reactions in the aerosol phase, which comprises aqueous $i = 1, \ldots, N_\mathrm{aq}$ and particulate $i = N_{\mathrm{aq}+1}, \ldots, N_\mathrm{a}$ species. The second term on the right side of Eq. (6) describes the mass transfer in the aqueous aerosol phase (compounds $i = 1, \ldots, N_\mathrm{aq}$) utilizing the Schwartz approach (Schwartz, 1986) with the dimensionless Henry's law coefficient H_i and the mass transfer coefficient $k_{\mathrm{t},m,i}$:

$$k_{\mathrm{t},m,i} = \left(\frac{r^2_{\mathrm{p},m}}{3D_\mathrm{g}} + \frac{4r_{\mathrm{p},m}}{3\nu\alpha_{\mathrm{aq},i}}\right)^{-1}. \tag{9}$$

Thereby, D_g denotes the gas diffusion coefficient, ν the molecular speed, and $\alpha_{\mathrm{aq},i}$ the mass accommodation coefficient for the aqueous compounds ($0 \leq \alpha_{\mathrm{aq},i} \leq 1$). The prefactor κ_i of the Henry term denotes the solubility index (1 means soluble and 0 insoluble) of the aqueous solute. L_m indicates the volume fraction $[V_m / V_\mathrm{box}]$ of the m-th droplet class inside the box volume and $C_{\mathrm{a},m,i}$ denotes the corresponding aqueous aerosol phase concentration in the m-th droplet class. The parameters in the gas-to-particle mass transfer term are described above, whereby similar to the solubility index a partitioning index λ_i (1 for partitioning in the particle phase and 0 for staying in the gas phase) is introduced for the individual compounds ($i = N_{\mathrm{aq}+1}, \ldots, N_\mathrm{a}$). There is the possibility to describe time-dependent entrainment/detrainment by the rate μ_i for the different gas-phase (Eq. 6, term IV) and aerosol-phase (Eq. 8, term V) species. For the aerosol species, a mass transfer between the

different droplet classes is also possible due to microphysical processes (e.g., by aggregation, break up, and condensation), which is described by term F in Eq. (8, term IV). In the present study, the terms of entrainment/detrainment in Eq. (6) and (8) can be neglected, because no entrainment is considered in the closed system of the box model simulations. Additionally, the terms of aqueous-phase transfer in the particle phase (Eq. 6 and 8, term II) are omitted because aqSOA formation is not considered in this SPACCIM model study.

2.2.3 Gas-phase chemistry mechanism

The basic gas-phase chemistry mechanism for the degradation of α-pinene, that is suitable for a box model or regional scale model, has been proposed by Chen and Griffin (2005). The oxidation mechanisms take into account the organic degradation protocol established by Jenkin et al. (1997) as well as experimental results and formation pathways of SVOCs (Jenkin et al., 2000; Winterhalter et al., 2000). The host gas-phase chemistry mechanism for the α-pinene oxidation is the Caltech Atmospheric Chemistry Mechanism (CACM, Griffin et al., 2002; Pun et al., 2003).

The oxidation mechanism for α-pinene degradation underlies a number of simplifications to reduce the amount of species and associated reactions in the model. The reduced computing time will allow the use of this mechanism in future 3-D model studies. Therefore, the mechanism does not include the reactions on the carbon positions in hydrocarbon skeletons that are less likely to be attacked by the OH radical (Chen and Griffin, 2005). Peroxy radicals (RO_2) are explicitly considered in the mechanism if their further chemical reactions can lead to the formation of multifunctional carbonyl compounds that may form SVOCs (Chen and Griffin, 2005; Griffin et al., 2002). Moreover, peroxy radicals are summed up in the model to simplify RO_2 cross permutations and self-reactions. Further details concerning the gas-phase chemistry mechanism are provided in the publication of Chen and Griffin (2005). The utilized chemical degradation reactions for α-pinene are compared with the MCM v3.3.1 (Master Chemical Mechanism) and the reaction rate coefficients have been updated, if necessary. Additionally, the recently measured HOM yields (Berndt et al., 2016) have been implemented in the existing gas-phase chemistry mechanism recalculating the former branching ratios for the last part of the sensitivity studies. The degradation reactions for α-pinene are summarized in Table S1 in the Supplement.

The vapor pressures of the SVOCS, which are assumed to partition into the particle phase, have been estimated with the group contribution method called EVAPORATION described by Compernolle et al. (2011). The tool is available online at the following URL (http://tropo.aeronomie.be/models/evaporation_run.htm). The vapor pressures of the HOMs from the reaction of α-pinene with OH are provided by Berndt et al. (2016) and were therein calculated with the COSMO-RS approach (Eckert and Klamt, 2002) as well as compared with estimates from SIMPOL (Pankow and Asher, 2008). Additionally, HOM vapor pressures are calculated with EVAPORATION for a comparison with the COSMO-RS values (see Table S4 in the Supplement for details). Up to now, the structural formulas of the HOMs from the α-pinene ozonolysis are not known from quantum chemical calculations. The HOM molecules formed from the reaction of α-pinene with O_3 might contain more functional groups than for the reaction of α-pinene with OH. Therefore, the HOMs from the ozone reaction pathway might have lower vapor pressures as indicated in the study of Kurtén et al. (2016) concerning vapor pressures of HOMs.

2.3 Performed sensitivity studies

According to Eqs. (2) and (3) the formed SOA mass predominantly depends on the following parameters: particle-phase bulk diffusion coefficient D_b, pseudo-first-order rate constant for particle phase reactions k_c, particle radius r_p, initial particle phase organic mass concentration OM_0, and the mass accommodation coefficient α. Sensitivity studies have been performed to characterize the influence of these five parameters on the SOA formation. This study has been limited to a single size-section m of particles. Polydisperse test cases have been performed, but for the conducted sensitivity studies, the consideration of a polydisperse aerosol distribution will increase the degree of freedom as well as the complexity. Further, for the simulation of the LEAK chamber studies, this feature was not required because of the nearly monodisperse aerosol spectrum existent within this type of experiment. For the sake of clarity, the results of the sensitivity studies regarding the mass accommodation coefficient α and initial particle phase organic mass concentration OM_0 are presented in the Supplement (see Sects. 2.2 and 2.3 in the Supplement, respectively). An overview of the parameters evaluated in the sensitivity studies is given in Table 1. The case studies 6 – 8 of Table 1 refer to the consideration of HOMs in the gas-phase chemistry mechanism and two further developments of the kinetic partitioning approach.

3 Results and discussion

3.1 Sensitivity studies

3.1.1 Impact of the particle-phase bulk diffusion coefficient D_b on SOA formation

To investigate the influence of the particle phase state on SOA formation, the particle-phase bulk diffusion coefficient D_b was varied from $10^{-9}\,m^2\,s^{-1}$ to $10^{-21}\,m^2\,s^{-1}$ (see Table 1, study 1). This range covers liquid particles, e.g. droplets with dissolved salts associated with D_b=$10^{-9}\,m^2\,s^{-1}$, and semi-solid/viscous particles starting at about $D_b < 10^{-14}\,m^2\,s^{-1}$ and ending up with $D_b = 10^{-21}\,m^2\,s^{-1}$. The latter value corresponds to a particle with the texture of pitch (Koop et al., 2011). The model results for the variation of D_b are shown in Fig. 1. Although, D_b is varied over thirteen orders of magnitude, the sensitivity study reveals that in general three main regimes for SOA formation occur. For liquid particles, $10^{-9}\,m^2\,s^{-1} \geq D_b \geq 10^{-14}\,m^2\,s^{-1}$, the highest SOA mass is observed. Thereby, rapid formation is achieved for $10^{-9}\,m^2\,s^{-1} \geq D_b \geq 10^{-13}\,m^2\,s^{-1}$. A slower SOA formation is observed for $D_b = 10^{-14}\,m^2\,s^{-1}$. However, for long equilibration times (about 20 – 24 hours) and fast particle phase reactions (Fig. 1), about 90 % of the maximum SOA mass is still achieved. Moreover, between $D_b = 10^{-14}\,m^2\,s^{-1}$ and $D_b = 10^{-15}\,m^2\,s^{-1}$, a reduced SOA mass is observed caused by the phase transition from liquid to semi-solid particles in this particle-phase bulk diffusion coefficient range (Koop et al., 2011). This second formation regime is characterized by the longer diffusion time as the particle-phase bulk diffusion coefficients are lower. Accordingly, the equilibration time between the gas and the particle phase is longer. SOA formation is delayed by the reduced diffusion into the particle phase, but can still be observed. The third regime is characterized by an extremely low or no SOA formation. For values $D_b < 10^{-16}\,m^2\,s^{-1}$ the SOA formation is inhibited because the condensed organic material does not diffuse sufficiently into the particle bulk.

Table 1. Varied model parameters in the sensitivity studies, whereby some cross checks concerning the sensitivity have been conducted.

#	Main parameter varied	Range	Additional parameter varied	Adjusted values	Remarks
1	D_b in $m^2\,s^{-1}$	$10^{-9}-10^{-21}$	k_c in s^{-1}	1, 10^{-1}, 10^{-2}, 10^{-4}, 10^{-6}	$r_p = 35$ nm; $OM_0 = 5.8\times10^{-2}\,g\,g^{-1}$
2	k_c in s^{-1}	$1-10^{-6}$	D_b in $m^2\,s^{-1}$	10^{-12}, 10^{-14}, 10^{-18}	$r_p = 35$ nm; $OM_0 = 5.8\times10^{-2}\,g\,g^{-1}$
3a	α [§] (dimensionless)	$1-10^{-2}$	D_b in $m^2\,s^{-1}$ and	10^{-12}, 10^{-14}, 10^{-18}	$r_p = 35$ nm; $OM_0 = 5.8\times10^{-2}\,g\,g^{-1}$
3b			k_c in s^{-1}	1, 10^{-1}, 10^{-2}, 10^{-4}	$r_p = 35$ nm; $OM_0 = 5.8\times10^{-2}\,g\,g^{-1}$
4a	r_p in nm	11 – 240	k_c in s^{-1} and	1, 10^{-1}, 10^{-2}, 10^{-4}, 10^{-6}	$OM_0 = 5.8\times10^{-2}\,g\,g^{-1}$
4b			D_b in $m^2\,s^{-1}$	10^{-12}, 10^{-14}, 10^{-18}	$OM_0 = 5.8\times10^{-2}\,g\,g^{-1}$
5	OM_0 [§] in $g\,g^{-1}$	$10^{-5}-5.8\times10^{-2}$	D_b in $m^2\,s^{-1}$	10^{-12}, 10^{-14}, 10^{-18}	$r_p = 35$ nm
6a	HOMs considered[†]		k_c in s^{-1} and	1, 10^{-2}, 10^{-4}, 10^{-6}	$r_p = 35$ nm and
6b			D_b in $m^2\,s^{-1}$	10^{-12}, 10^{-14}, 10^{-18}	$OM_0 = 10^{-6}\,g\,g^{-1}$
7	k_b in s^{-1} *	$1-10^{-6}$	k_c in s^{-1}	1, 10^{-2}, 10^{-4}	$D_b = 10^{-12}\,m^2\,s^{-1}$, $r_p = 35$ nm
8	Weighted particle-phase bulk diffusion coefficient	$D_{org} = 10^{-12}$ or $10^{-14} m^2\,s^{-1}$	k_b in s^{-1}	$10^{-2}-10^{-6}$	$k_c = 10^{-2} s^{-1}$, $r_p = 35$ nm

* Implementation of backward reactions in the particle phase, for more details see Sect. 3.3

† See reactions 1b and 3b in Table S1 in the Supplement

§ Results are presented in the Supplement

According to the classification of Mai et al. (2015), this case is named particle-phase-diffusion-limited partitioning. After the formation of a thin organic shell/film around the particle, no effective SOA formation takes place because of the long mixing time inside the particle. Thus, the gas-phase concentrations of the condensing organic compounds as well as the interfacial transport of these compounds are not the limiting factors of SOA formation under these conditions.

The three observed regimes for the variation of the particle-phase bulk diffusion coefficient are not shifted by the choice of the particle-phase reaction chemical rate constant k_c. The formed SOA mass is indeed reduced due to the lower particle phase reaction rate. For $D_b = 10^{-14}\,m^2\,s^{-1}$ less than 90 % of the maximum SOA mass is achieved (Fig. 1 b). Logarithmic scaled plots

for the variation of the particle-phase bulk diffusion coefficient are provided in the Supplement (see Fig. S1 in the Supplement) to illustrate the wide range of modeled SOA.

Viscosity measurements have mostly shown that organic aerosols become semi-solid, when relative humidity drops below $\approx 80/75\,\%$ (Renbaum-Wolff et al., 2013a; Zhang et al., 2015; Grayson et al., 2015). Afterwards, measured viscosity values were converted in diffusion coefficients via the Stokes-Einstein relation (Einstein, 1956). As a result, calculated particle-phase bulk diffusion coefficients for RH $< 80\,\%$ are lower than $5 \times 10^{-14}\,\mathrm{m^2\,s^{-1}}$ (Renbaum-Wolff et al., 2013a), which implies semi-solid organic aerosols. In the following, the measurement results by Renbaum-Wolff et al. (2013a), Zhang et al. (2015), and Grayson et al. (2016) are discussed from a perspective of the model results that are calculated with different particle-phase bulk diffusion coefficients. The estimated particle-phase bulk diffusion coefficients from measurements imply that the simulated regime, where SOA mass formation is highest, might be relevant for wet conditions only ($\approx$ RH $> 90\,\%$). The second regime, with intermediate SOA production, could only be reached within a narrow relative humidity range ($\approx 90\,\% >$ RH $> 70\,\%$). In this range, the transition from liquid to semi-solid particles might occur following the available viscosity measurements (Renbaum-Wolff et al., 2013a; Zhang et al., 2015). We can assume $D_\mathrm{b} < 10^{-16}\,\mathrm{m^2\,s^{-1}}$ (Renbaum-Wolff et al., 2013a, results of poke-and-flow technique) for a relative humidity below $70\,\%$. The sensitivity study reveals almost no SOA formation. Considering the relative humidity levels typical for chamber studies (0 to $70\,\%$ RH), it is quite difficult to interpret observed SOA formation in line with the stated particle-phase bulk diffusion coefficients (Renbaum-Wolff et al., 2013a) and related model results from the present study. However, under ambient conditions the broad spectrum of particle-phase bulk diffusion coefficients and the linked SOA mass have to be taken into account. A recent investigation concerning SOA phase state using fluorescence lifetime imaging (FLIM) by Hosny et al. (2016) provides a lower microviscosity than bulk viscosity measurements over the full RH-range (Renbaum-Wolff et al., 2013a; Zhang et al., 2015; Grayson et al., 2016). Therefore, local friction of a single particle is lower than bulk friction and hence local diffusion can be more efficient than bulk diffusion.

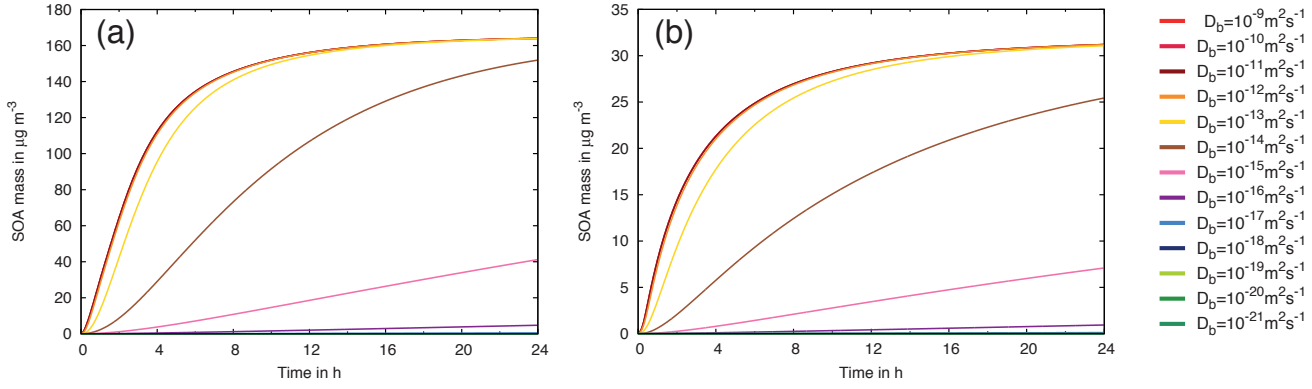

Figure 1. Simulated SOA mass for different particle-phase bulk diffusion coefficients in the range of D_b: $10^{-9}\,\mathrm{m^2\,s^{-1}} - 10^{-21}\,\mathrm{m^2\,s^{-1}}$ (model case 1 of Table 1) using a particle reaction rate constant of a) $k_\mathrm{c} = 1\,\mathrm{s^{-1}}$ and b) $k_\mathrm{c} = 10^{-6}\,\mathrm{s^{-1}}$.

3.1.2 Importance of the pseudo-first-order rate constant of particle phase reactions k_c on SOA formation

The pseudo-first-order rate constant of particle phase reactions k_c has been varied from $1\,s^{-1}$ to $10^{-6}\,s^{-1}$ to examine the influence of high and low particle phase reactivity on SOA formation in the second sensitivity study (see Table 1, study 2). As indicated in Eq. (1), the organic compounds, which are partitioned from the gas phase into the particle phase, can further react in the particle phase with a constant reaction rate k_c. The from the gas into the particle phase partitioned organic compounds are named p-products. The products, which have been caused due to the reactions in the particle phase, are termed r-products. The r-products do not stay in equilibrium with the gas-phase compounds and, therefore, can not evaporate from the particle phase. The r-products comprise particle-phase compounds resulting from aging of the condensed organic compounds (e.g., dimers, trimers or oligomers). Fig. 2 depicts the results of the particle-phase rate constant variation for liquid and semi-solid particles. A higher rate constant leads to an increased SOA mass independent of the phase state. The pseudo-first-order rate constant can also be understood as a reactive SOA uptake. The efficiency of this reactive uptake is different for liquid and semi-solid particles. For liquid particles ($D_b = 10^{-12}\,m^2\,s^{-1}$) the mass enhancement factor is about 6 for a seven order of magnitude higher k_c. This means that the SOA mass is increased due to a higher particle phase reactivity, since the organic mass is shifted more effectively from the partitioning products (p-products) to the reacted products (r-products). For semi-solid particles, the kinetic approach is predominantly sensitive for particle-phase reactions as indicated in Zaveri et al. (2014). The particle-phase-diffusion-limited partitioning for the viscous aerosol particles has been step-wise raised due to the increased particle-phase reaction rate constant (see Fig. 2b). The mass enhancement factor is about 2.5 for a seven orders of magnitude higher reactivity. It is noted that organic aerosol particles might exhibit such low particle-phase diffusivities $D_b \leq 10^{-18}\,m^2\,s^{-1}$ mainly under dry conditions (RH $< 40\,\%$). As a result, a higher pseudo-first-order rate constant for a chemical particle phase reaction leads to a distinct increase in SOA mass. Processes such as dimerization, oligomerization or other SOA aging processes can be represented in SOA models by means of particle reactions. Rate constants for oligomerization processes are not well characterized and only estimates from product studies exist. For example, Hosny et al. (2016) simulated the evolution of oleic acid droplets with the kinetic multilayer model KM-SUB (Shiraiwa et al., 2010) including monomer to tetramer products for the ozonolysis of oleic acid, comparing the results with experimental data.

3.1.3 Influence of the particle radius r_p on SOA formation

The effect of the variation of the particle radius r_p in the range from 11 nm to 240 nm on SOA formation is analyzed in this subsection. Additionally, the particle-phase bulk diffusion coefficient and the particle phase reaction rate constant have been varied to characterize the influence of the different parameters on the SOA formation for different particle sizes (see Table 1, model study 4a and 4b). The influence of the particle radius on the SOA formation is moderate for liquid aerosol particles ($D_b = 10^{-12}\,m^2\,s^{-1}$) when particle phase reactions are fast (Fig. 3a). For an about 22-fold larger particle, the SOA mass increase is by less than $10\,\%$. The maximum formed SOA mass is comparatively low for semi-solid particles and the particle size determines whether organic compounds condense or not (Fig. 3b). Therefore, the influence of the particle radius is higher for semi-solid particles. However, the formed SOA mass is rather small due to the limited diffusion into the particle and

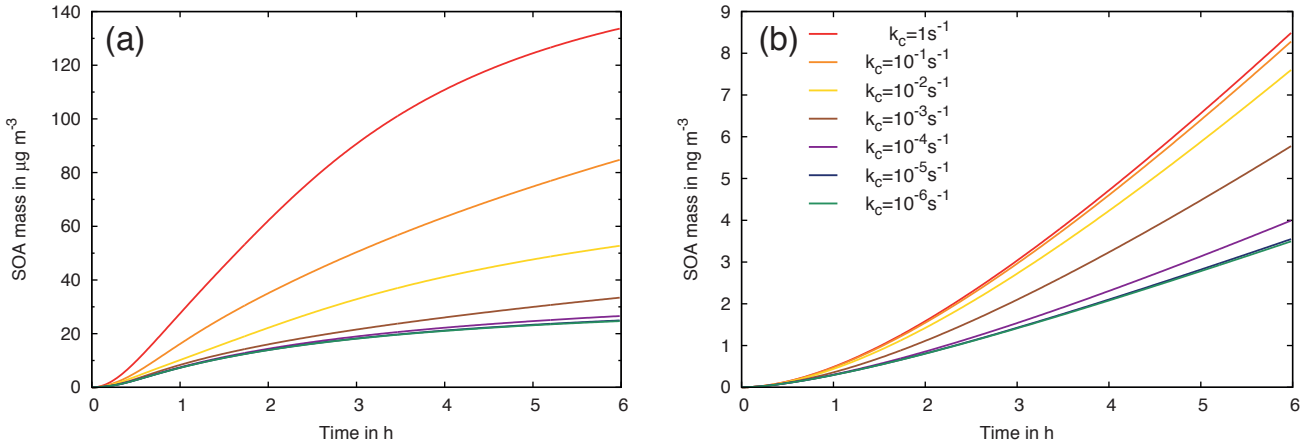

Figure 2. Simulated SOA mass for different pseudo-first-order rate constant of particle reactions k_c (model case 2 of Table 1) using particle-phase bulk particle diffusion coefficients for a) liquid ($D_b = 10^{-12}$ m^2 s^{-1}) and b) semi-solid ($D_b = 10^{-18}$ m^2 s^{-1}) aerosol particles.

it should be kept in mind that this diffusion coefficient is limited to dry conditions. For liquid particles, the increase in SOA mass caused by the larger particle size is for moderate particle-phase reactions about 40 % (see Fig. S5a in the Supplement). For semi-solid particles and moderate particle reactions, the same trend is observed but only very low SOA concentrations are formed (see Fig S5b in the Supplement). Due to the particle-phase-diffusion-limited partitioning for semi-solid particles combined with only moderate particle-phase rate constants, the formed SOA mass reaches quite small values, which are not observed under typical chamber study experiment conditions. Furthermore, the normalized increase of organic mass is highest for the smallest particles (Fig. S4a and S4b). This means smaller particles are characterized by a more effective uptake of organic mass related to the initial organic aerosol mass. This finding agrees with the surface ratio between smaller and larger particles. The influence of the particle radius r_p on SOA formation is characterized as moderate, but noticeable, particularly for semi-solid particles. The influence of the particle size is considerably smaller compared to the particle-phase bulk diffusion coefficient or the particle reactivity.

3.2 Importance of HOMs for initial SOA formation

Recently, ELVOCs (Ehn et al., 2014; Jokinen et al., 2015) and HOMs (Mutzel et al., 2015; Berndt et al., 2016) have been found to play a major role in aerosol formation from monoterpenes. Mutzel et al. (2015) have demonstrated the existence of HOMs during LEAK chamber experiments and ambient measurements at the TROPOS field site Melpitz. Laboratory measurements of Berndt et al. (2016) provide molar yields of HOMs for the α-pinene ozonolysis and α-pinene OH oxidation of 3.4 % and 2.4 %, respectively. The existing gas-phase chemistry mechanism of Chen and Griffin (2005) does not consider the formation of HOMs. Therefore, the mechanism of Chen and Griffin (2005) has been updated with the HOM formation from α-pinene implementing the yields measured by Berndt et al. (2016). The HOM compounds are lumped to one compound group and

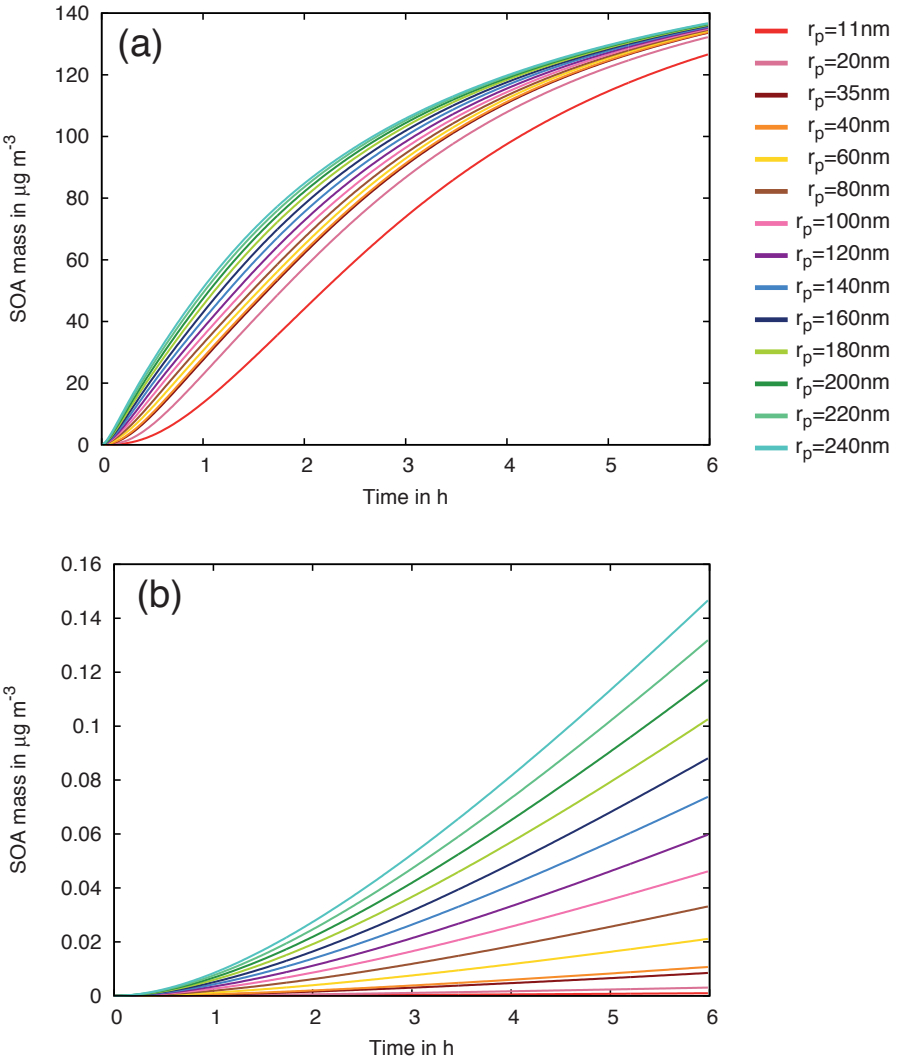

Figure 3. Model results of SOA mass for the variation of the particle radius r_p using a constant $k_\mathrm{c} = 1\,\mathrm{s}^{-1}$ (case 4a and 4b of Table 1) for a) liquid ($D_\mathrm{b} = 10^{-12}\,\mathrm{m}^2\,\mathrm{s}^{-1}$) and b) semi-solid ($D_\mathrm{b} = 10^{-18}\,\mathrm{m}^2\,\mathrm{s}^{-1}$) aerosol particles.

added to the gas-phase chemistry mechanism (see Table S1, reactions 1b and 3b). As an estimate for the vapor pressure of this compound group, the average vapor pressure of the compounds listed in Table S4 from COSMO-RS have been taken. To investigate the influence of the HOMs on the SOA mass, we have varied the pseudo-first-order rate constant of particle reactions and the particle-phase bulk diffusion coefficient (see Table 1 model case 6a and 6b for details). Thus, the effect of HOMs is characterized under different particle phase conditions and reaction regimes, however, for HOMs no further reactions in the particle phase have been considered in this study. Almost no initial organic mass OM_0 is utilized for the simulations

with HOMs. Nevertheless, the conducted simulations account not for new particle formation. The simulations without initial organic mass is consistent to previous studies, initialized with inorganic seed aerosol particles. The simulation results of Sect. 3.1.2 have been chosen as a reference case to characterize the influence of HOMs on the formed SOA mass. In contrast the reference simulations have been conducted with an initial organic aerosol mass concentration of $OM_0 = 5.8 \times 10^{-2}\,g\,g^{-1}$. The particle radius is 35 nm for both simulation setups.

In Fig. 4a the formed SOA mass for liquid particles ($D_b = 10^{-12}\,m^2\,s^{-1}$) is compared with simulations with and without consideration of HOMs under additional variation of the pseudo-first-order rate constant of particle reactions. For the liquid phase state ($D_b = 10^{-12}\,m^2\,s^{-1}$) the formed SOA mass is always increased due to the consideration of HOMs. A rapid condensation of HOMs occurs due to their low vapor pressures (Fig. 4a and Fig. S6 in the Supplement). This circumstance leads to an effective SOA formation immediately with oxidation of α-pinene. Consequently, condensed HOMs serve as an organic medium on the particles and support the subsequent condensation of SVOCs on the particle surfaces. When considering HOMs, the initialization with initial organic particle mass is not required because the formed SOA mass quickly exceeds OM_0 due to the immediate partitioning of the HOMs. Fig. 4b depicts the same sensitivity study for the phase transition zone between a liquid and semi-solid phase state ($D_b = 10^{-14}\,m^2\,s^{-1}$). The main difference compared to the results for liquid particles is the convergence of the simulated SOA mass for $k_c = 1\,s^{-1}$ for both cases. However, for slower chemical reactions in the particle phase, the SOA mass is increased when considering HOMs. An explanation for this behavior might be the missing chemical reactions in the particle phase for HOMs. Very fast chemical particle phase reactions can increase the uptake flux of organic gaseous compounds and compensate longer diffusion times for viscous particles. This may be the reason for the convergence of formed SOA mass for $k_c = 1\,s^{-1}$ combined with $D_b = 10^{-14}\,m^2\,s^{-1}$. For semi-solid particles ($D_b = 10^{-18}\,m^2\,s^{-1}$, Fig. 4c), the SOA formation without consideration of HOMs is more effective. This circumstance is caused by the missing particle-phase reactions for HOMs because the utilized kinetic approach is for $D_b < 10^{-15}\,m^2\,s^{-1}$ mainly sensitive to particle-phase reactions (Zaveri et al., 2014). Further, for semi-solid particles a particle-phase-diffusion-limited partitioning of HOMs occur with proceeding simulation time (Mai et al., 2015). Therefore, the equilibrium between the gas and the particle phase is quickly established for HOMs and their effect on the SOA mass differ from that for liquid particles. As indicated before, semi-solid aerosol particles might occur for a limited range of atmospheric conditions when the relative humidity decreases below 40 %. Therefore, the HOMs might affect SOA formation as seen in Fig. 4a and 4b, regardless of their reactivity in the particle phase.

Fig. 5 demonstrates how much SOA mass is contained in the different component groups throughout the simulation time. In general, the HOMs provide about 27 % of the simulated final total SOA mass and initiate SOA mass formation. For the chosen pseudo-first-order rate constant of particle reactions $k_c = 10^{-4}\,s^{-1}$, the remaining SOA mass is subdivided equally between the partitioning and the reacted products, whereby, for the liquid particles the mass contributed by the r-products increases over time. Accordingly, HOMs are important for fresh SOA formation since they provide the organic medium for SVOCs to partition into the aerosol phase and secondly induce further organic particle growth.

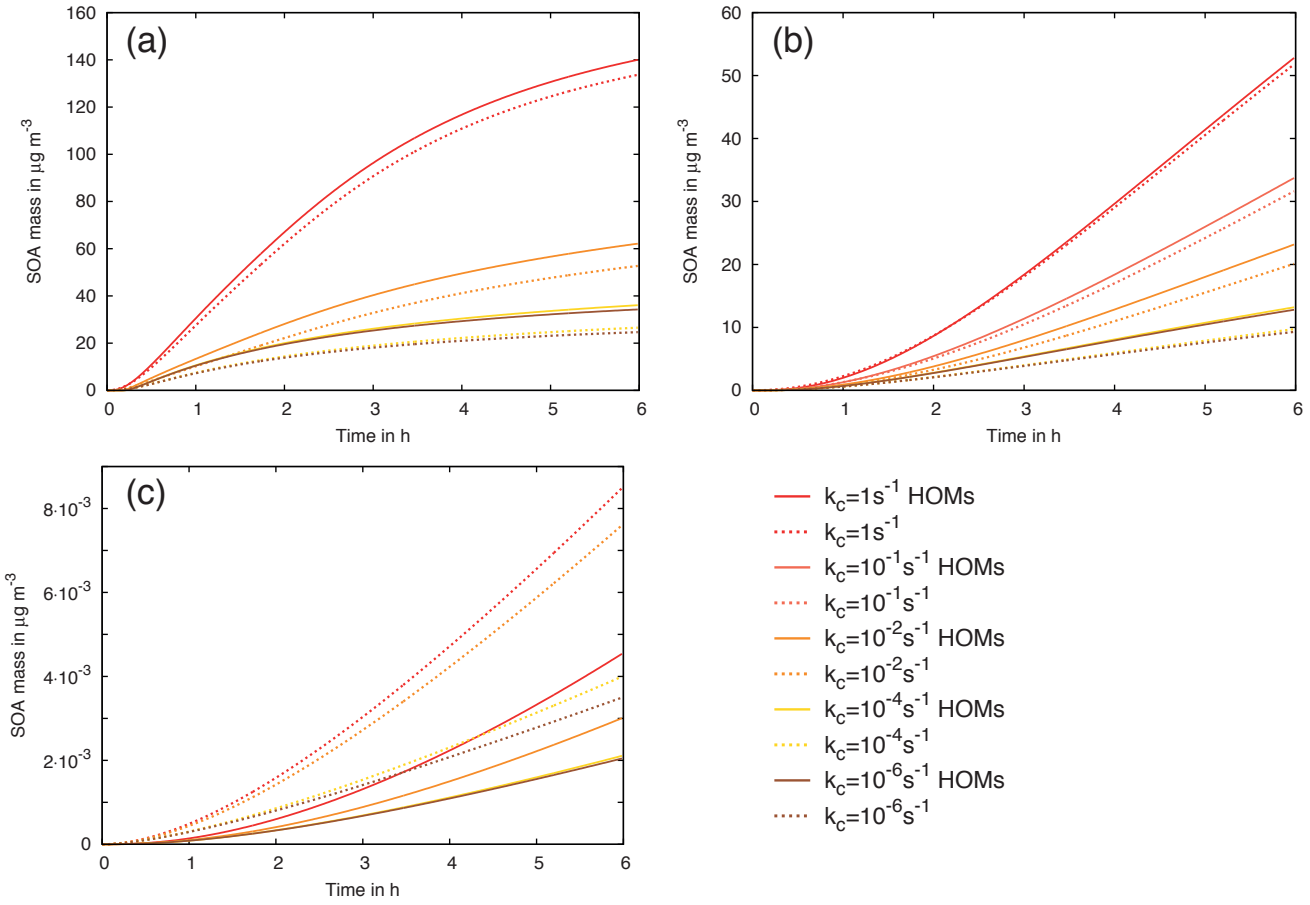

Figure 4. Simulated SOA mass including HOMs and additional variation of the pseudo-first-order rate constant of particle reactions k_c (case 6a and 6b of Table 1) for a) liquid ($D_b = 10^{-12}$ m^2 s^{-1}), b) transition between liquid and semi-solid ($D_b = 10^{-14}$ m^2 s^{-1}) as well as c) semi-solid ($D_b = 10^{-18}$ m^2 s^{-1}) aerosol particles.

3.3 Representation of reversible SOA formation pathways and the impacts on SOA

An additional backward reaction for every partitioned species has been implemented to further improve/refine the approach of Zaveri et al. (2014) and, thus, investigate the influence of particle phase chemical reactions in more detail. Backward reactions describe the reaction from the aged organic particle phase compounds to the original partitioned organic compounds that exchange directly with the gas phase. Organic aerosol-phase reactions can be irreversible reactions such as oxidation reactions or reversible reactions as for instance dimerization/oligomerization (Hallquist et al., 2009; Ziemann and Atkinson, 2012). For the observed particle-phase dimerization, different possible reaction mechanisms can be found in the literature: (i) hemiacetal formation due to reactions between alcohols and aldehydes or carbonyl compounds (Iinuma et al., 2004; Ziemann and Atkinson,

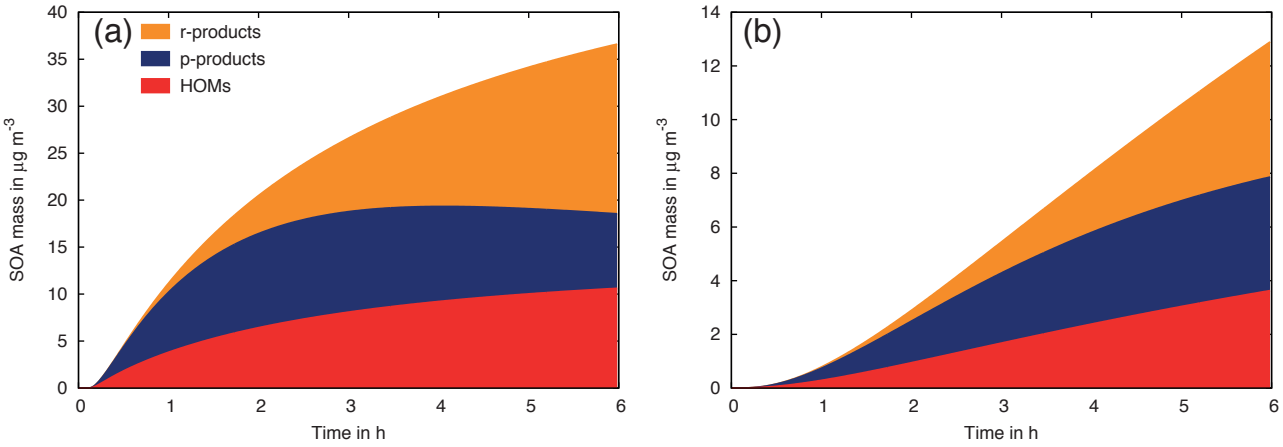

Figure 5. Simulated SOA mass including HOMs resolved for the different components for a) liquid ($D_b = 10^{-12}$ m^2 s^{-1}) and b) the transition between liquid and semi-solid ($D_b = 10^{-14}$ m^2 s^{-1}) aerosol particles and $k_c = 10^{-4}$ s^{-1}. Therein, p-products represent compounds which are partitioned from the gas phase in the particle phase and the r-phase includes compounds which are chemically processed by particle phase reactions.

2012; Carey and Sundberg, 2007), (ii) peroxyhemiacetal formation between hydroperoxides and carbonyl compounds (Tobias and Ziemann, 2000; Ziemann and Atkinson, 2012), (iii) aldol reaction products from the acid-catalyzed dimerization of a ketone or aldehyde (Carey and Sundberg, 2007; Casale et al., 2007), and (iv) esterfication due to reactions of carboxylic acids with alcohols (Surratt et al., 2006; Ziemann and Atkinson, 2012; Carey and Sundberg, 2007). Thermodynamic calculations indicate ester formation and peroxyhemiacetal formation as most likely (Barsanti and Pankow, 2006; DePalma et al., 2013) and suggest hemiacetal formation as thermodynamically unfavorable (Barsanti and Pankow, 2004; DePalma et al., 2013). Therefore, an irreversible representation of the aerosol chemistry might lead to an overprediction of the formed SOA mass, which means that can be only considered as an upper limit approach. The formed oligomers are complex compounds, which consist of a few monomer units. The oligomer equilibrium can be influenced by ambient conditions such as the temperature, relative humidity, and the chemical composition of the aerosol. A reversible representation of oligomerization reactions can be considered by means of an implemented backward reaction. E.g. Roldin et al. (2014) treats the kinetics of the reversible dimerization also with two separate reactions. However, an advanced kinetic treatment of particle-phase reactions is utilized considering monomer concentrations combined with second-order rate constants and dimer first-order degradation rates separated for bulk and surface layers. However, measurement data concerning dimerization reaction rates are scarce for condensed organic compounds and vary over several orders of magnitude (Antonovskii and Terent'ev, 1967). For the sensitivity study concerning the influence of the backward reaction on the predicted SOA mass, a simplified approach is tested. Therefore, we considered different backward reaction rate constants for particle-phase reactions (see Table 1, case 7) in addition to the pseudo-first-order rate constants. The implemented reactions are given in Table S3 in the Supplement. Fig. 6 shows the influence of the backward reactions in the

liquid particle phase on the formation of SOA. For a backward reaction rate of k_b=10^{-6} s^{-1} the SOA formation is almost equal to the cases without a backward reaction. The formed SOA concentrations decrease for the cases with fast backward reactions $k_b \geq 10^{-3}$ s^{-1}. This value is lower than for the reference case with a 10-fold lower chemical rate constant (see Fig. 6a and 6b). Fast particle-phase reactions (see Fig. 6a) combined with backward reactions $k_b \geq 10^{-2}$ s^{-1} induce slower SOA formation and decrease SOA concentrations with respect to a second reference case ($k_c = 10^{-1}$ s^{-1}). The SOA formation was faster than the base case with k_c=10^{-1} s^{-1} at the beginning, when k_c=1 s^{-1} combined with k_b=10^{-3} s^{-1}. However, for model runs considering backward reactions, the formed SOA is lower than for the reference case without backward reactions. Fig. 6b reveals a similar SOA formation for a more moderate chemical rate constant in the particle phase k_c=10^{-2} s^{-1} in comparison to the previous results using fast reactions. In combination with the slowest backward reactions k_b=10^{-6} s^{-1}, the formed SOA mass is almost equal to the reference case with k_c=10^{-2} s^{-1} and no backward reactions. Model simulations using backward reaction constants of $k_b \geq 10^{-3}$ s^{-1} show lowered SOA production. The formed SOA mass is lower than the reference case using k_c=10^{-3} s^{-1}. During the first hour of the simulation, the SOA formation evolves almost in the same way for all different cases. Afterwards, the three cases with a slow backward reaction k_b=$10^{-6} - 10^{-4}$ s^{-1} follow the SOA formation of the reference case with k_c=10^{-2} s^{-1}. The SOA formation for backward reactions with k_b=10^{-2} s^{-1} and k_b=10^{-3} s^{-1} behaves in the same way as described above for fast particle phase reactions (see Fig. 6b). The main benefit of the implementation of a sufficiently fast backward reaction ($k_b \leq 10^{-2}$ s^{-1}) is the asymptotic curve shape of the SOA mass for proceeding simulation times. This behavior is also observed during chamber studies (Ng et al., 2006), which indicate an equilibrium state of the gas and the particle phase after a proceeding oxidation time and concomitant consumption of the hydrocarbon.

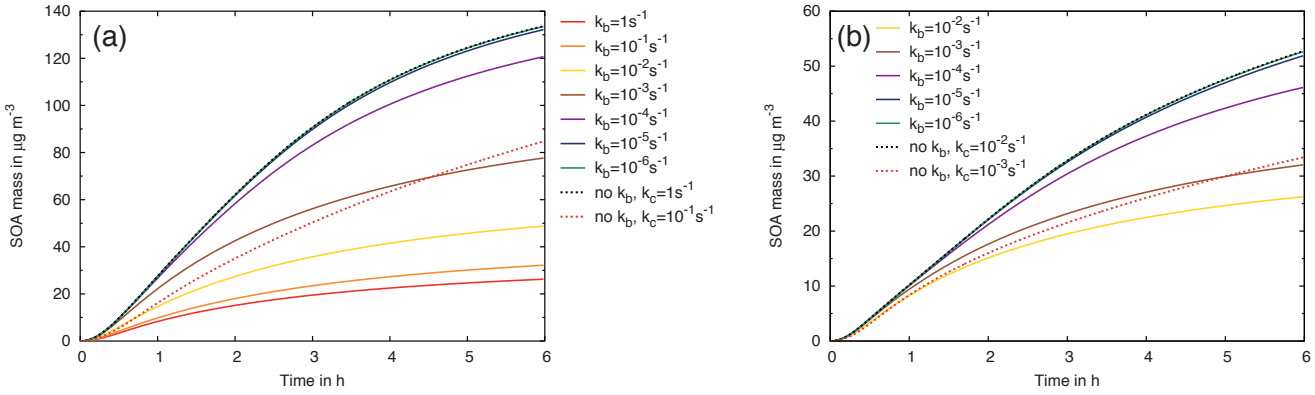

Figure 6. Simulated SOA mass including a chemical backward reaction in the particle phase for liquid ($D_b = 10^{-12}$ m^2 s^{-1}) aerosol particles (case 7 of Table 1) with a) a fast chemical reaction in the particle phase k_c=1 s^{-1} and b) a reduced rate constant k_c=10^{-2} s^{-1}, whereby backward reactions with different rate constants k_b are additionally included. The reference simulations for the respective k_c without backward reactions (indicated by "no k_b" in the key) are shown with dashed lines.

3.4 Impact of a weighted particle-phase bulk diffusion coefficient considering particle composition on SOA formation

This subsection examines the particle-phase bulk diffusion coefficient extensively, namely the influence of the effective particle-phase bulk diffusion coefficient on SOA formation. Inorganic seed is usually utilized for chamber experiments. The seed is often composed of a dissolved salt (e.g., ammonium sulfate) and water. For water and ionic molecules in concentrated aqueous solutions, diffusion coefficients are well known. A temperature-dependent diffusion coefficient for water is provided by Holz et al. (2000). Diffusion coefficients for ions in aqueous solution are listed in Cussler (2009). However, diffusion coefficients for organic compounds are not known and depend on the other compounds that exist in the particle phase. Literature data are available for bulk viscosity values of SOA under different RH conditions (Renbaum-Wolff et al., 2013a; Zhang et al., 2015; Grayson et al., 2016). However, these measurements represent the phase state of processed SOA particles after several hours in the chamber and various treatment steps. Also the conversion of viscosity to diffusion coefficients is an uncertainty factor as outlined by Marshall et al. (2016). The main goal of this sensitivity study is to calculate a composition weighted particle-phase bulk diffusion coefficient D_m for the particles over the entire simulation time. The individual diffusion coefficients are weighted by applying a Vignes type rule (Vignes, 1966; Wesselingh and Bollen, 1997) concerning the mole fractions x_i:

$$D_\mathrm{m} = \left[D_\mathrm{org}^{x_\mathrm{org}}\right] \times \left[D_\mathrm{inorg}^{x_\mathrm{inorg}}\right] \times \left[D_\mathrm{water}^{x_\mathrm{water}}\right]. \tag{10}$$

Equation (10) describes the calculation of a mean or weighted particle-phase bulk diffusion coefficient D_m under consideration of the compound specific diffusion coefficients for water D_water, dissolved ions D_inorg (here ammounium sulfate), and organic compounds D_org including their corresponding mole fractions x_water, x_inorg, and x_org, respectively (more details are given in the Supplement). However, the diffusion coefficient of the pure organic compound mixture is not known from measurements or tabulated for the single compounds. Therefore, we utilize the results from Sect. 3.1.1 to estimate D_org in an appropriate way. We conducted two sensitivity studies, one with $D_\mathrm{org} = 10^{-12}\,\mathrm{m^2\,s^{-1}}$ and the second with $D_\mathrm{org} = 10^{-14}\,\mathrm{m^2\,s^{-1}}$ under additional variation of the pseudo-first-order rate constant of particle reactions k_c (see Table 1, case 8). The impact of increasing organic mole fractions of aerosols on the time evolution of SOA formation has been investigated with this approach. Thereby, the variation of the chemical rate constants for particle phase reactions induces different time evolutions of organic mass increase (see Sect. 3.1.2). In Fig. 7a the modeled SOA formation is shown for applying a weighted particle-phase bulk diffusion coefficient with $D_\mathrm{org} = 10^{-12}\,\mathrm{m^2\,s^{-1}}$ and for comparison with a constant particle-phase bulk diffusion coefficient of $D_\mathrm{b} = 10^{-12}\,\mathrm{m^2\,s^{-1}}$, respectively. The main difference of this study is the slightly faster increase of SOA mass at the beginning of the simulation for the weighted particle-phase bulk diffusion coefficient. The reason for this behavior is the higher initial particle-phase bulk diffusion coefficient in the order of $D_\mathrm{m} = 10^{-12}\,\mathrm{m^2\,s^{-1}}$ of the seed composed of ammonium sulfate and water. The simulation results under consideration of $D_\mathrm{org} = 10^{-14}\,\mathrm{m^2\,s^{-1}}$ are compared to the results using a constant particle-phase bulk diffusion coefficient of $D_\mathrm{b} = 10^{-12}\,\mathrm{m^2\,s^{-1}}$ (Fig. 7b) and $D_\mathrm{b} = 10^{-14}\,\mathrm{m^2\,s^{-1}}$ (Fig. 7c). A faster uptake of organic mass occurs in the first minutes for a weighted particle-phase bulk diffusion coefficient (Fig. 7b). With an increasing organic mass the weighted particle-phase bulk diffusion coefficient drops below a value of $D_\mathrm{b} = 10^{-12}\,\mathrm{m^2\,s^{-1}}$ with the consequence of slower and less effective SOA formation (about 37 % decrease for k_c=1 $\mathrm{s^{-1}}$). Fig. 7 reveals that the total SOA mass is increased by about 40 – 50 % for a weighted particle-phase bulk diffusion coefficient ($D_\mathrm{org} = 10^{-14}\,\mathrm{m^2\,s^{-1}}$) compared to simulation results

with a constant particle-phase bulk diffusion coefficient of $D_b = 10^{-14}\,m^2\,s^{-1}$. Additionally, the SOA formation is faster for the weighted particle-phase bulk diffusion coefficient.

Overall, the simulations have shown that the obtained model results are sensitive to a composition-dependent particle-phase bulk diffusion coefficient, which is obvious when compared with results for constant particle-phase bulk diffusion coefficient. The assumption of a slower diffusion coefficient for the organic material might be justified due to the high bulk viscosity from measurements (Renbaum-Wolff et al., 2013a; Zhang et al., 2015; Grayson et al., 2016). The application of a modified Vignes type rule for the calculation of a weighted particle-phase bulk diffusion coefficient is already mentioned and applied by Lienhard et al. (2014, 2015) and Price et al. (2015) for the water diffusion coefficient in SOA particles. The applicability of Eq. (10) within the kinetic approach of Zaveri et al. (2014) is checked and verified under the utilization of the model by Zobrist et al. (2011) as basis for evaluation (S. O'Meara, personal communication). Fig. S7a and S7b in the Supplement display the differences for the numerical solution from the model of Zobrist et al. (2011) and the analytical solution of the kinetic approach with the weighted particle-phase bulk diffusion coefficient for $D_{org} = 10^{-11}\,m^2\,s^{-1}$ and $D_{org} = 10^{-13}\,m^2\,s^{-1}$, respectively. For both assumed self-diffusion coefficients of the organic fraction, the numerical and analytical solution are equal within 1×10^{-6} s and 1×10^{-4} s. Thus, Eq. (10) can applied to the kinetic approach instead of a constant bulk diffusion coefficient. However, improved particle-phase bulk diffusion coefficient data depending on relative humidity and organic mass loading will be needed to improve current model implementations.

3.5 Comparison with performed LEAK chamber measurements

Selected simulation results have been compared with measurements from the aerosol chamber LEAK for α-pinene ozonolysis investigations. The simulations show only results for the narrow range of the investigated parameter setup. Figure 8a and 8b present simulation results for the combination of the three newly implemented model features from Sects. 3.2 to 3.4 in comparison with the results from the base kinetic approach and measurements. Wall loss effects are not considered in this study, due to the short experiment time (2 h). However, for longer experiment duration particle and gas wall loss might be an important process for chamber studies and have to be considered in modeling (Zhang et al., 2014). The simulations shown in Fig. 8a are conducted with an effective particle-phase bulk diffusion coefficient considering an organic diffusion coefficient of $D_{org} = 10^{-12}\,m^2\,s^{-1}$. The pseudo-first-order rate constant of particle reactions is set to $k_c = 10^{-2}\,s^{-1}$ and only the backward reaction constants have been varied. Simulations with a particle-phase bulk diffusion coefficient of $D_b = 10^{-12}\,m^2\,s^{-1}$ and $k_c = 10^{-2}\,s^{-1}$ (ref. case I) as well as $k_c = 10^{-3}\,s^{-1}$ (ref. case II) are selected as reference cases. In general, the reference simulation with $k_c = 10^{-3}\,s^{-1}$ is in good agreement with the LEAK measurements (Fig. 8a, ref. case II). However, the simulated SOA mass is systematically underestimated for the first 1.5 h. This might be caused by not considered HOM yields and a too low particle-phase bulk diffusion coefficient for the early stage of SOA formation. For $k_c = 10^{-2}\,s^{-1}$ this initial underestimation is marginal (Fig. 8a, ref. case I). On the other hand, the overestimation of SOA becomes obvious for $k_c = 10^{-2}\,s^{-1}$ after 1 h simulation time and characterizes the simulated SOA mass till the end of the experiment time. Therefore, the formed SOA mass for the base parametrization appears to lead to initial underestimation or final overestimation. Consideration of the weighted particle-phase bulk diffusion coefficient and HOMs lead to a faster SOA mass increase at the beginning of the

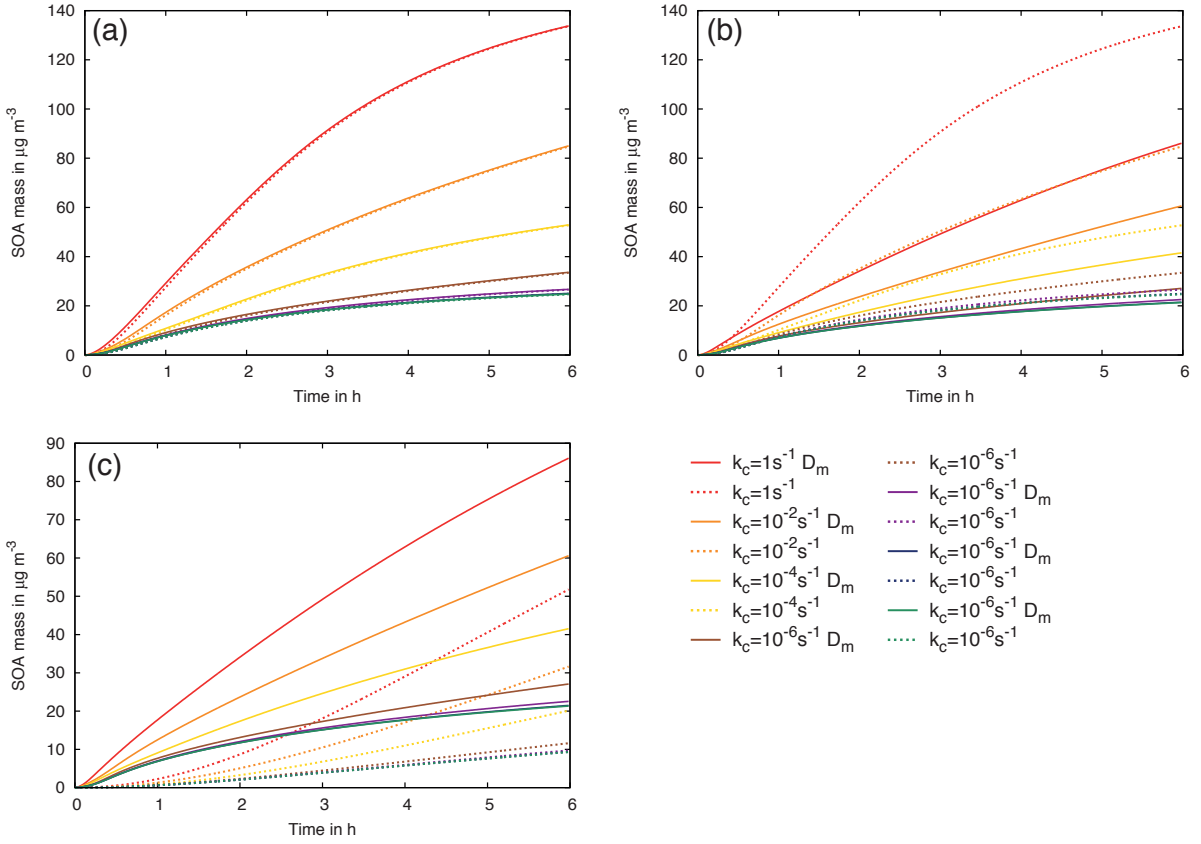

Figure 7. Simulated SOA mass considering an effective particle-phase bulk diffusion coefficient under additional variation of the pseudo-first-order rate constant of particle reactions k_c (case 8 of Table 1). a) Organic material is considered with a diffusion coefficient of $D_{org} = 10^{-12}\,m^2\,s^{-1}$ in the weighted particle-phase bulk diffusion coefficient D_m (solid lines) and for comparison the results for $D_b = 10^{-12}\,m^2\,s^{-1}$ are shown (dashed lines); b) Organic material is considered with a diffusion coefficient of $D_{org} = 10^{-14}\,m^2\,s^{-1}$ in the weighted particle-phase bulk diffusion coefficient D_m (solid lines) and for comparison the results for $D_b = 10^{-12}\,m^2\,s^{-1}$ are shown (dashed lines); c) Organic material is considered with a diffusion coefficient of $D_{org} = 10^{-14}\,m^2\,s^{-1}$ in the weighted particle-phase bulk diffusion coefficient D_m (solid lines) and for comparison the results for $D_b = 10^{-14}\,m^2\,s^{-1}$ are shown (dashed lines).

simulation when the organic amount is low in the particle phase. The decreasing particle-phase bulk diffusion coefficient due to the uptake of further organic material and the backward reactions in the particle phase induce a flattening of the mass increase. Nevertheless, the SOA mass is highly overestimated, which might be caused by the high particle-phase bulk diffusion coefficient of the organic material. The simulations with an effective particle-phase bulk diffusion coefficient (Fig. 8a) are reproduced with a smaller diffusion coefficient for the organic material $D_{org} = 10^{-14}\,m^2\,s^{-1}$. The results for these simulations are presented in Fig. 8b where the same reference simulations as shown in Fig. 8a are utilized. Figure 8b reveals that all five simulations with the weighted particle-phase bulk diffusion coefficient start nearly at the same time as observed in the exper-

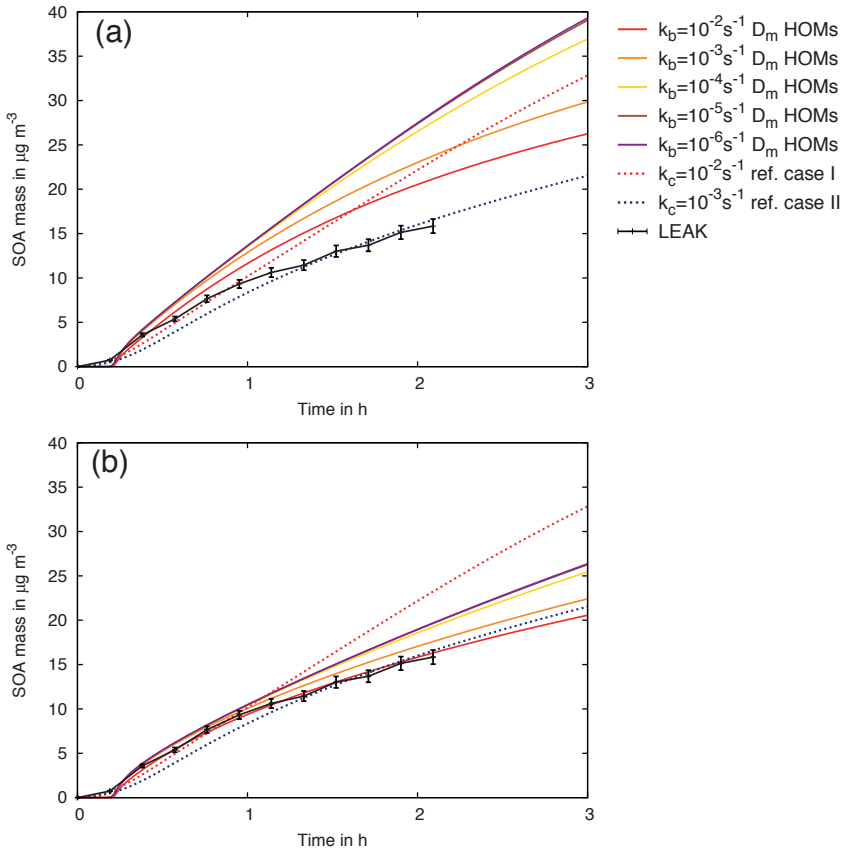

Figure 8. Simulated SOA mass considering an effective particle-phase bulk diffusion coefficient as well as HOMs, a constant pseudo-first-order rate constant of particle reactions $k_c = 10^{-2}\,s^{-1}$ and under additional variation of the chemical backward reaction rate constant of particle reactions k_b in comparison with aerosol chamber measurements from LEAK. a) Organic material is considered with a diffusion coefficient of $D_{org} = 10^{-12}\,m^2\,s^{-1}$ in the weighted diffusivity D_m (solid lines); b) Organic material is considered with a diffusion coefficient of $D_{org} = 10^{-14}\,m^2\,s^{-1}$ in the weighted diffusivity D_m (solid lines). For comparison, in both plots the results for a constant particle-phase bulk diffusion coefficient $D_b = 10^{-12}\,m^2\,s^{-1}$ combined with two different pseudo-first-order rate constants of particle reactions $k_c = 10^{-2}\,s^{-1}$ (ref. case I) and $k_c = 10^{-3}\,s^{-1}$ (ref. case II) are included (dashed lines).

iment with the formation of SOA. After 1 h simulation time, it is obvious that the simulated concentration profile agrees well with the experimentally observed SOA mass when using a backward reaction rate constant of k_b=$10^{-2}\,s^{-1}$. The high initial particle-phase bulk diffusion coefficient, $D_m \approx 2 \times 10^{-9}\,m^2\,s^{-1}$ (see Fig. 9), for the aqueous ammonium sulfate seed particles enables a fast diffusion in the aerosol particles. Thus, immediately partitioning HOMs can be absorbed quickly into the particle phase. Within the first 30 min of the simulation time, the SOA mass sharply increases and the weighted particle-phase bulk diffusion coefficient drops about three orders of magnitude. Consequently, the mixing time in the particle phase increases and this leads to a slower SOA mass formation. This process is depicted in Fig. 9, where for the first hour of simulation time the major

changes in the weighted particle-phase bulk diffusion coefficient and the SOA mass can be seen. After the weighted particle-phase bulk diffusion coefficient has reduced to a value $D_m \approx 10^{-13}$ m^2 s^{-1}, the longer mixing time will cause a slower SOA formation as already shown in Fig. 1b. This effect is further pronounced due to continuous SOA formation and a concomitant decrease in particle-phase diffusion. By means of the implementation of HOMs, no initial organic particle mass is necessary to enable partitioning after a short oxidation time ($\approx$ 8 min). The effective particle-phase bulk diffusion coefficient is reduced and the mixing time increases by increasing the organic mass over the time, slowing down SOA mass formation (see Fig. 9). Furthermore, the chemical backward reactions in the particle phase induce an equilibrium state, e.g. for the oligomer formation. Accordingly, an equilibrium is also achieved between the gas and the p-products in the particle phase for the semi-volatile compounds. Additionally, to the good agreement of simulated total SOA mass, the flattening with increasing organic mass better represents the time profile of SOA. Here, HOMs provide about 27 % of the simulated total SOA mass at the end of the simulation time (see Fig. 10). This points out the important role of HOMs for initial SOA formation. Additionally, the chemical analysis of the filter measurements from LEAK revealed that organic peroxides contribute to the formed organic mass, which agrees with the simulated partitioning of HOMs into the particle phase. Moreover, Fig. 10b shows that the HOMs mainly parti-

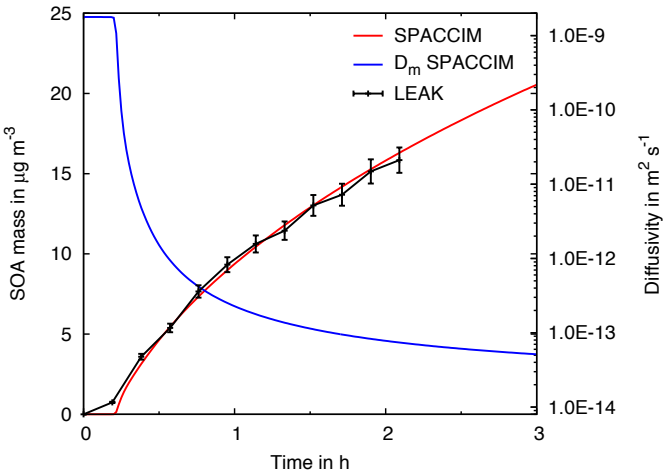

Figure 9. Simulated SOA mass as shown in Fig. 8 for $k_c = 10^{-2}$ s^{-1}, $k_b = 10^{-2}$ s^{-1}, under consideration of HOMs, and with the weighted diffusion coefficient utilizing $D_{org} = 10^{-14}$ m^2 s^{-1} in comparison to the measured SOA mass from the LEAK experiment. The corresponding weighted particle-phase bulk diffusion coefficient D_m from the simulation is displayed on the secondary y-axis.

tion in the first minutes of the simulation into the particle phase. For the simulation of SOA formation shown in Fig. 8 and Fig. 10, the vapor pressure estimates of the HOM compounds have been taken as given by Berndt et al. (2016) for the calculation with COSMO-RS (Eckert and Klamt, 2002). COSMO-RS is based on quantum chemical methods and the calculation of the molecular surface (Eckert and Klamt, 2002), which enables a more accurate estimation of thermodynamic properties and might be more precise than group contribution methods (Kurtén et al., 2016). For comparison, the vapor pressures of the HOMs have been estimated with the group contribution methods SIMPOL (Pankow and Asher, 2008) and EVAPORATION (Compernolle

et al. (2011), see Table S4 in the Supplement) and accordingly, the SOA formation have been simulated for every method. The total SOA mass deviates maximally by 11 % from the SOA mass formed with COSMO-RS vapor pressure estimates (see Fig. S8a in the Supplement). However, the temporal curve shape of SOA formation and the relative contribution of the three product classes to the total organic mass deviates between model simulations utilizing different HOM vapor pressures. Thus, for the vapor pressures estimated by EVAPORATION, the HOMs contribute in the first 15 minutes of SOA formation between 97 and 100 % to the organic mass (see Fig. S8d in the Supplement). This is a higher contribution as for the other model simulations (see Fig. S8b and S8c in the Supplement) and the time period for this high contribution is longer. Due to the fact that the vapor pressures of the HOMs from α-pinene ozonolysis might be lower than the utilized values, the relative contribution of HOMs to the initial SOA formation could be higher than indicated by the simulation with COSMO-RS vapor pressures.

Gas-phase concentrations of the reactants α-pinene and ozone (see Fig. 11a and 11b) as well as a first reaction product named

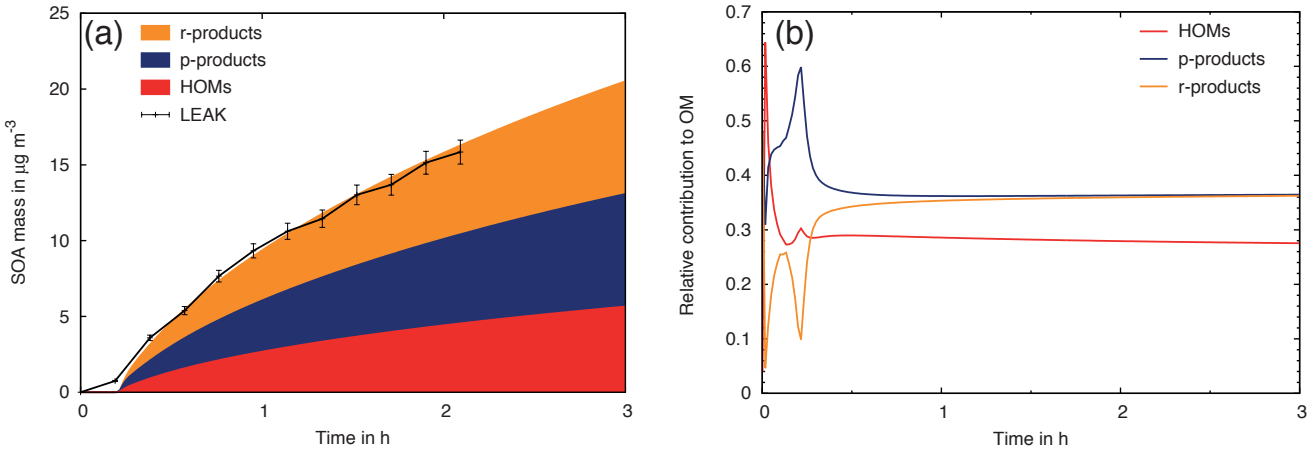

Figure 10. a) Simulated SOA mass as shown in Fig. 8b for $k_b = 10^{-2}\,s^{-1}$ resolved for the different components and compared with aerosol chamber measurements from LEAK. b) Relative contribution of the individual product classes to the total organic mass.

pinonaldehyde (Fig. 11c) have also been compared with smog chamber measurements. Corresponding gas-phase concentrations for the preferred model setup of Fig. 8b, with $k_b = 10^{-2}\,s^{-1}$, of the reactants α-pinene and ozone (see Fig. 8a and 8b) as well as a first reaction product named pinonaldehyde (Fig. 8c) have also been compared with smog chamber measurements. The simulation for the α-pinene depletion is in a very good agreement with the measured concentration decrease of α-pinene (Fig. 11a). The depletion of ozone is slightly overestimated by the model (see Fig. 11b). After half an hour, the measured ozone concentration decreases not so fast as initially started. Experimentally, ozone is measured with an ozone monitor (49c Ozone Analyzer, Thermo Scientific, USA) and this device is based on measuring absorption on characteristic wavelengths. For measuring ozone, the absorption at 254 nm is utilized. According to Docherty et al. (2005), the ozonolysis of α-pinene yields up to 47 % organic peroxides. As organic peroxides absorb light at 254 nm, an overestimation of the signal detected by the ozone monitor caused by the high amount of organic peroxides cannot be excluded. Therefore, with the increase of the hydroperoxide concentration over the experiment time the overestimation of the ozone concentration by the monitoring

system might increase and the underestimation by the model can be caused. Further, the measured gas-phase concentration of pinonaldehyde is underestimated by the model (Fig. 11c). This cannot be caused by an excessive partitioning of pinonaldehyde into the particle phase because pinonaldehyde is characterized by a high saturation vapor pressure and there is no effective partitioning into the particle phase. However, the formation of pinonaldehyde is measured by a proton-transfer-reaction mass spectrometer (PTR-MS) at *m/z* 169 ($[M+H]^+$). The PTR-MS technique enables only the detection of the *m/z* ratio. No further information were obtained. Thus, compounds or fragments with the same *m/z* were detected as well resulting in an overestimation of the pinonaldehyde concentration measured by PTR-MS. This circumstance can cause the underestimation of the gas-phase concentration of pinonaldehyde (see Fig. 11c). To investigate the underestimation of pinonaldehyde concentration additionally from the site of the model, we evaluated the branching ratios of the α-pinene with ozone reaction. Based on the results of Berndt et al. (2003), the pinonaldehyde yield was artificially increased in the mechanism to investigate the sensitivity of the pinonaldehyde on this yield. The results of this modification in the gas-phase chemistry mechanism are shown within Figs. 11a to 11d. For the reactants, no difference between the two simulations is observed (Fig. 11a and 11b). However, the pinonaldehyde concentrations fit very well with the measured values from the smog chamber (Fig. 11c). Due to the high vapor pressure of pinonaldehyde, the SOA mass decreases by about 20 % due to the increased pinonaldehyde yield in the modified gas-phase chemistry mechanism (see Fig. 11d). Nevertheless, the results of the modified kinetic partitioning approach fit better with the measurements than the reference simulations.

3.6 Limitations of the present studies

The presented model studies do not account for the Kelvin effect. The Kelvin effect describes the change of the vapor pressure due to a curved liquid-vapor interface and is especially important for small particles because of their higher curvature (Seinfeld and Pandis, 2006; Pruppacher and Klett, 2010). The vapor pressure of a compound i over a flat surface $p_{\mathrm{sat},i}$ (atm) can be corrected to the partial vapor pressure over a curved interface $p_i^{\ominus}$ (atm, Seinfeld and Pandis, 2006). The correction factor depends strongly on the particle size and the surface tension of the considered aerosol particle/droplet. The surface tension varies with the composition of the aerosol particle (Facchini et al., 1999; Hitzenberger et al., 2002; Ervens et al., 2004, 2005), e.g. it is increased by dissolved salts (Seinfeld and Pandis, 2006) and decreased by organic compounds (Facchini et al., 1999; Ervens et al., 2005). However, for the estimation of the vapor pressures for the partitioning compounds a group contribution method (EVAPORATION, Compernolle et al., 2011) is applied in this study. An investigation of O'Meara et al. (2014) reveals that the vapor pressure estimates from the different group contribution methods vary from each other and deviate from existing measurements up to six orders of magnitude. Further, Kurtén et al. (2016) showed the differences between the vapor pressures estimated by three different group contribution methods and COSMO-RS (conductor-like screening model for real solvents, Eckert and Klamt, 2002). Therein, 8 orders of magnitude lower vapor pressures are estimated by group contribution methods than COSMO-RS for some highly oxidized monomers. Therefore, the correction of the vapor pressure by the Kelvin effect might be in the order of the error range of the applied group contribution method. For this reason, we have not considered the Kelvin effect in our calculations.

This study utilizes a simplified scheme to consider particle-phase reactions in order to account for SOA aging. The kinetic

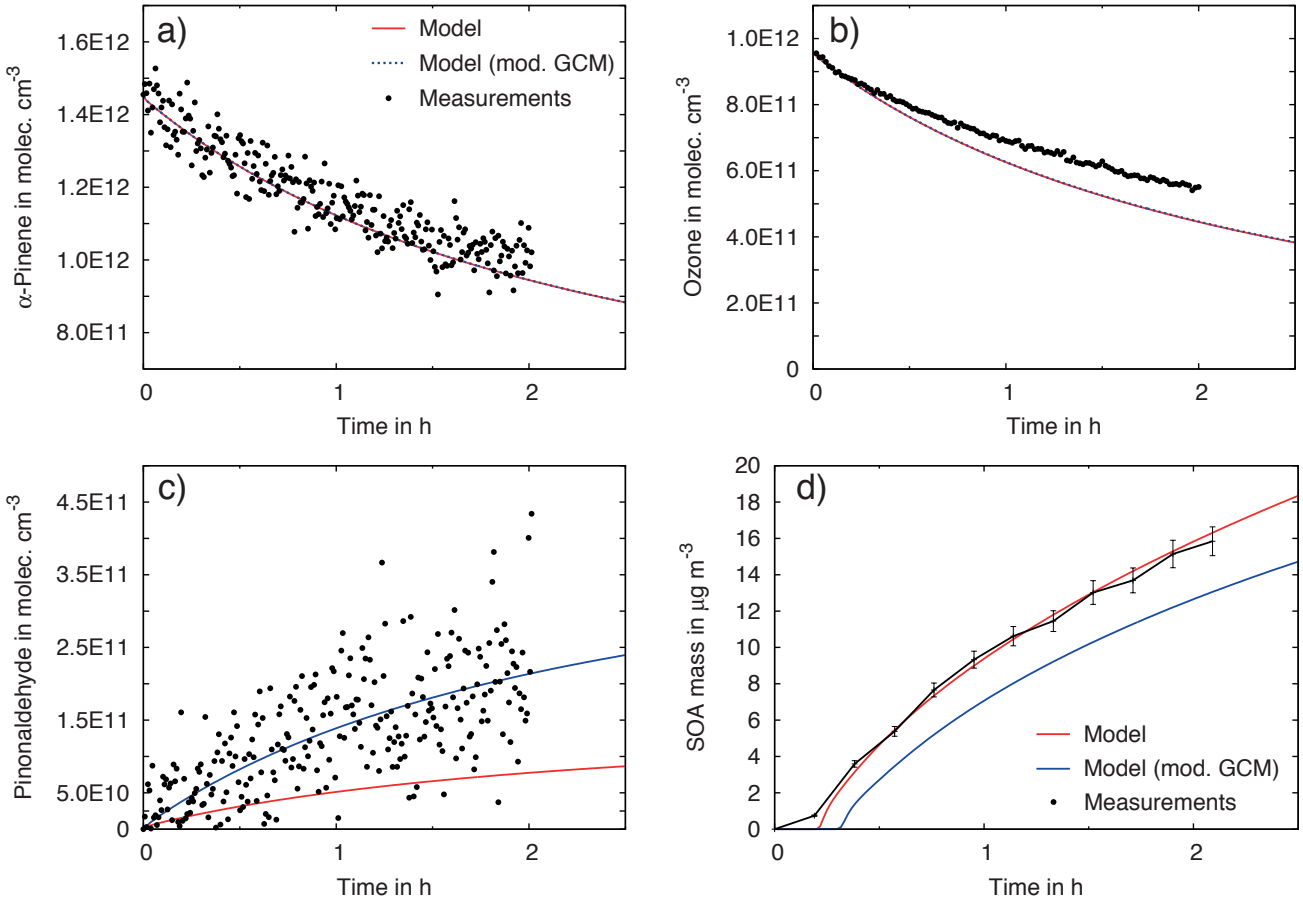

Figure 11. Simulation results for the preferred case of Fig. 8b with $k_b = 10^{-2}\,s^{-1}$ (solid red line) and an additional model run with modified gas-phase chemistry mechanism (GCM, pinonaldehyde yield as provided by Berndt et al. (2003) dashed/ solid blue line) in comparison with measurements from LEAK (black dots). Gas-phase concentrations for the reactants a) α-pinene and b) ozone are shown as well as a first-order product c) pinonaldehyde and d) the SOA mass.

approach of Zaveri et al. (2014) is divided into two reaction cases according to the rate of the particle-phase reactivity based on the achievement of the steady state. In Sect. 3.3, a modification of the particle-phase reactivity is presented in order to improve the representation of SOA aging under preservation of the basic classification/separation in fast and slow particle-phase reactions. This simplified approach is appropriate for application in 3-D models, treating organic compounds in lumped groups, and saves computational effort. However, for future chamber simulations with the focus on SOA processes combined with advanced measurement data, accounting for SOA aging or oxidation state, an improved representation of particle-phase reactivity will be implemented to further develop SPACCIM. Therefore, the pseudo-first-order rate constants will be replaced, e.g. by second-order equilibrium reactions under consideration of equilibrium rates provided by Barsanti and Pankow (2004)

for hydrate and hemiacetal formation or thermodynamic calculations for equilibrium constants of DePalma et al. (2013) for individual dimers.

4 Conclusions

The kinetic partitioning approach by Zaveri et al. (2014) has been implemented in the SPACCIM model in this study. Extensive sensitivity studies were performed to investigate the dependence of the SOA formation on i) the particle-phase bulk diffusion coefficient D_b, ii) the chemical reaction rate constant of the solute within the particle phase k_c, iii) particle radius r_p, and iv) the initial organic particle phase mass OM_O. The influence of HOMs on SOA formation was additionally investigated. Moreover, the kinetic approach was extended by both a chemical backward reaction of the solute within the particle phase k_b and a composition-dependent particle-phase bulk diffusion coefficient D_m.

Overall, the conducted sensitivity studies reveal that the particle-phase bulk diffusion coefficient is the key parameter for the simulation of SOA formation and processes. In liquid particles ($D_b = 10^{-9} - 10^{-13}\,m^2\,s^{-1}$) 310-times or 66-times more SOA is formed than in higher viscous aerosol particles ($D_b = 10^{-17} - 10^{-21}\,m^2\,s^{-1}$), using a high or a negligible particle-phase reactivity, respectively. For a wide range of particle-phase bulk diffusion coefficients ($D_b = 10^{-9} - 10^{-14}\,m^2\,s^{-1}$) almost the same SOA mass can be produced if long equilibration times are considered. However, on the time scale of chamber experiments, the observed equilibration time for SOA formation is shorter than that observed from the simulation with a constant particle-phase bulk diffusion coefficient of $D_b = 10^{-14}\,m^2\,s^{-1}$. Nevertheless, for a high particle-phase bulk diffusion coefficient ($D_b > 10^{-14}\,m^2\,s^{-1}$), the SOA mass is overestimated by about 40 % if the initial increase of organic mass is in good agreement due to a fast and irreversible particle phase reaction. The pseudo-first-order rate constant for particle reactions k_c is shown to be a second key parameter for the description of organic mass in the particle phase to reflect oligomerization and aging. A large fraction of the formed SOA (61 % for model case 6) consists of chemically processed organic compounds, for liquid particles and a moderate rate of chemical particle reactions (k_c=$10^{-4}\,s^{-1}$). Up to now, the rate constants for such processes are not extensively evaluated, which introduces a large uncertainty to the applicability of this parameter in the model. Therefore, further kinetic and mechanistic studies are needed to better characterize the aerosol particle reactivity and the resulting contribution to the SOA processing. Additionally, the results of the sensitivity studies have revealed that the SOA mass continues to be formed if there are chemical backward reactions in the particle phase are neglected or the particle-phase bulk diffusion coefficient is not reduced due to the increase in organic material. However, the simulated temporal curve shape of constant SOA formation is in contrast to the result of the experiment. The performed studies with the advanced model show a benefit for SOA modeling particularly for the predicted SOA concentration-time profile and the overall SOA mass. The overprediction of the SOA mass has been reduced by about 40 % and the simulated temporal curve shape of SOA formation shows a much better agreement with measured SOA yields from the LEAK chamber. Besides the development of the partitioning approach, the extension of the gas-phase chemistry mechanism for α-pinene considering HOMs has been shown to be a key factor for modeling SOA formation, particularly at the early stage of the chamber experiments. HOMs play a major role for initial SOA formation from α-pinene because up to 65 % of OM is provided by them at the early stage of the simulation

and about 27 % of the SOA mass is formed by HOMs at the end of the simulation. Additionally, due to the consideration of the low-volatile HOMs, no need for initial organic particle mass exists and a better agreement with the observed SOA time profiles can be achieved. In conclusion, this study has (i) demonstrated the applicability of the kinetic approach (Zaveri et al., 2014) in the SPACCIM model, (ii) revealed the main key factors controlling the SOA formation, (iii) pointed out the current uncertainties/limitations of the approach, and (iv) showed the needs for further laboratory measurements as well as advanced model comparisons with chamber experimental data.

Appendix A: Description of the kinetic partitioning approach according to Zaveri et al. (2014)

The existing model framework has been extended by the implementation of the kinetic partitioning approach established by Zaveri et al. (2014). The basic assumption of this approach is the description of the diffusive flux of a solute in the particle phase via Fick's second law extended by a particle phase reaction of the solute:

$$\frac{\partial A_i(r,t)}{\partial t} = D_{\mathrm{b},i}\frac{1}{r^2}\frac{\partial}{\partial r}\left(r^2\frac{\partial A_i(r,t)}{\partial r}\right) - k_{\mathrm{c},i}A_i(r,t)\,. \tag{A1}$$

Thereby, the utilized parameters are the particle-phase concentration A_i of the solute i as a function of the radius r and the time t, the particle-phase bulk diffusion coefficient of the solute $D_{\mathrm{b},i}$, and the chemical reaction rate constant $k_{\mathrm{c},i}$ of the solute within the particle phase. Equation (A1) is in spherical coordinates and there is a fundamental simplification concerning the diffusion coefficient. Here, the diffusion coefficient is assumed to be constant and, therefore, a bulk diffusion coefficient $D_{\mathrm{b},i}$ for the particle phase is introduced. This assumption simplifies the calculation of the integral (Eq. A1). For the solution of the transient partial differential equation (Eq. A1) the particle is assumed to be spherically symmetrical concerning the concentration profiles of the solute inside the considered particle. Therefore, the following initial and boundary conditions are defined by Zaveri et al. (2014):

Initial condition: $A_i(r,0) = 0\,,$ (A2a)

Boundary condition 1: $A_i(r_{\mathrm{p}},t) = A_i^{\mathrm{s}}\,,$ (A2b)

Boundary condition 2: $\dfrac{\partial A_i(0,t)}{\partial r} = 0\,.$ (A2c)

First, Eq. (A1) is analytically solved by means of (Eq. A2a to A2c) without consideration of the chemical reaction (Carslaw and Jaeger, 1959; Crank, 1975). The solution for taking account of a first-order chemical reaction in the particle phase is provided by Danckwarts (1951) and the integration of this solution in order to quantify the average particle-phase concentration $\overline{A}(t)$ yields:

$$\frac{\overline{A}_i(t)}{A_i^{\mathrm{s}}} = \frac{\int_0^{r_{\mathrm{p}}} 4\pi r^2 \frac{A_i(r,t)}{A_i^{\mathrm{s}}}\mathrm{d}r}{\frac{4}{3}\pi r_{\mathrm{p}}^3} = Q_i - U_i(t)\,, \tag{A3}$$

where

$$Q_i = 3\left(\frac{q_i \coth q_i - 1}{q_i^2}\right), \tag{A4}$$

$$U_i(t) = \frac{6}{\pi^2}\sum_{n=1}^{\infty}\frac{exp\left\{-\left(k_{\mathrm{c},i} + \frac{n^2\pi^2 D_{\mathrm{b},i}}{r_{\mathrm{p}}^2}\right)t\right\}}{(q_i/\pi)^2 + n^2}. \tag{A5}$$

Thereby, r_{p} is the particle radius and $q_i = r_{\mathrm{p}}\sqrt{k_{\mathrm{c},i}/D_{\mathrm{b},i}}$ is a dimensionless diffusion–reaction parameter. Zaveri et al. (2014) describe Q_i as steady state term and $U_i(t)$ as transient term, which equals Q_i at $t = 0$ and decreases exponentially to zero when $t \to \infty$. Whereby, t denotes here the time since the start, which can only be monitored in a Lagrangian box model for a "closed system". Zaveri et al. (2014) review that the gas-phase concentration profile of the solute around the particle is at a quasi-steady state. To describe the gas-particle partitioning, Zaveri et al. (2014) propose an ordinary differential equation:

$$\frac{\mathrm{d}\overline{A}_i}{\mathrm{d}t} = \frac{3}{r_{\mathrm{p}}}k_{\mathrm{g},i}\left(\overline{C}_{\mathrm{g},i} - C_{\mathrm{g},i}^{\mathrm{s}}\right) - k_{\mathrm{c},i}\overline{A}_i, \tag{A6}$$

whereby, $\overline{C}_{\mathrm{g},i}$ is the average bulk gas-phase concentration, $C_{\mathrm{g},i}^{\mathrm{s}}$ is the gas-phase concentration of the solute just outside the surface of the aerosol particle, and $k_{\mathrm{g},i}$ denotes the gas-side mass-transfer coefficient. The gas-side mass transfer coefficient depends on the gas diffusion coefficient, the particle radius, and the transition regime correction factor (Fuchs and Sutugin, 1971), which is a function of the Knudsen number and the mass accommodation coefficient ($0 \leq \alpha_i \leq 1$). Under atmospheric conditions interfacial phase equilibrium is achieved in a fractional amount of a second, which is meaningful for the description of gas-to-particle mass transfer. The concentrations of an individual compound in the gas and the aerosol phase are linked by means of the effective saturation vapor concentration $C_{\mathrm{g},i}^{*}$ and the total organic aerosol mass at the surface $\sum_j A_j^{\mathrm{s}}$:

$$C_{\mathrm{g},i}^{\mathrm{s}} = \frac{A_i^{\mathrm{s}}}{\sum_j A_j^{\mathrm{s}}}C_{\mathrm{g},i}^{*}. \tag{A7}$$

Under consideration of Eq. (A3) and (A7) with the approximation of $\sum_j A_j^{\mathrm{s}}$ by $\sum_j \overline{A}_j$, the mass transfer in Eq. (A6) yields to:

$$\frac{\mathrm{d}\overline{A}_i}{\mathrm{d}t} = \frac{3}{r_{\mathrm{p}}}k_{\mathrm{g},i}\left\{\overline{C}_{\mathrm{g},i} - \frac{\overline{A}_i}{\sum_j \overline{A}_j}\frac{C_{\mathrm{g},i}^{*}}{(Q_i - U_i(t))}\right\} - k_{\mathrm{c},i}\overline{A}_i. \tag{A8}$$

Due to the time-dependent transient term $U_i(t)$ the approach is limited for usage in box models for "closed systems". To use the approach also in 3-D models without restrictions, some modifications have been proposed by Zaveri et al. (2014). According to their general sensitivity study concerning the time scales for a quasi-steady state, they can resolve that a distinction between two different reaction regimes is meaningful in this context. For chemical reactions with $k_{\mathrm{c},i} \geq 0.01$ s, a quasi-steady state is reached in less than 1 minute and this is fast enough for usage in atmospheric Eulerian 3-D models. Therefore, this first case is valid for fast reactions and the term $U_i(t)$ can be neglected. The ordinary differential equation is rewritten for fast reactions to:

$$\frac{\mathrm{d}\overline{A}_i}{\mathrm{d}t} = \frac{3}{r_{\mathrm{p}}}k_{\mathrm{g},i}\left\{\overline{C}_{\mathrm{g},i} - \frac{\overline{A}_i}{\sum_j \overline{A}_j}\frac{C_{\mathrm{g},i}^{*}}{Q_i}\right\} - k_{\mathrm{c},i}\overline{A}_i. \tag{A9}$$

Thus, the second case comprises slow reactions, which means quasi-steady state times longer than 1 min and $k_{\mathrm{c},i} < 0.01$ s. For the description of the gas-particle interface in the slow reaction case the two-film theory (Lewis and Whitman, 1924) is utilized. Therefore, the gradients in the gas and the particle phase are limited on the hypothetical gas-side and particle-side film next to the interface between the aerosol and the gas phase. The usage of the two-film theory needs the formulation of an overall gas-side mass transfer coefficient $K_{\mathrm{g},i}$ (Zaveri et al., 2014):

$$\frac{1}{K_{\mathrm{g},i}} = \frac{1}{k_{\mathrm{g},i}} + \frac{1}{k_{\mathrm{p},i}} \left(\frac{C^*_{\mathrm{g},i}}{\sum_j \overline{A}_j} \right) . \tag{A10}$$

The particle-side mass transfer coefficient $k_{\mathrm{p},i}$ is not general known and, therefore, estimated by Zaveri et al. (2014) for the limiting case ($k_{\mathrm{c},i} \to 0$, $q \to 0$, $Q \to 1$) of a nonreactive solute:

$$k_{\mathrm{p},i} = 5 \frac{D_{\mathrm{b},i}}{r_{\mathrm{p}}} . \tag{A11}$$

Thus, for slow reactions the ordinary differential equation is rewritten to:

$$\frac{\mathrm{d}\overline{A}_i}{\mathrm{d}t} = \frac{3}{r_{\mathrm{p}}} K_{\mathrm{g},i} \left\{ \overline{C}_{\mathrm{g},i} - \frac{\overline{A}_i}{\sum_j \overline{A}_j} C^*_{\mathrm{g},i} \right\} - k_{\mathrm{c},i} \overline{A}_i . \tag{A12}$$

Finally, Zaveri et al. (2014) also provides equations for polydisperse aerosol, whereby the total average concentration $\overline{C}_{\mathrm{a},i,m}$ of a solute i in size-section m is represented by:

$$\overline{C}_{\mathrm{a},i,m} = \frac{4}{3} \pi r^3_{\mathrm{p},m} N_{\mathrm{m}} A_{i,m} . \tag{A13}$$

Here, N_m denotes number concentration. For fast reactions the following equation is proposed:

$$\frac{\mathrm{d}\overline{C}_{\mathrm{a},i,m}}{\mathrm{d}t} = \xi_m k_{\mathrm{g},i,m} \left(\overline{C}_{\mathrm{g},i} - \overline{C}_{\mathrm{a},i,m} \frac{S_{i,m}}{Q_i} \right) - k_{\mathrm{c},i} \overline{C}_{\mathrm{a},i,m} , \tag{A14}$$

and for slow reactions holds:

$$\frac{\mathrm{d}\overline{C}_{\mathrm{a},i,m}}{\mathrm{d}t} = \xi_m K_{\mathrm{g},i,m} \left(\overline{C}_{\mathrm{g},i} - \overline{C}_{\mathrm{a},i,m} S_{i,m} \right) - k_{\mathrm{c},i} \overline{C}_{\mathrm{a},i,m} , \tag{A15}$$

whereby, ξ_m denotes the surface area of the respective size-section m:

$$\xi_m = 4\pi r^2_{\mathrm{p},m} N_m , \tag{A16}$$

and $S_{i,m}$ is the saturation ratio:

$$S_{i,m} = \frac{C^*_{\mathrm{g},i}}{\sum_j \overline{C}_{\mathrm{a},j,m}} . \tag{A17}$$

The simulations in this study have been conducted after implementation of the general model equations for polydisperse aerosol (Eq. A14 and A15). This has been done with the aim to test the kinetic approach in the box model SPACCIM for a following implementation in the 3-D regional model framework COSMO-MUSCAT (Wolke et al., 2012), which requires the implementation of the general system.

Acknowledgements. We thank Dr. Simon O'Meara and Dr. David O. Topping for their help with the evaluation of applicability of the weighted particle-phase bulk diffusion coefficient. We thank Prof. Dr. Ina Tegen and Prof. Dr. Hartmut Herrmann for helpful discussions and comments on the manuscript.

References

Abramson, E., Imre, D., Beranek, J., Wilson, J., and Zelenyuk, A.: Experimental determination of chemical diffusion within secondary organic aerosol particles, Phys. Chem. Chem. Phys., 15, 2983 – 2991, doi:10.1039/c2cp44013j, 2013.

Andreae, M. O. and Crutzen, P. J.: Atmospheric Aerosols: Biogeochemical Sources and Role in Atmospheric Chemistry, Science, 276, 1052 – 1058, doi:10.1126/science.276.5315.1052, 1997.

Antonovskii, V. L. and Terent'ev, V. A.: Effect of the Structure of Hydroperoxides and Some Aldehydes on the Kinetics of the Noncatalytic Formation of α-Hydroxy Peroxides, Zhurnal Organicheskoi Khimii, 3, 1011 – 1015, 1967.

Barsanti, K. C. and Pankow, J. F.: Thermodynamics of the formation of atmospheric organic particulate matter by accretion reactions-Part 1: aldehydes and ketones, Atmospheric Environment, 38, 4371 – 4382, doi:10.1016/j.atmosenv.2004.03.035, 2004.

Barsanti, K. C. and Pankow, J. F.: Thermodynamics of the formation of atmospheric organic particulate matter by accretion reactions-Part 3: Carboxylic and dicarboxylic acids, Atmospheric Environment, 40, 6676 – 6686, doi:10.1016/j.atmosenv.2006.03.013, 2006.

Berndt, T., Böge, O., and Stratmann, F.: Gas-phase ozonolysis of α-pinene: gaseous products and particle formation, Atmospheric Environment, 37, 3933 – 3945, doi:10.1016/S1352-2310(03)00501-6, 2003.

Berndt, T., Richters, S., Jokinen, T., Hyttinen, N., Kurtén, T., Otkjær, R. V., Kjaergaard, H. G., Stratmann, F., Herrmann, H., Sipilä, M., Kulmala, M., and Ehn, M.: Hydroxyl radical-induced formation of highly oxidized organic compounds, Nature Communications, 7, doi:10.1038/ncomms13677, 2016.

Cappa, C. D. and Wilson, K. R.: Evolution of organic aerosol mass spectra upon heating: implications for OA phase and partitioning behavior, Atmospheric Chemistry and Physics, 11, 1895 – 1911, doi:10.5194/acp-11-1895-2011, 2011.

Carey, F. and Sundberg, R.: Advanced Organic Chemistry, Part A. Structure and Mechanisms, 5th Edition, Springer US, doi:10.1007/978-0-387-44899-2, 2007.

Carslaw, H. S. and Jaeger, J. C.: Conduction of Heat in Solids, 2nd ed., Clarendon Press, Oxford, 1959.

Casale, M. T., Richman, A. R., Elrod, M. J., Garland, R. M., Beaver, M. R., and Tolbert, M. A.: Kinetics of acid-catalyzed aldol condensation reactions of aliphatic aldehydes, Atmospheric Environment, 41, 6212 – 6224, doi:10.1016/j.atmosenv.2007.04.002, 2007.

Champion, D., Hervet, H., Blond, G., Meste, M. L., , and Simatos, D.: Translational Diffusion in Sucrose Solutions in the Vicinity of Their Glass Transition Temperature, The Journal of Physical Chemistry B, 101, 10 674 – 10 679, doi:10.1021/jp971899i, 1997.

Chen, J. and Griffin, R. J.: Modeling secondary organic aerosol formation from oxidation of α-pinene, β-pinene, and d-limonene, Atmospheric Environment, 39, 7731 – 7744, doi:10.1016/j.atmosenv.2005.05.049, 2005.

Compernolle, S., Ceulemans, K., and Müller, J.-F.: EVAPORATION: a new vapour pressure estimation method for organic molecules including non-additivity and intramolecular interactions, Atmospheric Chemistry and Physics, 11, 9431 – 9450, doi:10.5194/acp-11-9431-2011, 2011.

Crank, J.: The Mathematics of Diffusion, 2nd ed., Oxford University Press Inc., New York, doi:10.1088/0031-9112/26/11/044, 1975.

Cussler, E. L.: Diffusion: mass transfer in fluid systems, 3rd Edition, Cambridge University Press, doi:10.1017/cbo9780511805134, 2009.

Danckwarts, P. V.: Absorption and simultaneous diffusion and chemical reaction into particles of various shapes and into falling drops, Transactions of the Faraday Society, pp. 1014 – 1023, doi:10.1039/tf9514701014, 1951.

DePalma, J. W., Horan, A. J., Hall IV, W. A., and Johnston, M. V.: Thermodynamics of oligomer formation: implications for secondary organic aerosol formation and reactivity, Phys. Chem. Chem. Phys., 15, 6935 – 6944, doi:10.1039/C3CP44586K, 2013.

Docherty, K. S., Wu, W., Lim, Y. B., and Ziemann, P. J.: Contributions of Organic Peroxides to Secondary Aerosol Formed from Reactions of Monoterpenes with O_3, Environmental Science & Technology, 39, 4049 – 4059, doi:10.1021/es050228s, 2005.

Donahue, N. M., Kroll, J. H., Pandis, S. N., and Robinson, A. L.: A two-dimensional volatility basis set – Part 2: Diagnostics of organic-aerosol evolution, Atmospheric Chemistry and Physics, 12, 615 – 634, doi:10.5194/acp-12-615-2012, 2012.

Donahue, N. M., Ortega, I. K., Chuang, W., Riipinen, I., Riccobono, F., Schobesberger, S., Dommen, J., Baltensperger, U., Kulmala, M., Worsnop, D. R., and Vehkamaki, H.: How do organic vapors contribute to new-particle formation?, Faraday Discussions, 165, 91 – 104, doi:10.1039/C3FD00046J, 2013.

Eckert, F. and Klamt, A.: Fast solvent screening via quantum chemistry: COSMO-RS approach, AIChE Journal, 48, doi:10.1002/aic.690480220, 2002.

Ehn, M., Kleist, E., Junninen, H., Petäjä, T., Lönn, G., Schobesberger, S., Dal Maso, M., Trimborn, A., Kulmala, M., Worsnop, D. R., Wahner, A., Wildt, J., and Mentel, T. F.: Gas phase formation of extremely oxidized pinene reaction products in chamber and ambient air, Atmospheric Chemistry and Physics, 12, 5113 – 5127, doi:10.5194/acp-12-5113-2012, 2012.

Ehn, M., Thornton, J. a., Kleist, E., Sipilä, M., Junninen, H., Pullinen, I., Springer, M., Rubach, F., Tillmann, R., Lee, B., Lopez-Hilfiker, F., Andres, S., Acir, I.-H., Rissanen, M., Jokinen, T., Schobesberger, S., Kangasluoma, J., Kontkanen, J., Nieminen, T., Kurtén, T., Nielsen, L. B., Jørgensen, S., Kjaergaard, H. G., Canagaratna, M., Maso, M. D., Berndt, T., Petäjä, T., Wahner, A., Kerminen, V.-M., Kulmala, M., Worsnop, D. R., Wildt, J., and Mentel, T. F.: A large source of low-volatility secondary organic aerosol, Nature, 506, 476 – 9, doi:10.1038/nature13032, 2014.

Einstein, A.: Investigations on the Theory of Brownian Motion, Dover, New York, 1956.

Ervens, B., Feingold, G., Clegg, S. L., and Kreidenweis, S. M.: A modeling study of aqueous production of dicarboxylic acids: 2. Implications for cloud microphysics, Journal of Geophysical Research: Atmospheres, 109, doi:10.1029/2004JD004575, 2004.

Ervens, B., Feingold, G., and Kreidenweis, S. M.: Influence of water-soluble organic carbon on cloud drop number concentration, Journal of Geophysical Research: Atmospheres, 110, doi:10.1029/2004JD005634, 2005.

Ervens, B., Turpin, B. J., and Weber, R. J.: Secondary organic aerosol formation in cloud droplets and aqueous particles (aqSOA): a review of laboratory, field and model studies, Atmospheric Chemistry and Physics, 11, 11 069 – 11 102, doi:10.5194/acp-11-11069-2011, 2011.

Facchini, M. C., Mircea, M., Fuzzi, S., and Charlson, R. J.: Cloud albedo enhancement by surface-active organic solutes in growing droplets, Nature, 40, 257 – 259, doi:10.1038/45758, 1999.

Fuchs, N. and Sutugin, A.: HIGH-DISPERSED AEROSOLS, in: Topics in Current Aerosol Research, edited by Hidy, G. and Brock, J., International Reviews in Aerosol Physics and Chemistry, Pergamon, doi:10.1016/B978-0-08-016674-2.50006-6, 1971.

Goldstein, A. H. and Galbally, I. E.: Known and Unexplored Organic Constituents in the Earth's Atmosphere, Environmental Science & Technology, 41, 1514–1521, doi:10.1021/es072476p, 2007.

Grayson, J. W., Song, M., Sellier, M., and Bertram, A. K.: Validation of the poke-flow technique combined with simulations of fluid flow for determining viscosities in samples with small volumes and high viscosities, Atmospheric Measurement Techniques, 8, 2463 – 2472, doi:10.5194/amt-8-2463-2015, 2015.

Grayson, J. W., Zhang, Y., Mutzel, A., Renbaum-Wolff, L., Böge, O., Kamal, S., Herrmann, H., Martin, S. T., and Bertram, A. K.: Effect of varying experimental conditions on the viscosity of α-pinene derived secondary organic material, Atmospheric Chemistry and Physics, 16, 6027 – 6040, doi:10.5194/acp-16-6027-2016, 2016.

Griffin, R. J., Dabdub, D., and Seinfeld, J. H.: Secondary organic aerosol 1. Atmospheric chemical mechanism for production of molecular constituents, Journal of Geophysical Research: Atmospheres, 107, 1 – 26, doi:10.1029/2001jd000541, 2002.

Hallquist, M., Wenger, J. C., Baltensperger, U., Rudich, Y., Simpson, D., Claeys, M., Dommen, J., Donahue, N. M., George, C., Goldstein, A. H., Hamilton, J. F., Herrmann, H., Hoffmann, T., Iinuma, Y., Jang, M., Jenkin, M. E., Jimenez, J. L., Kiendler-Scharr, A., Maenhaut, W., McFiggans, G., Mentel, T. F., Monod, A., Prévôt, A. S. H., Seinfeld, J. H., Surratt, J. D., Szmigielski, R., and Wildt, J.: The formation, properties and impact of secondary organic aerosol: current and emerging issues, Atmospheric Chemistry and Physics, 9, 5155 – 5236, doi:10.5194/acp-9-5155-2009, 2009.

Harrison, R. and Yin, J.: Particulate matter in the atmosphere: which particle properties are important for its effects on health?, Sci. Total Environ., 249, 85 – 101, doi:10.1016/s0048-9697(99)00513-6, 2000.

Haywood, J. and Boucher, O.: Estimates of the direct and indirect radiative forcing due to tropospheric aerosols: A review, Reviews of Geophysics, 38, 513 – 543, doi:10.1029/1999RG000078, 2000.

Hitzenberger, R., Berner, A., Kasper-Giebl, A., Löflund, M., and Puxbaum, H.: Surface tension of Rax cloud water and its relation to the concentration of organic material, Journal of Geophysical Research: Atmospheres, 107, AAC 5–1 – AAC 5–6, doi:10.1029/2002JD002506, 2002.

Hoffmann, E., Tilgner, A., Schrödner, R., Bräuer, P., Wolke, R., and Herrmann, H.: An advanced modeling study on the impacts and atmospheric implications of multiphase dimethyl sulfide chemistry, Proceedings of the National Academy of Sciences, 113, 11 776 – 11 781, doi:10.1073/pnas.1606320113, 2016.

Holz, M., Heil, S. R., and Sacco, A.: Temperature-dependent self-diffusion coefficients of water and six selected molecular liquids for calibration in accurate 1H NMR PFG measurements, Physical Chemistry Chemical Physics, 2, 4740 – 4742, doi:10.1039/B005319H, 2000.

Hosny, N. A., Fitzgerald, C., Tong, C., Kalberer, M., Kuimova, M. K., and Pope, F. D.: Fluorescent lifetime imaging of atmospheric aerosols: a direct probe of aerosol viscosity, Faraday Discussions, 165, 343 – 356, doi:10.1039/c3fd00041a, 2013.

Hosny, N. A., Fitzgerald, C., Vyšniauskas, A., Athanasiadis, A., Berkemeier, T., Uygur, N., Pöschl, U., Shiraiwa, M., Kalberer, M., Pope, F. D., and Kuimova, M. K.: Direct imaging of changes in aerosol particle viscosity upon hydration and chemical aging, Chemical Science, 7, 1357 – 1367, doi:10.1039/c5sc02959g, 2016.

Iinuma, Y., Böge, O., Gnauk, T., and Herrmann, H.: Aerosol-chamber study of the α-pinene/O_3 reaction: influence of particle acidity on aerosol yields and products, Atmospheric Environment, 38, 761 – 773, doi:10.1016/j.atmosenv.2003.10.015, 2004.

Iinuma, Y., Böge, O., Kahnt, A., and Herrmann, H.: Laboratory chamber studies on the formation of organosulfates from reactive uptake of monoterpene oxides, Physical Chemistry Chemical Physics, 11, 7985 – 7997, doi:10.1039/B904025K, 2009.

IPCC: Climate Change 2013: The Physical Science Basis. Contribution of Working Group I to the Fifth Assessment Report of the Intergovernmental Panel on Climate Change, Cambridge University Press, Cambridge, United Kingdom and New York, NY, USA, doi:10.1017/CBO9781107415324, 1535 pp, 2013.

Jenkin, M. E., Saunders, S. M., and Pilling, M. J.: The tropospheric degradation of volatile organic compounds: a protocol for mechanism development, Atmospheric Environment, 31, 81 – 104, doi:10.1016/s1352-2310(96)00105-7, 1997.

Jenkin, M. E., Shallcross, D. E., and Harvey, J. N.: Development and application of a possible mechanism for the generation of cis-pinic acid from the ozonolysis of α- and β-pinene, Atmospheric Environment, 34, 2837 – 2850, doi:10.1016/s1352-2310(00)00087-x, 2000.

Jimenez, J. L., Canagaratna, M. R., Donahue, N. M., Prevot, A. S. H., Zhang, Q., Kroll, J. H., DeCarlo, P. F., Allan, J. D., Coe, H., Ng, N. L., Aiken, A. C., Docherty, K. S., Ulbrich, I. M., Grieshop, A. P., Robinson, A. L., Duplissy, J., Smith, J. D., Wilson, K. R., Lanz, V. A., Hueglin, C., Sun, Y. L., Tian, J., Laaksonen, A., Raatikainen, T., Rautiainen, J., Vaattovaara, P., Ehn, M., Kulmala, M., Tomlinson, J. M., Collins, D. R., Cubison, M. J., Dunlea, J., Huffman, J. A., Onasch, T. B., Alfarra, M. R., Williams, P. I., Bower, K., Kondo, Y., Schneider,

J., Drewnick, F., Borrmann, S., Weimer, S., Demerjian, K., Salcedo, D., Cottrell, L., Griffin, R., Takami, A., Miyoshi, T., Hatakeyama, S., Shimono, A., Sun, J. Y., Zhang, Y. M., Dzepina, K., Kimmel, J. R., Sueper, D., Jayne, J. T., Herndon, S. C., Trimborn, A. M., Williams, L. R., Wood, E. C., Middlebrook, A. M., Kolb, C. E., Baltensperger, U., and Worsnop, D. R.: Evolution of Organic Aerosols in the Atmosphere, Science, 326, 1525 – 1529, doi:10.1126/science.1180353, 2009.

Jokinen, T., Sipilä, M., Richters, S., Kerminen, V.-M., Paasonen, P., Stratmann, F., Worsnop, D., Kulmala, M., Ehn, M., Herrmann, H., and Berndt, T.: Rapid Autoxidation Forms Highly Oxidized RO_2 Radicals in the Atmosphere, Angewandte Chemie International Edition, 53, 14 596 – 14 600, doi:10.1002/anie.201408566, 2014.

Jokinen, T., Berndt, T., Makkonen, R., Kerminen, V.-M., Junninen, H., Paasonen, P., Stratmann, F., Herrmann, H., Guenther, A. B., Worsnop, D. R., Kulmala, M., Ehn, M., and Sipilä, M.: Production of extremely low volatile organic compounds from biogenic emissions: Measured yields and atmospheric implications, Proceedings of the National Academy of Sciences, 112, 7123 – 7128, doi:10.1073/pnas.1423977112, 2015.

Kahnt, A., Iinuma, Y., Böge, O., Mutzel, A., and Herrmann, H.: Denuder sampling techniques for the determination of gas-phase carbonyl compounds: A comparison and characterisation of in situ and ex situ derivatisation methods, Journal of Chromatography B, 879, 1402 – 1411, doi:10.1016/j.jchromb.2011.02.028, 2011.

Kidd, C., Perraud, V., Wingen, L. M., and Finlayson-Pitts, B. J.: Integrating phase and composition of secondary organic aerosol from the ozonolysis of α-pinene, Proceedings of the National Academy of Sciences, 111, 7552 – 7557, doi:10.1073/pnas.1322558111, 2014.

Köhler, H.: The nucleus in and the growth of hygroscopic droplets, Transactions of the Faraday Society, 32, 1152 – 1161, doi:10.1039/TF9363201152, 1936.

Koop, T., Bookhold, J., Shiraiwa, M., and Pöschl, U.: Glass transition and phase state of organic compounds: dependency on molecular properties and implications for secondary organic aerosols in the atmosphere, Phys. Chem. Chem. Phys., 13, 19 238 – 19 255, doi:10.1039/c1cp22617g, 2011.

Kuimova, M. K.: Molecular Rotors Image Intracellular Viscosity, CHIMIA International Journal for Chemistry, 66, doi:10.2533/chimia.2012.159, 2012.

Kulmala, M., Toivonen, A., Mäkelä, J., and Laaksonen, A.: Analysis of the growth of nucleation mode particles observed in Boreal forest, Tellus B, 50, doi:10.3402/tellusb.v50i5.16229, 1998.

Kurtén, T., Tiusanen, K., Roldin, P., Rissanen, M., Luy, J., Boy, M., Ehn, M., and Donahue, N.: α-Pinene Autoxidation Products May Not Have Extremely Low Saturation Vapor Pressures Despite High O:C Ratios, The Journal of Physical Chemistry A, 120, 2569 – 2582, doi:10.1021/acs.jpca.6b02196, 2016.

Lewis, W. K. and Whitman, W. G.: Principles of Gas Absorption., Industrial & Engineering Chemistry, 16, 1215 – 1220, doi:10.1021/ie50180a002, 1924.

Lienhard, D. M., Huisman, A. J., Bones, D. L., Te, Y.-F., Luo, B. P., Krieger, U. K., and Reid, J. P.: Retrieving the translational diffusion coefficient of water from experiments on single levitated aerosol droplets, Physical Chemistry Chemical Physics, 16, 16 677 – 16 683, doi:10.1039/C4CP01939C, 2014.

Lienhard, D. M., Huisman, A. J., Krieger, U. K., Rudich, Y., Marcolli, C., Luo, B. P., Bones, D. L., Reid, J. P., Lambe, A. T., Canagaratna, M. R., Davidovits, P., Onasch, T. B., Worsnop, D. R., Steimer, S. S., Koop, T., and Peter, T.: Viscous organic aerosol particles in the upper troposphere: diffusivity-controlled water uptake and ice nucleation?, Atmospheric Chemistry and Physics, 15, 13 599 – 13 613, doi:10.5194/acp-15-13599-2015, 2015.

Mai, H., Shiraiwa, M., Flagan, R. C., and Seinfeld, J. H.: Under What Conditions Can Equilibrium Gas-Particle Partitioning Be Expected to Hold in the Atmosphere?, Environmental Science & Technology, 49, 11 485 – 11 491, doi:10.1021/acs.est.5b02587, 2015.

Marshall, F. H., Miles, R. E. H., Song, Y.-C., Ohm, P. B., Power, R. M., Reid, J. P., and Dutcher, C. S.: Diffusion and reactivity in ultraviscous aerosol and the correlation with particle viscosity, Chemical Science, 7, 1298 – 1308, doi:10.1039/C5SC03223G, 2016.

Mendoza, C. I., Santamaría-Holek, I., and Pérez-Madrid, A.: Effective temperatures and the breakdown of the Stokes-Einstein relation for particle suspensions, The Journal of Chemical Physics, 143, 104 506, doi:10.1063/1.4930550, 2015.

Mentel, T. F., Springer, M., Ehn, M., Kleist, E., Pullinen, I., Kurtén, T., Rissanen, M., Wahner, A., and Wildt, J.: Formation of highly oxidized multifunctional compounds: autoxidation of peroxy radicals formed in the ozonolysis of alkenes - deduced from structure-product relationships, Atmospheric Chemistry and Physics, 15, 6745 – 6765, doi:10.5194/acp-15-6745-2015, 2015.

Mutzel, A., Poulain, L., Berndt, T., Iinuma, Y., Rodigast, M., Böge, O., Richters, S., Spindler, G., Sipilä, M., Jokinen, T., Kulmala, M., and Herrmann, H.: Highly Oxidized Multifunctional Organic Compounds Observed in Tropospheric Particles: A Field and Laboratory Study, Environmental Science & Technology, 49, 7754 – 7761, doi:10.1021/acs.est.5b00885, 2015.

Mutzel, A., Rodigast, M., Iinuma, Y., Böge, O., and Herrmann, H.: Monoterpene SOA – Contribution of first-generation oxidation products to formation and chemical composition, Atmospheric Environment, 130, 136 – 144, doi:10.1016/j.atmosenv.2015.10.080, 2016.

Ng, N., Kroll, J., Keywood, M., Bahreini, R., Varutbangkul, V., Flagan, R., Seinfeld, J., Lee, A., and Goldstein, A.: Contribution of First- versus Second-Generation Products to Secondary Organic Aerosols Formed in the Oxidation of Biogenic Hydrocarbons, Environmental Science & Technology, 40, 2283 – 2297, doi:10.1021/es052269u, 2006.

O'Meara, S., Booth, A. M., Barley, M. H., Topping, D., and McFiggans, G.: An assessment of vapour pressure estimation methods, Phys. Chem. Chem. Phys., 16, 19 453 – 19 469, doi:10.1039/C4CP00857J, 2014.

O'Meara, S., Topping, D. O., and McFiggans, G.: The rate of equilibration of viscous aerosol particles, Atmospheric Chemistry and Physics, 16, 5299 – 5313, doi:10.5194/acp-16-5299-2016, 2016.

Pajunoja, A., Malila, J., Hao, L., Joutsensaari, J., Lehtinen, K. E. J., and Virtanen, A.: Estimating the Viscosity Range of SOA Particles Based on Their Coalescence Time, Aerosol Science and Technology, 48, i – iv, doi:10.1080/02786826.2013.870325, 2014.

Pankow, J. F.: An absorption model of the gas/aerosol partitioning involved in the formation of secondary organic aerosol, Atmospheric Environment, 28, 189 – 193, doi:10.1016/1352-2310(94)90094-9, 1994.

Pankow, J. F. and Asher, W. E.: SIMPOL.1: a simple group contribution method for predicting vapor pressures and enthalpies of vaporization of multifunctional organic compounds, Atmospheric Chemistry and Physics, 8, 2773 – 2796, doi:10.5194/acp-8-2773-2008, 2008.

Pope, C. and Dockery, D.: Health Effects of Fine Particulate Air Pollution: Lines that Connect, J. Air Waste Manage., 56, 709 – 742, doi:10.1080/10473289.2006.10464485, 2006.

Power, R. M., Simpson, S. H., Reid, J. P., and Hudson, A. J.: The transition from liquid to solid-like behaviour in ultrahigh viscosity aerosol particles, Chemical Science, 4, 2597 – 2604, doi:10.1039/c3sc50682g, 2013.

Price, H. C., Mattsson, J., Zhang, Y., Bertram, A. K., Davies, J. F., Grayson, J. W., Martin, S. T., O'Sullivan, D., Reid, J. P., Rickards, A. M. J., and Murray, B. J.: Water diffusion in atmospherically relevant α-pinene secondary organic material, Chemical Science, 6, 4876 – 4883, doi:10.1039/C5SC00685F, 2015.

Pruppacher, H. and Klett, J.: Microphysics of Clouds and Precipitation, 2nd Edition, Springer Netherlands, doi:10.1007/978-0-306-48100-0, 2010.

Pun, B. K., Wu, S.-Y., Seigneur, C., Seinfeld, J. H., Griffin, R. J., and Pandis, S. N.: Uncertainties in Modeling Secondary Organic Aerosols: Three-Dimensional Modeling Studies in Nashville/Western Tennessee, Environmental Science & Technology, 37, 3647 – 3661, doi:10.1021/es0341541, 2003.

Rampp, M., Buttersack, C., and Lüdemann, H.-D.: c,T-Dependence of the viscosity and the self-diffusion coefficients in some aqueous carbohydrate solutions, Carbohydrate Research, 328, 561 – 572, doi:10.1016/s0008-6215(00)00141-5, 2000.

Renbaum-Wolff, L., Grayson, J. W., Bateman, A. P., Kuwata, M., Sellier, M., Murray, B. J., Shilling, J. E., Martin, S. T., and Bertram, A. K.: Viscosity of α-pinene secondary organic material and implications for particle growth and reactivity, Proceedings of the National Academy of Sciences, 110, 8014 – 8019, doi:10.1073/pnas.1219548110, 2013a.

Renbaum-Wolff, L., Grayson, J. W., and Bertram, A. K.: Technical Note: New methodology for measuring viscosities in small volumes characteristic of environmental chamber particle samples, Atmospheric Chemistry and Physics, 13, 791 – 802, doi:10.5194/acp-13-791-2013, 2013b.

Riipinen, I., Yli-Juuti, T., Pierce, J. R., Petaja, T., Worsnop, D. R., Kulmala, M., and Donahue, N. M.: The contribution of organics to atmospheric nanoparticle growth, Nature Geosciences, 5, doi:10.1038/ngeo1499, 2012.

Roldin, P., Eriksson, A. C., Nordin, E. Z., Hermansson, E., Mogensen, D., Rusanen, A., Boy, M., Swietlicki, E., Svenningsson, B., Zelenyuk, A., and Pagels, J.: Modelling non-equilibrium secondary organic aerosol formation and evaporation with the aerosol dynamics, gas- and particle-phase chemistry kinetic multilayer model ADCHAM, Atmospheric Chemistry and Physics, 14, 7953 – 7993, doi:10.5194/acp-14-7953-2014, 2014.

Rusumdar, A. J., Wolke, R., Tilgner, A., and Herrmann, H.: Treatment of non-ideality in the SPACCIM multiphase model – Part 1: Model development, Geoscientific Model Development, 9, 247 – 281, doi:10.5194/gmd-9-247-2016, 2016.

Saukko, E., Lambe, A. T., Massoli, P., Koop, T., Wright, J. P., Croasdale, D. R., Pedernera, D. A., Onasch, T. B., Laaksonen, A., Davidovits, P., Worsnop, D. R., and Virtanen, A.: Humidity-dependent phase state of SOA particles from biogenic and anthropogenic precursors, Atmospheric Chemistry and Physics, 12, 7517 – 7529, doi:10.5194/acpd-12-4447-2012, 2012.

Schwartz, S. E.: Mass-Transport Considerations Pertinent to Aqueous Phase Reactions of Gases in Liquid-Water Clouds, pp. 415 – 471, Springer Berlin Heidelberg, Berlin, Heidelberg, doi:10.1007/978-3-642-70627-1_16, 1986.

Seinfeld, J. H. and Pandis, S. N.: Atmospheric Chemistry and Physics: from Air Pollution to Climate Change, 2nd Edition, John Wiley, New York, doi:10.1029/2007JD009735, 2006.

Shiraiwa, M., Pfrang, C., and Pöschl, U.: Kinetic multi-layer model of aerosol surface and bulk chemistry (KM-SUB): the influence of interfacial transport and bulk diffusion on the oxidation of oleic acid by ozone, Atmospheric Chemistry and Physics, 10, 3673 – 3691, doi:10.5194/acp-10-3673-2010, 2010.

Shiraiwa, M., Ammann, M., Koop, T., and Pöschl, U.: Gas uptake and chemical aging of semisolid organic aerosol particles, Proceedings of the National Academy of Sciences, 108, 11 003 – 11 008, doi:10.1073/pnas.1103045108, 2011.

Shiraiwa, M., Pfrang, C., Koop, T., and Pöschl, U.: Kinetic multi-layer model of gas-particle interactions in aerosols and clouds (KM-GAP): linking condensation, evaporation and chemical reactions of organics, oxidants and water, Atmospheric Chemistry and Physics, 12, 2777 – 2794, doi:10.5194/acp-12-2777-2012, 2012.

Shiraiwa, M., Yee, L. D., Schilling, K. A., Loza, C. L., Craven, J. S., Zuend, A., Ziemann, P. J., and Seinfeld, J. H.: Size distribution dynamics reveal particle-phase chemistry in organic aerosol formation, Proceedings of the National Academy of Sciences, 110, 11 746 – 11 750, doi:10.1073/pnas.1307501110, 2013a.

Shiraiwa, M., Zuend, A., Bertram, A. K., and Seinfeld, J. H.: Gas-particle partitioning of atmospheric aerosols: interplay of physical state, non-ideal mixing and morphology, Phys. Chem. Chem. Phys., 15, 11 441 – 11 453, doi:10.1039/C3CP51595H, 2013b.

Simmel, M. and Wurzler, S.: Condensation and activation in sectional cloud microphysical models, Atmospheric Research, 80, 218 – 236, doi:10.1016/j.atmosres.2005.08.002, 2006.

Simmel, M., Diehl, K., and Wurzler, S.: Numerical simulation of the microphysics of an orographic cloud: Comparison with measurements and sensitivity studies, Atmospheric Environment, 39, 4365 – 4373, doi:10.1016/j.atmosenv.2005.02.017, 2005.

Surratt, J. D., Murphy, S. M., Kroll, J. H., Ng, N. L., Hildebrandt, L., Sorooshian, A., Szmigielski, R., Vermeylen, R., Maenhaut, W., Claeys, M., Flagan, R. C., and Seinfeld, J. H.: Chemical Composition of Secondary Organic Aerosol Formed from the Photooxidation of Isoprene, The Journal of Physical Chemistry A, 110, 9665 – 9690, doi:10.1021/jp061734m, 2006.

Tarjus, G. and Kivelson, D.: Breakdown of the Stokes-Einstein relation in supercooled liquids, The Journal of Chemical Physics, 103, 3071 – 3073, doi:10.1063/1.470495, 1995.

Tilgner, A., Bräuer, P., Wolke, R., and Herrmann, H.: Modelling multiphase chemistry in deliquescent aerosols and clouds using CAPRAM3.0i, Journal of Atmospheric Chemistry, 70, 221 – 256, doi:10.1007/s10874-013-9267-4, 2013.

Tobias, H. and Ziemann, P.: Thermal Desorption Mass Spectrometric Analysis of Organic Aerosol Formed from Reactions of 1-Tetradecene and O_3 in the Presence of Alcohols and Carboxylic Acids, Environmental Science & Technology, 34, 2105 – 2115, doi:10.1021/es9907156, 2000.

Vaden, T. D., Imre, D., Beránek, J., Shrivastava, M., and Zelenyuk, A.: Evaporation kinetics and phase of laboratory and ambient secondary organic aerosol, Proceedings of the National Academy of Sciences, 108, 2190 – 2195, doi:10.1073/pnas.1013391108, 2011.

Vignes, A.: Diffusion in Binary Solutions. Variation of Diffusion Coefficient with Composition, Industrial & Engineering Chemistry Fundamentals, 5, 189 – 199, doi:10.1021/i160018a007, 1966.

Virtanen, A., Joutsensaari, J., Koop, T., Kannosto, J., Yli-Pirilä, P., Leskinen, J., Mäkelä, J. M., Holopainen, J. K., Pöschl, U., Kulmala, M., Worsnop, D. R., and Laaksonen, A.: An amorphous solid state of biogenic secondary organic aerosol particles, Nature, 467, 824 – 827, doi:10.1038/nature09455, 2010.

Virtanen, A., Kannosto, J., Kuuluvainen, H., Arffman, A., Joutsensaari, J., Saukko, E., Hao, L., Yli-Pirilä, P., Tiitta, P., Holopainen, J. K., Keskinen, J., Worsnop, D. R., Smith, J. N., and Laaksonen, A.: Bounce behavior of freshly nucleated biogenic secondary organic aerosol particles, Atmospheric Chemistry and Physics, 11, 8759 – 8766, doi:10.5194/acp-11-8759-2011, 2011.

Wesselingh, J. and Bollen, A.: Distillation Multicomponent Diffusivities from the Free Volume Theory, Chemical Engineering Research and Design, 75, 590 – 602, doi:10.1205/026387697524119, 1997.

Winterhalter, R., Neeb, P., Grossmann, D., Kolloff, A., Horie, O., and Moortgat, G.: Products and Mechanism of the Gas Phase Reaction of Ozone with β-Pinene, Journal of Atmospheric Chemistry, 35, 165 – 197, doi:10.1023/A:1006257800929, 2000.

Wolke, R. and Knoth, O.: Numerical Solution of Differential and Differential-Algebraic Equations, 4 – 9 September 2000, Halle, Germany Time-integration of multiphase chemistry in size-resolved cloud models, Applied Numerical Mathematics, 42, 473 – 487, doi:10.1016/S0168-9274(01)00169-6, 2002.

Wolke, R., Sehili, A., Simmel, M., Knoth, O., Tilgner, A., and Herrmann, H.: SPACCIM: A parcel model with detailed microphysics and complex multiphase chemistry, Atmospheric Environment, 39, 4375 – 4388, doi:10.1016/j.atmosenv.2005.02.038, 2005.

Wolke, R., Schröder, W., Schrödner, R., and Renner, E.: Influence of grid resolution and meteorological forcing on simulated European air quality: A sensitivity study with the modeling system COSMO-MUSCAT, Atmospheric Environment, 53, 110 – 130, doi:10.1016/j.atmosenv.2012.02.085, 2012.

Zaveri, R. A., Easter, R. C., Shilling, J. E., and Seinfeld, J. H.: Modeling kinetic partitioning of secondary organic aerosol and size distribution dynamics: representing effects of volatility, phase state, and particle-phase reaction, Atmospheric Chemistry and Physics, 14, 5153 – 5181, doi:10.5194/acp-14-5153-2014, 2014.

Zelenyuk, A., Imre, D., Beránek, J., Abramson, E., Wilson, J., and Shrivastava, M.: Synergy between Secondary Organic Aerosols and Long-Range Transport of Polycyclic Aromatic Hydrocarbons, Environmental Science & Technology, 46, 12 459 – 12 466, doi:10.1021/es302743z, 2012.

Zhang, X., Cappa, C. D., Jathar, S. H., McVay, R. C., Ensberg, J. J., Kleeman, M. J., and Seinfeld, J. H.: Influence of vapor wall loss in laboratory chambers on yields of secondary organic aerosol, Proceedings of the National Academy of Sciences, 111, 5802 – 5807, doi:10.1073/pnas.1404727111, 2014.

Zhang, Y., Sanchez, M. S., Douet, C., Wang, Y., Bateman, A. P., Gong, Z., Kuwata, M., Renbaum-Wolff, L., Sato, B. B., Liu, P. F., Bertram, A. K., Geiger, F. M., and Martin, S. T.: Changing shapes and implied viscosities of suspended submicron particles, Atmospheric Chemistry and Physics, 15, 7819 – 7829, doi:10.5194/acp-15-7819-2015, 2015.

Zhao, J., Ortega, J., Chen, M., McMurry, P. H., and Smith, J. N.: Dependence of particle nucleation and growth on high-molecular-weight gas-phase products during ozonolysis of α-pinene, Atmospheric Chemistry and Physics, 13, 7631 – 7644, doi:10.5194/acp-13-7631-2013, 2013.

Zhu, L., Cai, T., Huang, J., Stringfellow, T. C., Wall, M., and Yu, L.: Water Self-Diffusion in Glassy and Liquid Maltose Measured by Raman Microscopy and NMR, The Journal of Physical Chemistry B, 155, 5849 – 5899, doi:10.1021/jp202663r, 2011.

Ziemann, P. J. and Atkinson, R.: Kinetics, products, and mechanisms of secondary organic aerosol formation, Chem. Soc. Rev., 41, 6582 – 6605, doi:10.1039/C2CS35122F, 2012.

Zobrist, B., Soonsin, V., Luo, B. P., Krieger, U. K., Marcolli, C., Peter, T., and Koop, T.: Ultra-slow water diffusion in aqueous sucrose glasses, Phys. Chem. Chem. Phys., 13, 3514 – 3526, doi:10.1039/c0cp01273d, 2011.